AN INVESTIGATION ON AIRBORNE PARTICULATE MATTER COMPOSITION AT THE SARITEPE CAMPUS, BOĞAZİÇİ UNIVERSITY

by

Ezelnur Çıtak

B.Sc. in Environmental Engineering, Fatih University, 2015

Submitted to the Institute of Environmental Sciences in partial fulfillment of

the requirements for the degree of

Master of Science

in

Environmental Technology

Boğaziçi University

2019

AN INVESTIGATION ON AIRBORNE PARTICULATE MATTER COMPOSITION AT THE SARITEPE CAMPUS, BOĞAZİÇİ UNIVERSITY

APPROVED BY:

Prof. Dr. Nadim Copty . . . .
Thesis Advisor

Prof. Dr. Burak Demirel . . . .

Dr. Ulaş İm . . . .

DATE OF APPROVAL: 04/04/2019

ACKNOWLEDGEMENTS

I would like to express my indebtedness and blessing to numerous people having supported me on this long journey.

First and foremost, I would like to express my special thanks to my advisor, Professor Nadim Copty, for his valuable support and trust to my work, personally by his unique combination of high intelligence and modesty, and academically by his comments, evaluations, discussions. I am grateful to him for sparing his valuable time and sharing his valuable experiences helping me to accomplish of this work.

Secondly, I am also very grateful to Prof. Dr. Burak Demirel, for helping and supporting me throughout my study, sparing his valuable time and sharing his experiences on this very broad field of air quality and providing me the trust for accomplishment of this work. I am also grateful to Dr. Ulaş İm from Aarhus University, for sparing his valuable time and sharing his experiences on this very broad field of air quality modelling.

Very special thanks to Filiz Ayılmaz from Boğaziçi University, for sparing her valuable time and sharing her valuable technical experience in laboratory methodologies. I would like to express my gratitude to academic team in Sarıtepe Campus, for their collaboration and support to this work.

Most especially, I would like to express my special thanks to my husband, Yusuf Ensar Çıtak, mentally by his pep talks, encouragement, patience, and technically by his extensive experience in technological devices. I am in debt to him for his tolerability and not losing his faith in me for a moment. I would like to express my gratitude and blessing to my nuclear family, Canan Aydemir, Metin Aydemir and Gökçe Aydemir, for encouraging me during my academic life (more than 20 years) and their love and trust.

Last but not the least, I am also grateful to my extended family, all my friends and colleagues, for their encouragement and support. Finally, the financial support provided by Boğaziçi University Research Fund project 13461.

ABSTRACT

AN INVESTIGATION ON AIRBORNE PARTICULATE MATTER COMPOSITION AT THE SARITEPE CAMPUS, BOĞAZİÇİ UNIVERSITY

Particulate matter (PM) are released into the atmosphere from both anthropogenic sources such as transport and biomass burning and from natural sources such sea-salt, soil dust and vegetation. The purpose of this study is to evaluate chemical composition and possible sources of airborne particulate matter (PM) at the Sarıtepe campus of Boğaziçi University which is located along the Black Sea coast. The campus is also close to the forests of northwestern Istanbul and the newly opened highway connecting to the Yavuz Sultan Selim Bridge. Particulate matter samples were collected from various locations. The study extended over a period of 10 months (21 March 2017 to 20 January 2018). Sensitive laboratory techniques (ICP-OES, IC, AAS) were used for the analysis of the collected solid and aqueous phases. In total 360 samples were analyzed for 26 parameters: F^-, Cl^-, NO_2^-, NO_3^-, SO_4^{2}, PO_4^{3-}, Br^-, Mg^+, Ca^{2+}, K^+, Na^+, Cr, Mn, Fe, Ni, Cu, Zn, Al, Cd, Pb, Si, Co, Mo, pH, TDS and electrical conductivity. Potential sources of the collected PM were investigated using a multivariate factor analysis technique (PMF). Results of the study show that the metal compositions are highly correlated to each other. Concentrations of some metals are higher than some reported data in the literature. The composition of the collected PM indicates that both anthropogenic and natural sources have contributed to the PM in the study area. Specifically, PMF analysis suggests that the PM most likely originates from 4 sources: agricultural activity, burning processes, marine aerosol, and roadway transportation.

ÖZET

BOĞAZİÇİ ÜNİVERSİTESİ SARITEPE KAMPÜS'TEKİ PARTİKÜL MADDE KONSANTRASYONUNUN ARAŞTIRILMASI

Partiküler madde ulaşım biokütle yakımı gibi antropojenik kaynaklardan ve deniz tuzu toprak tozu vejetasyon gibi doğal kaynaklardan atmosfere salınır. Bu çalışmanın amacı, Boğaziçi Üniversitesinin Karadeniz kıyısında yer almakta olan Sarıtepe Kampüsü'ndeki hava kaynaklı partiküler madde kompozisyonunu ve muhtemel kaynaklarını belirlemektir. Kampüs İstanbulun kuzeybatı ormanlarına ve Yavuz Sultan Selim köprüsüne bağlı yeni açılan otoban yakın bir konumdadır. Partiküler madde örnekleri farklı lokasyonlardan toplanmıştır. Çalışma 10 aylık (21 Mart 2017-20 Ocak 2018) bir süreci kapsamaktadır. Toplanan katı ve sıvı fazların analizleri için hassas laboratuvar teknikleri (ICP-OES, IC, AAS) kullanılmıştır. Toplamda 360 adet numune 26 parametre için analiz edilmiştir. F^-, Cl^-, NO_2^-, NO_3^-, SO_4^{2-}, PO_4^{3-}, Br, Mg^+, Ca^{2+}, K^+, Na^+, Cr, Mn, Fe, Ni, Cu, Zn, Al, Cd, Pb, Si, Co, Mo. Toplanan partiküler maddenin muhtemel kaynakları çok değişkenli bir faktör analiz tekniği kullanılarak (PMF) araştırılmıştır. Çalışma sonuçları metal kompozisyonlarının yüksek oranda birbirleriyle ilintili olduğunu göstermiştir. Bazı metallerin konsantrasyonları literatürde rapor edilmiş datalara oranla daha yüksek olduğu görülmüştür. Toplanan PM konsantrasyonu gösteriyorki hem antropojenik hemde doğal kaynaklar çalışma alanındaki partiküler maddeye katkıda bulunmuştur. Özellikle PMF analizi partiküler maddenin büyük bir olasılıkla 4 kaynaktan-tarımsal faaliyet, yanma prosesleri, deniz tuzu aerosolleri ve karayolu ulaşımı ileri geldiğini belirtmiştir.

TABLE OF CONTENTS

LIST OF FIGURES

LIST OF TABLES

LIST OF SYMBOLS/ABBREVIATIONS

Symbol	**Explanation**	**Unit**
HNO_3	Nitric Acid	ml
µg	Microgram	

Abbreviation	**Explanation**
AAS	Flame Atomic Absorption Spectrophotometry
BC	Black Carbon
C	Coarse Mode
CMAQ	Community Multiscale Air Quality Modeling System
F	Fine Mode
IC	Ion Chromatography
ICP	Inductively Coupled Plasma
IGMAQN	Istanbul Greater Municipality Air Quality Network
PM	Particulate Matter
PMF	Positive Matrix Factorization
SSA	Sea Salt Aerosol
TDS	Total Dissolved Solids
WHO	World Health Organization
WS	Wind Speed
WD	Wind Direction
SE	South East
SSE	South South East
SW	South West
SSW	South South West

1. INTRODUCTION

Byzanz, Constantinople, Istanbul- capital of three past empires - is currently the most populous city of Turkey and one of the largest megacities worldwide. In recent decades, Istanbul has undergone rapid population growth, from 2 million in 1970 to 15.1 million in 2018, leading to extensive urbanization, and consequently, high levels of air pollution (Koçak et al., 2011; Im, 2009). Air pollution, which is one of the leading environmental problems facing Turkey, originates primarily from low-quality fuel usage, low quality burning devices, insufficient combustion technology applications and traffic-derived emissions. In megacities like Istanbul, urban air pollution is considered as one of the world's major environmental challenges, due to its direct effects on public health and the environment (Koçak et al., 2011; Demir et al., 2010). Figure 1.1 shows the potential impact of air pollution exposure on human health which can range from minor effects that require no health care up to serious effects necessitating hospitalization and that may ultimately lead to increased mortality rates. Recent studies estimate that about 9 million premature deaths worldwide are due to exposure to pollution; of these 9 million about 6.5 million are due to air pollution alone (Lancet, 2018). Most of these health effects are concentrated in urban areas, especially in countries that have undergone rapid industrialization.

Air pollution in urban environment has been known for decades. Notwithstanding, endeavors to deal with it were insufficient and unsystematic. In fact, urban air pollution was considered in the early 20th century as a sign of power and development in the industrialized world. Thenceforward worldwide energy consumption and population in urban areas have increased by more than a factor 5 and 4, respectively and the number of cars has increased by nearly 10 times compared to 50 years ago (Cohen et al., 2004).

Recent research has shown that air pollution in the form of airborne particles can lead to numerous health problems. High levels of particulate matter (PM) can lead to a broad range of diseases such as asthma, altered cardiac, systemic inflammation, accelerated atherosclerosis, lung cancer, reduction of heart rate variability, and thrombosis (Im, 2009; Demir et al., 2010; Kabatas et al., 2014; Rizza et al., 2017). Individuals with existing health problems, children and elderly people are most influenced by exposure to PM. High PM levels can ultimately lead to increased mortality. According to Hernández-Escamilla et al. (2015), the rate of exposure to PM and its adverse health effects are directly proportional to each other. Dangerous consequences of exposure to high levels of urban air pollution have been understood since the mid-20th century, by the time of notorious cases of the urban air pollution history such as the 1952 Great Smog of London and 1948 Donora Smog (Cohen et al.,2004). According to the 5/12/2012 dated Guardian newspaper, the estimated mortality rate for the Great Smog of London was more than 4000 in 4 days.

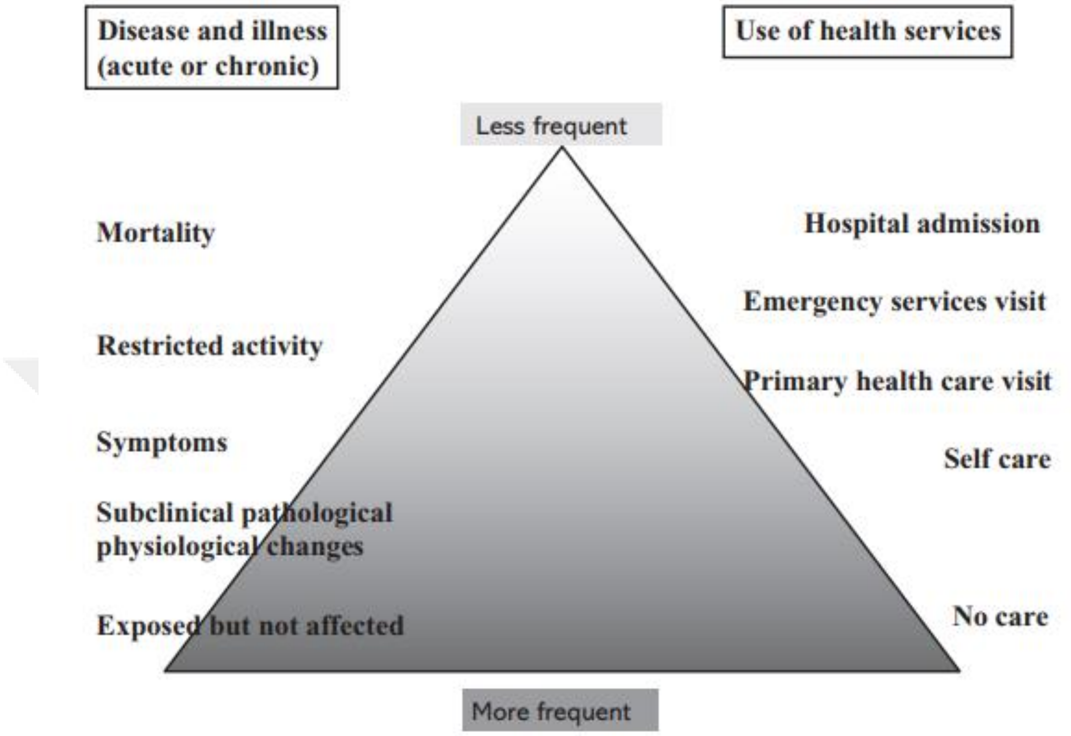

Figure 1.1. Relative frequencies of health events associated with exposure to air pollution (adapted from Cohen et al., 2004).

Capraz et al., (2016) examined the relation between daily changes of air pollutants (PM_{10}, SO_2, and NO_2) and mortality in Istanbul for a 6-year period (2007-2012). Results of the study show that short-term exposure to air pollution was related to increased cardiovascular, respiratory and total non-accidental mortality in the city of Istanbul during 2007-2012. Besides the health effects of PM, it has been reported that PM can influence climatic conditions and the environment through scattering and absorbing of shortwave solar radiation (Kabatas et al., 2014).

In urban areas particularly, PM originating from vehicular traffic is a major air pollutant especially for people who live near congested roadways or highways. Emissions caused by motor vehicles are major sources of fine fraction of PM ($PM_{2.5}$ and PM_{10}). Moreover, exhaust emissions from tailpipes and particles from tires, brakes, clutches, etc. are a significant contributor to road transport pollution (Manousakas et al., 2019). In addition to local sources, by virtue of the long residence times in the atmosphere, the fine fractions of PM can be transported over long distances

(Koçak et al., 2011; Demir et al., 2010). As a result, population living in much larger areas can be affected by road transport pollution (Manousakas et al., 2019).

In addition to urban areas, natural and agricultural areas are in danger due to urbanization. In this century, semi urban areas have become rapidly industrialized, also. Urbanization has a big impact on decrease in biodiversity and changes in habitat structure in semi-urban areas. (Hosokawa et al., 2019) Especially poor air quality, among the types of environmental problems, is most challenging. Due to its influence on ecosystem, agriculture, global climate and human health. Air pollution has become the biggest problem by the reason of the rapid industrialization in semi-urban and urban areas (Ghosh et al., 2018).

In addition to anthropogenic sources, there is a vast number of natural sources of PM such as release of particles from seas and oceans (sea spray aerosols), suspension of particles from soil such as windblown dust particles, secondary formation in the atmosphere from gases, wild land fire particles (fires from natural cause) and volcanoes (Demir et al., 2010, Hernández-Escamilla et al., 2015, EEA, 2012).

Atmospheric PM comprises of varied elements and substances including sulphates, nitrates, ammonium, organic compounds, marine salts, soil elements and heavy metals-which can be toxic even at very low concentrations (Demir et al.,2010). Silicate minerals and carbonates are generally the main component of windblown dust while NaCl is a major fraction of sea spray. Moreover, during a volcanic eruption, SO_2 is the major gas emitted which also promotes the formation of secondary PM. During wild land fires, large amounts of fine PM are emitted (EEA, 2012). Besides their direct impacts on human health, PM can also adsorb heavy metals after a prolonged exposure which can further threaten the environment due to their non-degradable nature. Heavy metals can also significantly increase human health problems such as, cardiovascular diseases and cancer (Demir et al., 2010, Qian et al., 2014)

Since publishing of the British Clean Air Act in 1956, awareness of negative health and environmental effects of particulate matter increased (Saliba et al., 2010). After becoming a public concern, PM limitations have been set all around the world. EU regulations limit annual and daily PM_{10} levels to 40µg/m^3 and 50 µg/m^3, respectively, and annual $PM_{2.5}$ has been limited to 17 µg/m^3 (Directive, 2008/50/EC of the European Parliament and the Council of 21 May 2008 on ambient air quality and cleaner Europe). In the US, the Environmental Protection Agency (EPA) published a "Criteria Document" in 1969 relating to air pollution, which was followed by the Clean Air Act in

1970 and subsequently the first National Ambient Air Quality Standards (NAAQS) was published. (Saliba et al., 2010). The National Ambient Air Quality Standards (40 CFR part 50) defined by EPA sets strict limits for major air pollutants such as CO, Pb, NO_2, O_3, PM, and SO_2. After the last revision of NAAQS for PM in 2012, annual $PM_{2.5}$ was limited to 12 $\mu g/m^3$, daily $PM_{2.5}$ retained at 35 $\mu g/m^3$, while annual and daily limits of PM_{10} were retained at 50 $\mu g/m^3$ and 150 $\mu g/m^3$, respectively (EPA, 2017).

In Turkey, PM limits have been defined in the document 'Air Quality Assessment and Management Directive' dated. Additionally, there have been other directives related to air quality such as the 07.02.2009 'Heating Based Air Pollution Control Directive' and the 03.07.2009 'Industrial Based Air Pollution Control Directive'. These regulations gradually decreased air quality limits for major pollutants. For particulate matter the standards were set to decrease annually until they are in line with EU and WHO standard by 1/1/2019 (TMMOB CMO Air Pollution Report, 2017, Air Quality Assessment and Management Directive, 2008).

2. LITERATURE SURVEY

2.1. Origin of Particulate Matter

PM emitted into the atmosphere can lead to various environmental problems such as air quality degradation, climate change, stratospheric ozone depletion, and human and ecosystem exposure to hazardous substances. To assess the overall impacts of PM it is important to quantify these emissions and their chemical profiles, their source apportionments, and seasonal variations (Im, 2009). PM emissions, derived from anthropogenic and natural sources on a global basis, are given in Table 2.1.

Studies have shown that major natural sources of PM include volcanic activities, soil and rock debris, combustion of biomass, sea spray, and reactions between natural gaseous emissions (Seinfeld et al., 2006). Anthropogenic sources of PM are commonly distinguished into four categories; fuel combustion, industrial processes, nonindustrial fugitive sources (roadway dust from paved and unpaved roads, wind erosion of cropland, construction, etc.), and transportation sources (automobiles, etc.). Numerous studies have focuses on evaluating the contributions of PM to air pollution in urban areas (e.g., Tao et al., 2017; Rizza et al., 2017; Diapouli et al., 2017).

These studies have generally identified different anthropogenic emissions that are the main contributors of low air quality. Other factors influencing air pollution include topography, economic structure of the urban area and its meteorological & climatic conditions. Guclu et al. (2019) combined innovative tend diagram (ITD) with air quality index (AQI) classification to evaluate compliance with USEPA health status. Esenler and Besiktas stations on the European side, and Kadikoy and Umraniye stations on the Asian side of the Istanbul megacity were used in the proposed methodology. PM_{10}, CO, SO_2, NO_2 were selected air pollutants for the monitoring. According to results of study, air quality of Esenler zone was noticeably different from the other stations due to the spread of natural gas services and fuel quality improvements.

Table 2.1. Global Emission Estimates for Major Aerosol Classes (adapted from Seinfeld et al., 2006).

Source	Estimated Flux, Tg yr^{-1}
Natural	
Primary	
Mineral Dust	
0.1-1.0 µm	48
0.1-10.0 µm	190
Seasalt	10,100
Volcanic Dust	30
Biological debris	50
Secondary	
Sulfates from DMS	12.4
Sulfates from volcanic SO$_2$	20
Organic aerosol from biogenic VOC	11.2
Anthropogenic	
Primary	
Industrial dust (except black carbon)	100
Black carbon	12^a
Organic aerosol	81^a
Secondary	
Sulfates from SO$_2$	48.6^b
Nitrates from NO$_x$	21.3^c

* a=Tg C, b=Tg S, c=Tg NO$_3$ (Tg is 10^{12} grams)

Diapouli et al. (2017) reported that domestic heating, biomass (wood) burning and exhaust & non-exhaust emissions from traffic are major sources of PM in Athens and Thessaloniki, Greece. In a recent study focusing on PM pollution in the city of Cassino, Italy, it was shown that PM originating from traffic vary significantly depending on the hour of the day, day of the week, and on meteorological conditions. Ozdemir et al., (2014) measured Black Carbon (BC)-which is a significant component of the PM, and PM$_{2.5}$ concentrations characterized by diversified traffic densities in Istanbul. The obtained results from the study show that annually averaged BC contributes the PM$_{2.5}$

levels and diurnal changes of BC concentrations followed those of traffic density (correlation coefficient of 0.87).

Table 2.2. General Descriptions of Primary and Secondary PM Emissions and Sources (adapted from Narsto, 2006).

Emissions	Source Types
Primary	Primary
Crustal/Soil Dust/Road Dust	Paved/unpaved roads, vehicle tire and brake wear, construction, agricultural and forestry operations, and high wind events.
Salt (NaCl)	Oceans, road salt and salt pans / dry lake beds
Biogenic material	Pollen, spores and plant waxes
Metals	Industrial processes and transportation
Black carbon	Fossil-fuel combustion (especially diesel engines)
Secondary	Secondary
Sulfur dioxide (forming sulfate particles)	Electrical utilities, transportation, mining and smelting, and industrial processes.
Ammonia (contributing to formation of ammonium sulfate and ammonium nitrate)	Agriculture and animal husbandry, with minimal contributions from transportation and industrial processes.
Nitrogen oxides (forming ammonium nitrate with ammonia)	All types of fossil-fuel combustion, and to a minor degree microbial processes in soils.

Tao et al. (2017) reported that ship emissions in south China are a major source of PM in the atmosphere. According to Li et al. (2019) meteorological factors are critical in determining both areal and temporal changes in PM pollution levels. Results of the study indicate that, PM concentrations were negatively correlated with precipitation, relative humidity, air temperature, and windspeed but were positively correlated with surface pressure. Duration of sunshine showed negative and positive impacts on PM in northern and southern cities of China, respectively. Uygur et al. (2013) investigated the contribution of different natural and anthropogenic sources of PM along the coast of Marmara

Sea and reported that, besides traffic and regional industries, the sea and earth crust are also main contributors of PM to the atmosphere.

A vast number of diversified origin types, meteorological and geographical effects generate a wide dynamic range of seasonal and diurnal differentiates in PM mass concentration and composition. Table 2.2 explains the source types of primary and secondary PM. Primary particles are directly emitted to the atmosphere. They can be either in coarse form or fine form. Secondary particles are generated in the atmosphere via condensation/deposition of gaseous precursors (Narsto,2006). As depicted in Figure 2.1, PM composition is correlated with PM size. According to Narsto (2006), the fine fraction of PM consists of metals, SO_4, NO_3, NH_4, and numerous kinds of organic carbon compounds. On the other hand, the coarser fraction includes suspended dust, construction debris, grinding processes.

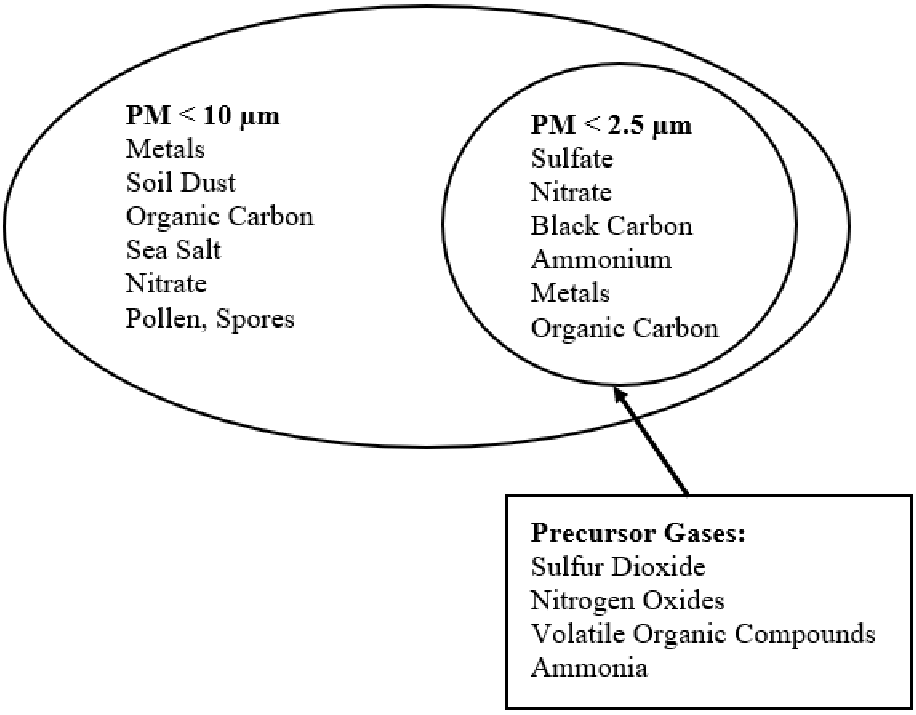

Figure 2.1. General Composition of PM. (from Narsto, 2006).

2.2. Chemical Composition and Size Distribution of PM

Several studies have examined the chemical composition of PM in Istanbul and the regions from which these PM levels originated such as the Balkans, Eastern Europe, Western Europe. Koçak et al. (2011) reported that the origin of 80% of the PM_{10} matter mass in the region is anthropogenic. The results were determined by conducting a source apportionment analysis using the Positive Matrix

Factorization (PMF) method. In addition, crustal soils and sea salt aerosols (SSA) contribute 10.2 and 7.5% of the particulate matter mass, respectively. Chemical composition of PM_{10} samples collected in Istanbul between November 2007 and June 2009 indicated that refuse incineration, solid fuel and traffic sources are major contributors of PM especially in winter. Emissions in Istanbul and local meteorology conditions can also have a large influence on circulation patterns of the particles originating within the city as well as from remote locations. Koçak et al. (2011) collected data from Boğaziçi University, Istanbul and compared thier findings with data obtained from the Istanbul Greater Municipality Air Quality Network (IGMAQN) at 9 urban and street-canyon stations across Istanbul (Aksaray, Alibeykoy, Besiktas, Esenler, Kartal, Sariyer, Umraniye, Uskudar and Yenibosna). Im et al. (2010) reported that high wintertime air quality in Istanbul is affected by lack of control strategies on primary particulate emissions and emissions emanating from local sources.

The size and composition distribution of urban aerosols or particulate matter is shown in Figure 2.2. The vertical axis of the figure depicts the change in concentration with diameter; a high value indicates that atmospheric concentrations at that diameter are relatively high. Atmospheric aerosol particles include hydrogen ions, nitrates, ammonium, organic material, sea salt, crustal species, metal oxides, sulphates, and water. Distinct size distributions are generally observed ranging from about 0.1 to 10 µm. Sulphate, ammonium, organic and elemental carbon, and transition metals can occur as finer particles with diameter smaller 1 µm. The coarser fraction includes crustal materials, including magnesium, aluminum, silicon, calcium, and iron, and biogenic organic particles (Seinfeld et al., 2006).

Marine aerosols are defined as sea salt aerosol (SSA) emissions and their reaction products with local air pollutants at coastal regions (Saliba et al., 2010). SSA is a significant constituent of aerosols due to the various heterogeneous reactions that can occur. SSA are derived by the action of waves breaking in the surf zone, which covers an area of about 25 to 50 m from the coastline, leading to bubbles bursting during whitecap formation. It is an important category of PM that should be generally considering in air quality studies, particularly in coastal areas. Specifically, SSA leads to increase in the PM levels in the coastal areas and influences atmospheric chemistry such as enhancement of nitrate formation (Im, 2013). SSA plays an important role in the formation atmospheric nitric acid (HNO_3) and sulfuric acid (H_2SO_4).

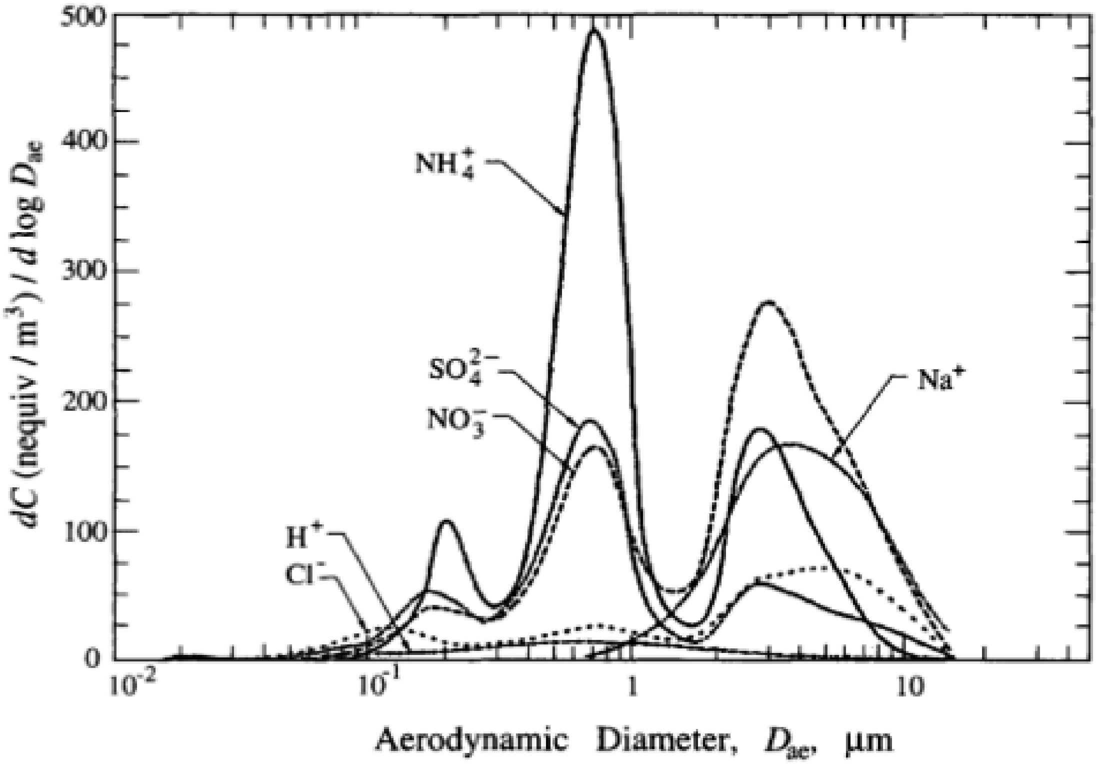

Figure 2.2. Measured size distributions of aerosols. (from Seinfeld et al., 2006).

Pérez et al. (2010) investigated atmospheric aerosols present at sea by measuring hourly PM_{10}, $PM_{2.5}$, and PM_1 concentrations. The data were also used to identify the chemical composition and the contributions of PM from crustal particles, sea spray, total carbon, and secondary inorganic aerosols. The course of the Oceanic II (The Scholar Ship) used for data collection in spring of 2008 was from the equatorial Atlantic to the Straits of Gibraltar, across the Mediterranean to Istanbul, and back via Lisbon to the English Channel. The study reported that clean air (PM_{10} <10μg m^{-3}) was gradually polluted as land is approached. Moreover, dust emissions from North Africa, biomass burning in sub-Saharan Africa and Russia, emissions transported from Europe, sea spray during rough seas, and plumes permeating from islands and industrial sulphate clouds were major sources of atmospheric pollution.

Im (2013) reported that SSA can be a major contributor of particulate matter. Surf zones could cause 10 times higher SSA in coastal areas, which could change the particulate matter levels and composition (Im, 2013). Demir et al. (2010) investigated trace metal concentrations on particulate matter samples at 3 different playgrounds' soil in İstanbul. Selected vicinities were Beşiktaş, Kabataş and Okmeydanı, and the sampling period was between March – April in 2009 (Demir et al., 2010). They reported that particulate matter deposition led to high heavy metal pollution in surface soil. The study revealed that soil and dust in playgrounds may contribute to heavy metal toxicity for children.

Additionally, Markakis et al. (2012) reported that that road traffic is a major origin of the CO, NMVOCs (Non-methane volatile organic compounds), NOx as well as PM pollution. The study was compiled for the area of Greater Istanbul on 2 km horizontal resolution consisting of 16 speciated gaseous/ particulate pollutants and 23 speciated NMVOCs.

Table 2.3. Concentrations (ng/m^3) and Size Distribution of Various Elements Found in Atmospheric Particles (adapted from Seinfeld et al., 2006).

Element	Mode*	Concentration (ng m^{-3})		
		Remote	Rural	Urban
Fe	F&C	0.6-4,200	55-14,500	130-13,800
Pb	F	0.01-65	2-1,700	30-90,000
Zn	F	0.03-450	10-400	15-8,000
Cd	F	0.01-1	0.4-1,000	0.2-7,000
As	F	0.01-2	1-28	2-2,500
V	F&C	0.01-15	3-100	1-1,500
Cu	F&C	0.03-15	3-300	3-5,000
Mn	F&C	0.01-15	4-100	4-500
Hg	_	0.01-1	0.05-160	1-500
Ni	F&C	0.01-60	1-80	1-300
Sb	F	0-1	0.5-7	0.5-150
Cr	F&C	0.01-10	1-50	2-150
Co	F&C	0-1	0.1-10	0.2-100
Se	F&C	0.01-0.2	0.01-30	0.2-3

*F= fine mode; C= coarse mode.

Composition data indicates that, as much as 40 trace metals can be found in atmospheric particulate matters. Table 2.3 summarizes the concentrations of these heavy metals. The origins of these elements were reported to be waste incineration, combustion of coal, oil, steel furnaces, boilers, smelters, dust, wood burning, etc. (Seinfeld et al., 2006). The impact of size on composition and chemical properties of particulate matter are summarized in Table 2.4.

Table 0.1. Comparison of Ambient Fine and Coarse Particles (from Seinfeld et al., 2006).

	Fine Particles	Coarse Particles
Formation Pathways	Chemical Reactions	Mechanical disruption
	Nucleation	Suspension of dusts
	Condensation	
	Cloud/fog processing	
Composition	Sulfate	Resuspended dust
	Nitrate	Coal and oil fly ash
	Ammonium	Crustal element
	Hydrogen ion	CaCO3, NaCl
	Organic compounds	Pollen animal debris
	Water	Tire wear debris
	Metals	
Solubility	Largely soluble, hygroscopic	Largely insoluble, non-hygroscopic
Sources	Combustion (coal, oil, diesel, etc.)	Resuspension of industrial dust and soil
	Smelters, mills, etc.	Suspension of soil
		Biological sources
		Construction/demolition
		Ocean spray
Atmospheric Lifetime	Days to weeks	Minutes to days
Travel Distance	100s to 1000s of km	< to 10s of km

2.3. PM Studies in Istanbul

Particulate matter compositions and concentrations vary greatly on temporal and spatial scales. PM concentrations generally peak in urban areas. Baykara et al. (2019) developed an up to date spatially distributed high-resolution emissions inventory based on local activity data and air quality simulations. The data are managed through the open-source project: Community Multiscale Air Quality Modeling System (CMAQ), version 5.2. Results of the study showed that accounting for high-resolution emissions of the residential heating sector in CMAQ significantly improves the spatial distribution and concentration of air pollutants (SO_2, PM_{10}, $PM_{2.5}$) for Istanbul especially in wintertime.

Figure 2.3 illustrates the transport range of various particulate matter and their residence times. Generally, the finer particulate matter stays longer in the atmosphere and are transported over greater distances. Kindap et al. (2006) noted that numerous studies have examined the transport of air pollutants in Europe but transport of air pollutants from Europe to Northern and Western parts of Turkey has not been studied adequately. To address this gap in the literature, the authors analyzed the contribution of long-range aerosol transport to air pollution in Istanbul. Meteorological and air quality modelling were used in this study. Based on the model simulations, it was reported that long range transboundary transport sources may be responsible for about 50% of the background PM_{10} in Istanbul.

Flores et al. (2017) investigated the impact of the dust transport on PM_{10} concentrations for the period of 2007-2014 in Aksaray, Istanbul. The Dust Regional Atmospheric Model (DREAM8b) was used to estimate dust loading in Istanbul. It was reported that PM_{10} concentrations exceeded the air quality standard of $50 \mu g/m^3$, 50% of the time, 40-60% of the dust loading occurred during the spring and, and that desert and non-desert dust sources contribute to 22-72% and 48-81%, respectively of the ground level PM_{10} concentrations in Aksaray. Results also showed that air masses arriving to Istanbul at 500 m elevation are divided into northern (52%) and southern (48%) components and hence PM_{10} level may be increased by long-range transport from the African Desert, Asian Desert, Arabian Peninsula, Russia, and Ukraine.

Kindap (2008) researched the NO_2 and SO_2 levels in Istanbul during a specific winter episode. The computer code MM5 was used for meteorological modelling while CMAQ was used to model atmospheric transport and chemistry. The modeling also incorporated tracer and trajectory investigations over the area of interest. Obtained results show that transboundary sources are an important contributor to the poor air quality of Istanbul as indicated by tracer and trajectory studies.

Theodasi et al. (2010) used factor analysis to identify six sources of aerosol species in PM_{10} in Istanbul during November 2007 to June 2009. Measured main ions were Na, Ca, nss SO_4 (non-sea-salt sulphates). Trace elements associated with anthropogenic sources (such as Pb, V, Cd and Ni) peaked in wintertime due to domestic heating. On the other hand, elements from natural sources (such as Al, Fe and Mn) peaked in the spring period due to dust transport from Northern Africa.

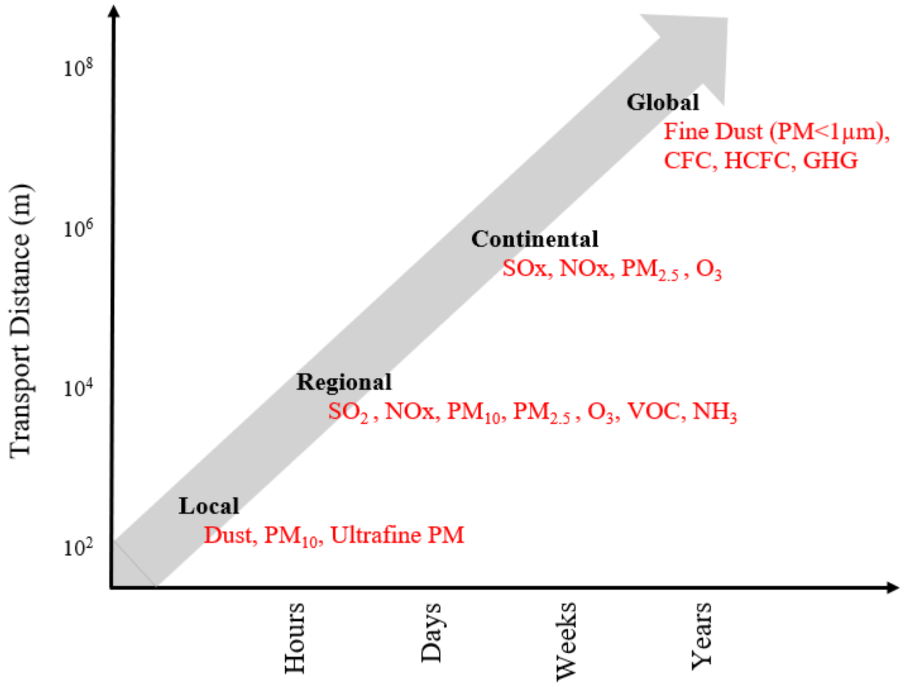

Figure 2.3. Illustration of Transport Scales of PM and other Atmospheric Pollutants (from Narsto, 2006).

Review of the literature clearly shows that particulate matter is a major source of pollution, particularly in urban areas such as Istanbul. The purpose of this study is to evaluate composition and possible sources of PM at the Saritepe campus of Bogazici University along the Black Sea coast. The Saritepe campus was selected for this study, because it is adjacent to the Black Sea, which is characterized by a highly active surf zone. While a number of studies have focused on PM in coastal areas of the East Mediterranean Sea, the contributions of Black Sea to PM has been less studied. The campus is also close to the forests of north western Istanbul and the newly opened major highway leading to the Yavuz Sultan Selim Bridge that connects the Asian and European sides of Istanbul. Specifically, PM samples were collected from various locations within the campus and at different distances from the coastline. The study extended over a 10 months period to study seasonal variations (summer vs. winter) in PM as well as the sensitivity of PM levels to wind speed and direction. The composition of the collected samples was analyzed and used to identify the contribution of different sources (natural and anthropogenic) to the total PM levels in the area. Meteorological data collected at the campus were used to correlate the PM concentrations and composition with the dominant wind speed and directions. The results of this study can provide important data on PM level in northern Istanbul and their likely sources.

3. MATERIALS AND METHODS

This chapter describes the field work, laboratory analyses and statistical tools uses to evaluate the spatial distribution of PM in the Saritepe Campus, their composition and potential sources.

3.1. Field Work

PM samples were collected from various locations within the campus and at different distances from the coastline. Samples were collected from 10 different locations within the campus for a period of 10 months to evaluate the seasonal variations in PM levels. The locations were selected at different distances from the Black Sea shoreline to assess different emission sources such as road transport, activities in residential area, sea breeze, etc. Sampling started on 21/03/2017 to 20/01/2018. Because meteorological data, such as precipitation, wind speed and wind direction, can have a significant impact on PM, the devices which are used in the study have 4 different section for sampling of PM in four different directions. The sampling points are shown in Figure 3.2 while the measuring devices are shown as Figure 3.3. Photographs of the measuring devices are shown in Figure 3.4. Samples were collected on a monthly basis. Each chamber of the sampling device collected both solids and water, mostly rainfall. A total of 360 samples were collected.

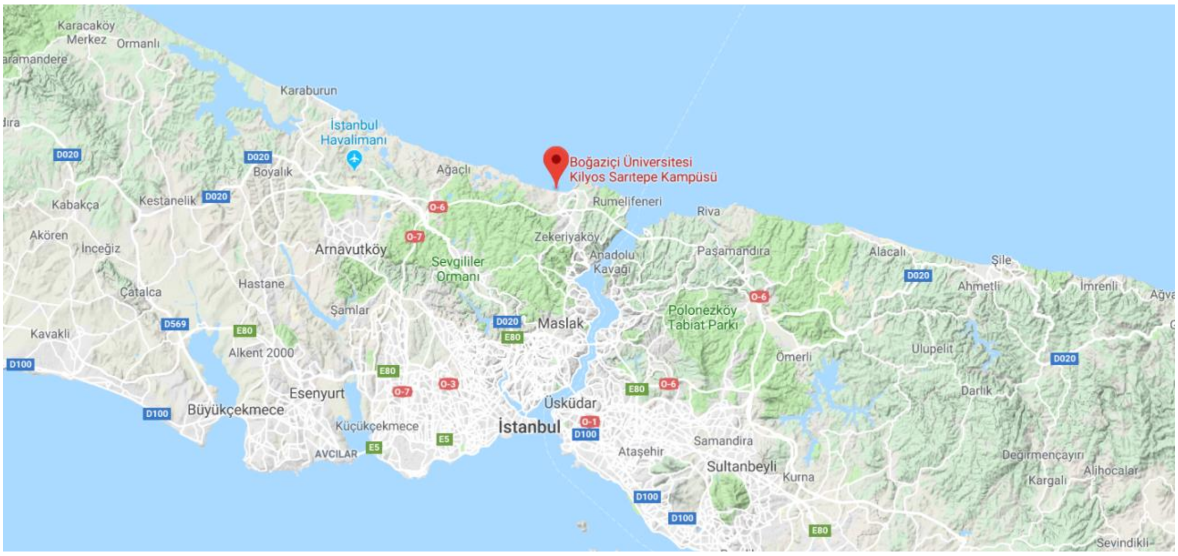

Figure 3.1. Location of Study Area (adapted from Google TerraMetrics, 2019).

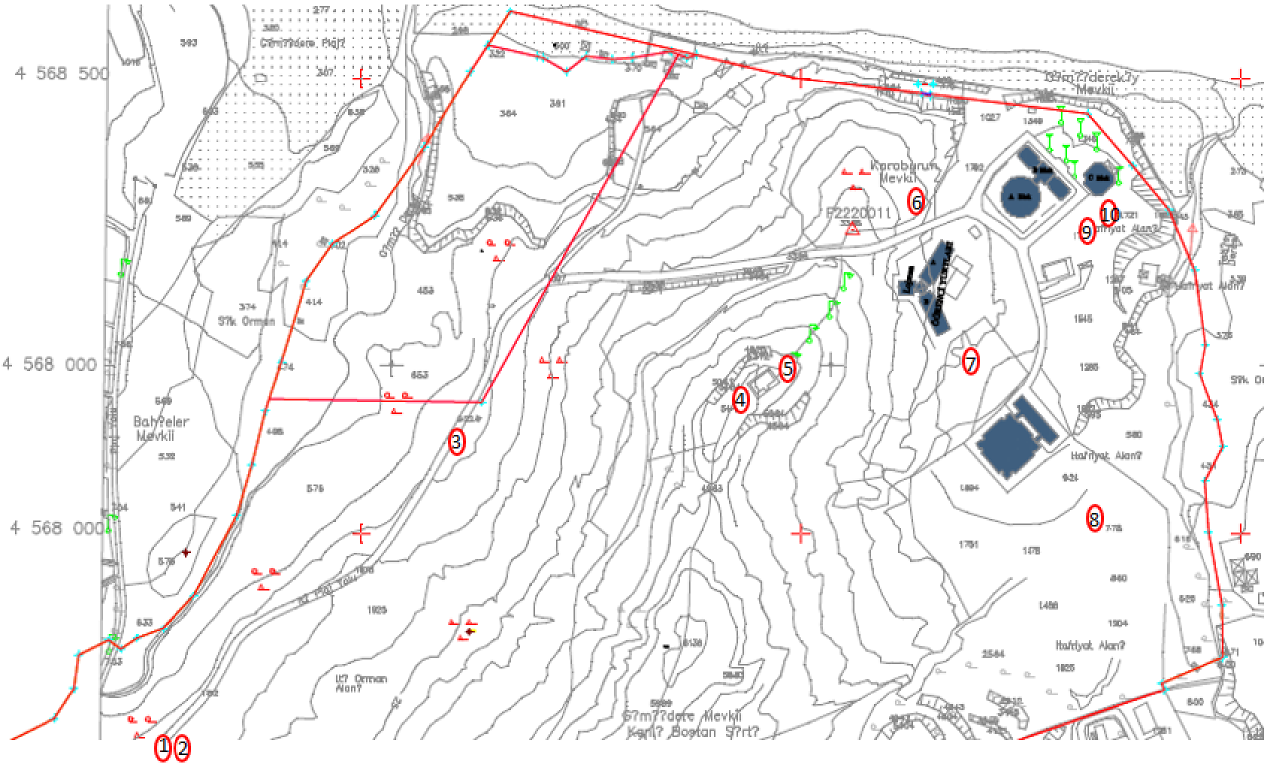

Figure 3.2. Topographic map of the Saritepe campus.

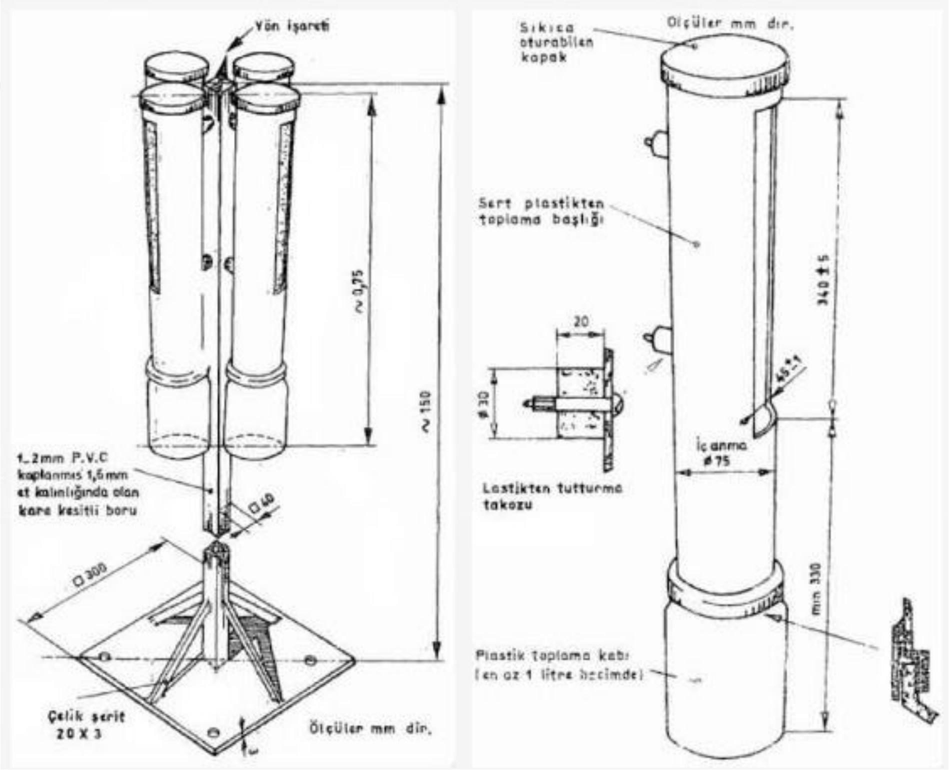

Figure 3.3. Schematic configuration of the devices.

Figure 3.4. Photographs of the sampling devices.

3.2. Laboratory Analysis

The collected samples were transported to the Institute of Environmental Sciences Laboratory at Bogazici University. For each collected sample, the following steps were performed:

Gravitational analysis: According to method TS 2341 and TS 2342, the samples were first oven dried and weighed to estimate the mass of PM collected.

Metal content: After drying, the solid samples were digested according to EPA 3051A and prepared for Inductively Coupled Plasma (ICP) (PerkinElmer Optima 2100DV) analysis-based method of EPA 6010D.

Analysis of aqueous samples: pH, total dissolved solids (TDS) and conductivity levels were measured according to EPA 150.2 and EPA 120.1, respectively. Anions and cations concentrations were measured using Ion Chromatography (IC) (DIONEX ICS-3000) and Atomic Absorption Spectroscopy (AAS) (PerkinElmer Analyst 300) according to EPA 9056A and EPA 7000B, respectively for the determination of fluoride, chloride, nitrite, nitrate, sulphate, phosphate, bromide, sodium, potassium, calcium, magnesium ion concentrations.

The standard methods are described below.

EPA METHOD 3051A: Microwave Assisted Acid Digestion: This technique is engineered to mimic extraction using conventional heating with nitric acid (HNO_3), or, nitric acid and hydrochloric acid (HCl). This method is applicable to the microwave-assisted acid dissolution of sediments, sludges, soils, and oils (USEPA, E., 2007). Combining Microwave Assisted Acid Digestion and Inductively Coupled Plasma has become popular for the analysis of metals in environmental samples including PM. This method provides low detection limits, wide linear dynamic range, multi-element capability, ability to measure isotope ratios and high sample throughput. However, the ICP-OES systems are equipped with liquid sample introduction systems which require the dissolution of solid samples prior to measurements.

Finding the best combination for dissolution is critical for reaching low detection limits (Celo et al., 2010). In this study, reagent combination was 9 ml nitric acid (HNO_3) to 3 ml hydrochloric acid (HCl). This method was used for the determination of trace elements by ICP-OES. The list of metals analyzed is given in Table 3.1.

Table 3.1. List of analyzed elements.

Element	Symbol
Aluminum	Al
Copper	Cu
Iron	Fe
Lead	Pb
Manganese	Mn
Chromium	Cr
Cadmium	Cd
Zinc	Zn
Silicon	Si
Cobalt	Co
Molybdenum	Mo
Nickel	Ni

METHOD 6010D: Inductively Coupled Plasma: The combination of optical emission spectrometry to atomization plasma technique brings forth Inductively Coupled Plasma-Optical Emission Spectrometry (ICP-OES). The ICP-OES is diversified from other techniques via its features as high selectivity and high sensitivity of the detection system. This technique has been used to determine trace elements in aqueous solutions. Argon plasma discharge where analytes are converted to gas-phase atoms, has an important role in this technique. The emitted energy in the form of light at wavelengths are specific for every element. The intensity of the emitted energy is directly related to the concentration (USEPA, E., 2018).

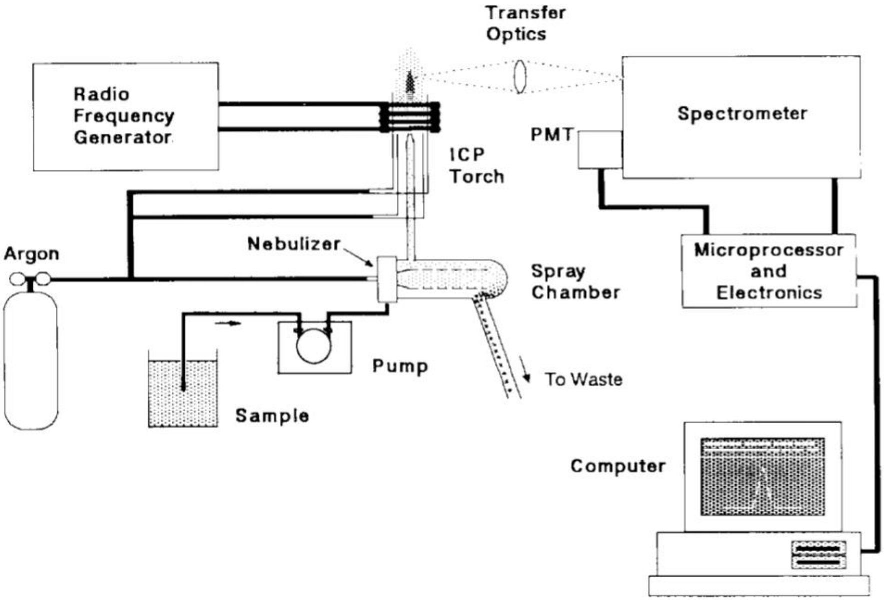

Figure 3.5. Typical Configuration of ICP-OES (from Charles et al., 1997).

METHOD 7000B: Flame Atomic Absorption Spectrophotometry: Except for the analyses for dissolved constituents, all samples require digestion prior to analysis such as filtration and then acidifying (USEPA, E., 2007, Campbell et al., 2014). Flame Atomic Absorption is a prevalent method for analyzing metals. The principle of the method is that metals absorb light at a specific wavelength and after supplying of the light of the correct wavelength, the amount of the light absorbed is measured. This allows the metal ions in samples to be converted to atomic state via the flame. Flame atomic absorption spectroscopy (AAS) was used to detect the concentrations of these four metal cations (Ca^{2+}, Mg^{2+}, Na^{+}, and K^{+}) present in the aqueous samples for this study.

METHOD 9056A: Determination of Inorganic Anions by Ion Chromatography: This technique was used to determine chloride (Cl), fluoride (F), bromide (Br), nitrate (NO_3), nitrite (NO_2), phosphate (PO_4), and sulphate (SO_4) anion concentrations in aqueous samples (USEPA, E., 2007). IC based on an ion-exchange separation has been studied in contrast to a vast number of different kinds of techniques available for determination of inorganic anions (Nagashima et al., 1999).

3.3. Statistical Analysis

In addition to the laboratory analysis, statistical analyses were conducted to evaluate the correlation between the observed concentrations and meteorological and environmental factors. Specifically, the following statistical analyses were performed:

Univariate Analysis: For all collected parameters, the statistical parameters consisting of mean, median, maximum, minimum, standard deviation, skewness, kurtosis and coefficient of variation were computed.

Correlation Analysis: Pearson's correlation coefficient between different parameter pairs were computed. These correlations describe the extent to which two variables are related to each other.

3.4. Source Apportionment

Positive Matrix Factorization (PMF) is a multivariate factor analysis technique used for the chemometric evaluation and modelling of environmental data sets (Comero et al., 2009) such as the air quality data sets. PMF decomposes the data into two matrices: factor profiles and factor contributions. Factor profiles gives the profiles of the sources contributing to the observed data while the factor contributions provide an estimate of the contribution of each source. As such, one can determine the contribution of different sources to the collected data (Norris et al., 2014), thus identifying the main sources of the collected PM for this study, particularly. Compared to the various kinds of available receptor models, PMF is seen as the best option because it is a non-data sensitive technique that can handle non-uniform large data sets without any previous univariate analysis (Comero et al., 2009). A vast number of studies has been used the PMF program. For example, in relation to air quality, Song et al., (2006) investigated the $PM_{2.5}$ levels of Beijing during the period of Jan. to Oct. in 2000, using PMF to be performed source apportionment. The application of the PMF program to the data collected in this study would help in determining the sources and their contribution to the collected particulate matter. Source apportionment was performed using the PMF computer program (EPA The Positive Matrix Factorization 5.0). Model applications consist of 6 steps: (1) model data, (2) base model results, (3) base model DISP (displacement) results, (4) base model boostrap results, (5) base model BS-DISP results, (6) error estimation summary. Each step has further subdivisions. Figure 4.38. shows the PMF result network which depicts the six steps of the model and the corresponding output. One of the most important section of results is ‘Base Model Results’ because it gives the contribution factor fingerprints of each source. Factor fingerprints diagram shows all selected parameters and contributions of factors in one figure which facilitates the understanding of the relations among the different factors. Pie charts show the specific percentages of contributions of sources on parameters one by one. That is significant particularly for the parameters which should be investigated individually such as trace elements.

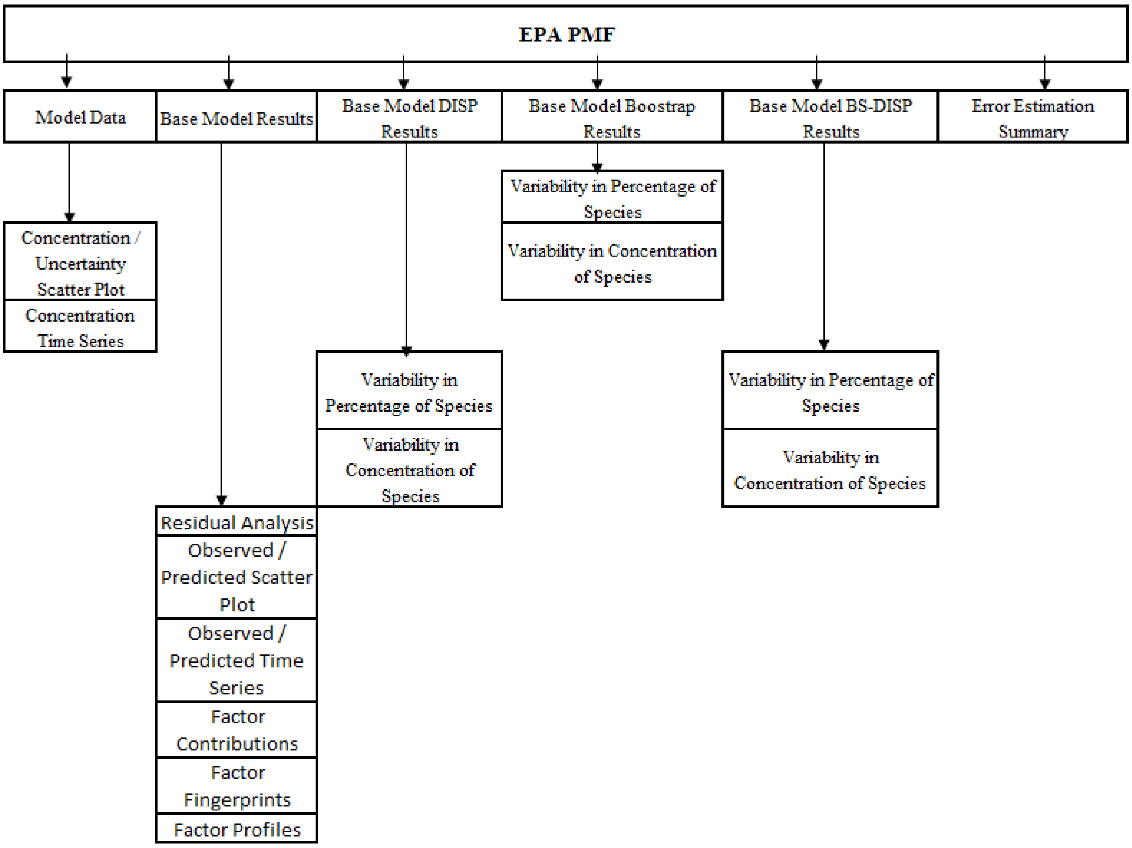

Figure 3.6. PMF result network.

In this study, PMF version 5.0 was applied to both the aqueous phase results and the particulate matter composition data. Seven sets of runs were made with the program. In the first set of runs, data from each sampling point were investigated separately for the 10 months period. In the second set of runs, the sampling points were divided into 4 groups depending on their proximity to the sea. Figure 4.42. shows the grouping of sampling points. The first group consisted of sampling points S1, S2 and S3 which were located closest to the roadway. The second group consisted of sampling points S4 and S5 which were located up the hill at the highest point of study area, near to wind turbine. The third group consisted of sampling points S6, S9 and S10 which were located closest to the sea. The fourth group consisted of sampling points S8 and S7 which were located close to the buildings. In the third set of runs the data were divided into two seasons (summer and winter) to evaluate any seasonal variations in the source apportionment. The summer months consisted of months May to September while the winter months consisted of the rest of months in study period.

4. RESULTS

The main findings of our study are as follows:

The Results Chapter consists of 5 main parts. In the first and the second parts the results of the laboratory analyses are presented. These consist of the analyses of the aqueous samples as well as the particulate particles collected at each sampling point. The third and fourth parts present the meteorological data and statistical analysis which consists of univariate descriptive statistics and correlations of the particulate matter compositional data to each other and to environmental factors. The fifth part of the study presents the source apportionment results using the PMF computer program (EPA Positive Matrix Factorization version 5.0). The data analyzed covers a 10-month period from 21-03-2017 to 20-01-2018.

4.1. Aqueous Phase Results

The accumulated water in the devices (Figure 3.4) were analyzed for the following ions: (i) F^-, Cl^-, NO_2^-, NO_3^-, SO_4^{2-}, PO_4^{3-}, Br^- (determined with IC), and (ii) Mg^{2+}, Ca^{2+}, K^+, Na^+ (determined with AAS).

Figures 4.1 to 4.7 show the monthly anion concentrations for each sampling point. Figures 4.8 to 4.11 show the cation concentration at each sampling point. Figures 4.12-4.14 present the pH, TDS and conductivity values. These data suggest that generally, there is a variation with time. In particular, the ions Cl^-, Br^-, Mg^{2+}, K^+, Na^+ concentrations were highest in the 5th month at the sampling locations S6, S9, S10 which were closest to the sea (Figure 3.2.). The 5th month covers the period from 21.07.2017 to 20.08.2017 and is labeled as August in the tables and figures. These ions are associated with sea water, suggesting that the impact of the sea is greatest close to the coast. TDS and conductivity levels show a similar trend. The rest of the ions such as NO_3^- and Ca^+ show no clear trend with time and location. The source of these ions is likely to be wet deposition through precipitation (Salve et. al., 2008). Since the precipitation is essentially the same at all sampled locations, no clear trend in time or space we observed.

The monthly averages of each ion are given in Table 4.1. Nine out of the eleven parameters analyzed had a maximum value in the 5th month. These ions are F^-, Cl^-, SO_4^{2-}, PO_4^{3-}, Br^-, Mg^{2+}, Ca^{2+}, K^+, Na^+. Highest values of these ions shown in bold in Table 4.1. For comparison purposes, Table

4.2. shows the chemical composition of typical seawater and the chemical composition of rainwater in a coastal environment of India (Gobre et. al., 2010). The results obtained from the current study are also shown in the table. The Cl^-, SO_4^{2-}, Mg^{2+}, Ca^{2+}, Na^+ values of the current study, which are marked in bold in Table 4.2, were higher than the referenced rainwater and seawater. This may be a result of evaporation of the collected water during the 1-month sampling period. Other ions such as Ca^{2+}, K^+, F^- ions fall between the concentration values of seawater and rainwater but closer to rainwater. The pH average of 6.38 is closer to that of rainwater (6.25).

Overall, comparison of aqueous ion content shows that the collected water collected in the sampling devices of the current study appear to be a mix of seawater and mostly rainwater. However, concentrations of Cl^-, SO_4^{2-}, Mg^{2+}, Ca^{2+}, Na^+, NO_3^- ions are greater than literature data, most probably due to evaporation.

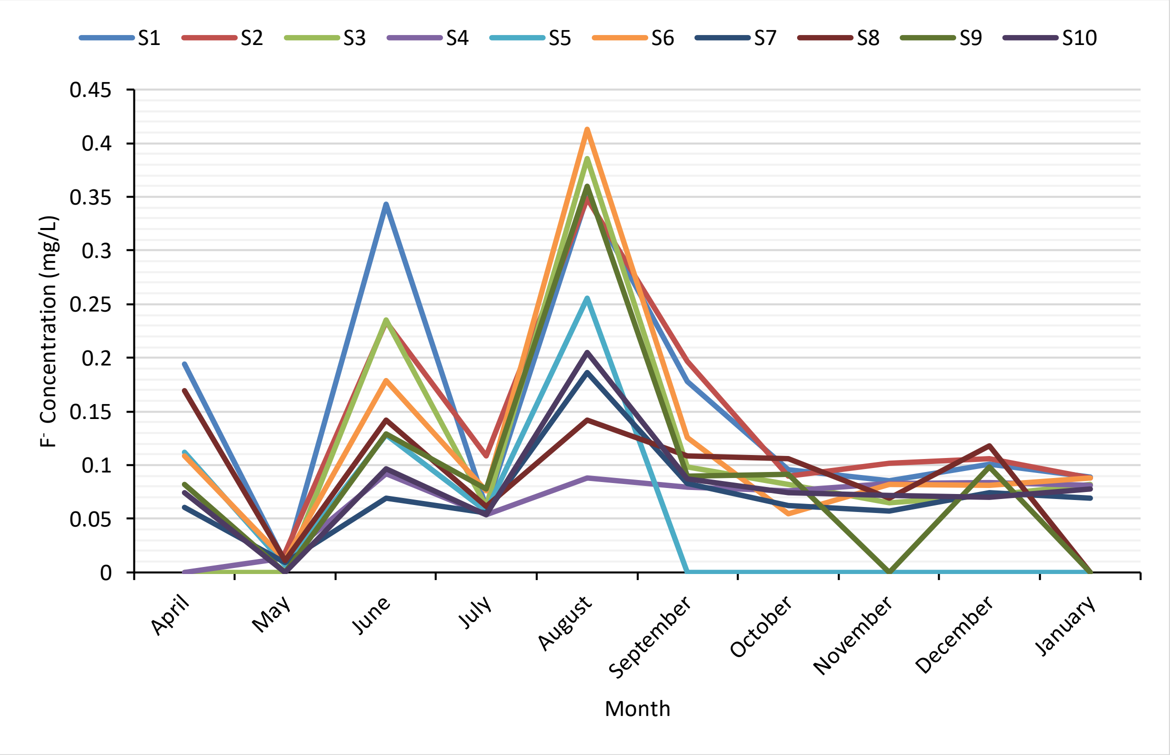

Figure 4.1. F^- concentration (mg/l) over the 10-month sampling period.

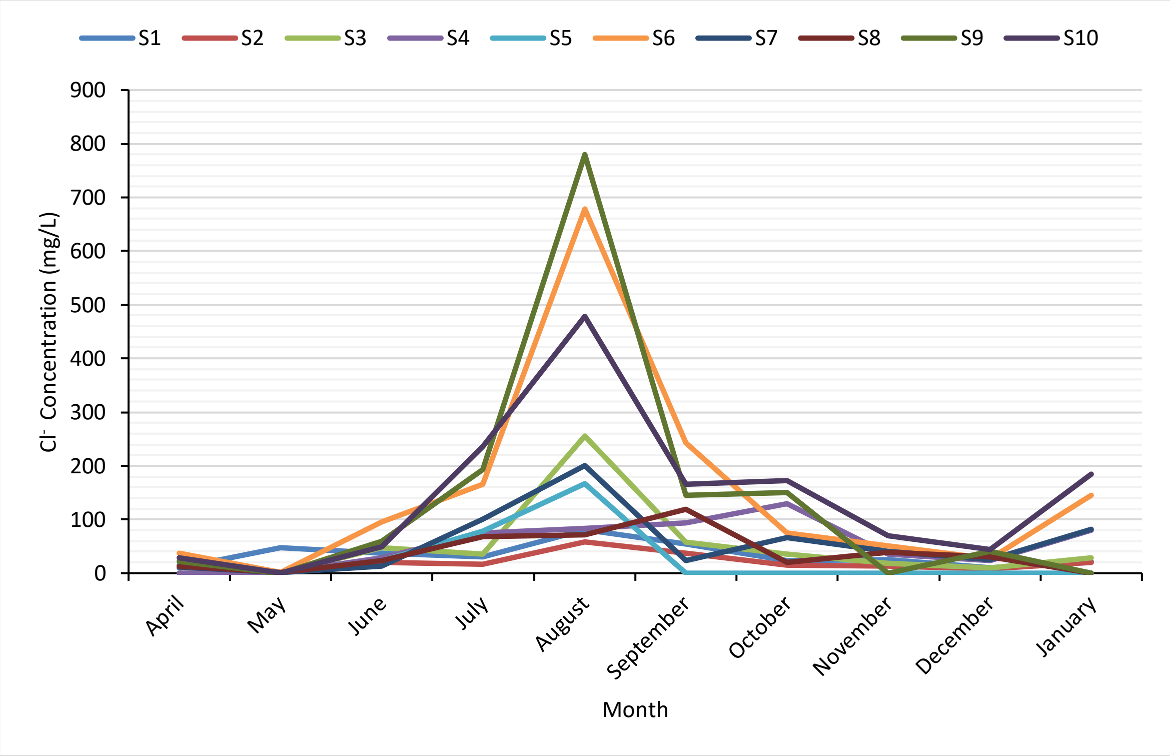

Figure 4.2. Cl^- concentration (mg/l) over the 10-month sampling period.

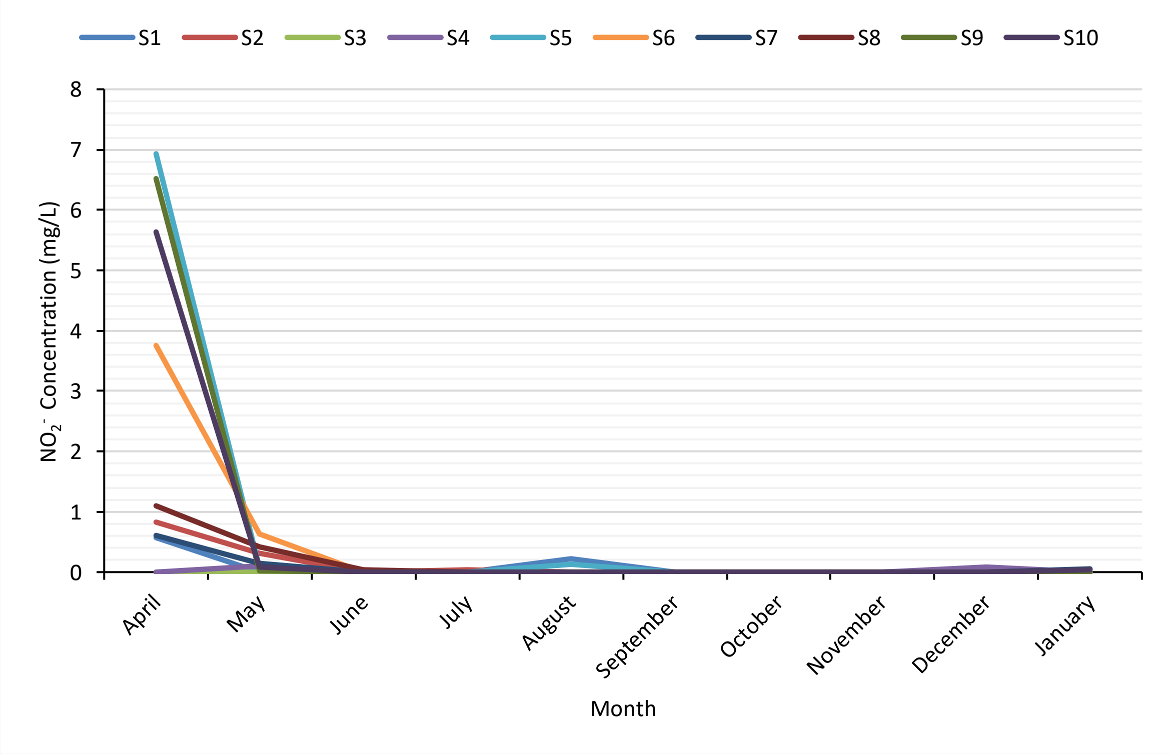

Figure 4.3. NO_2^- concentration (mg/l) over the 10-month sampling period.

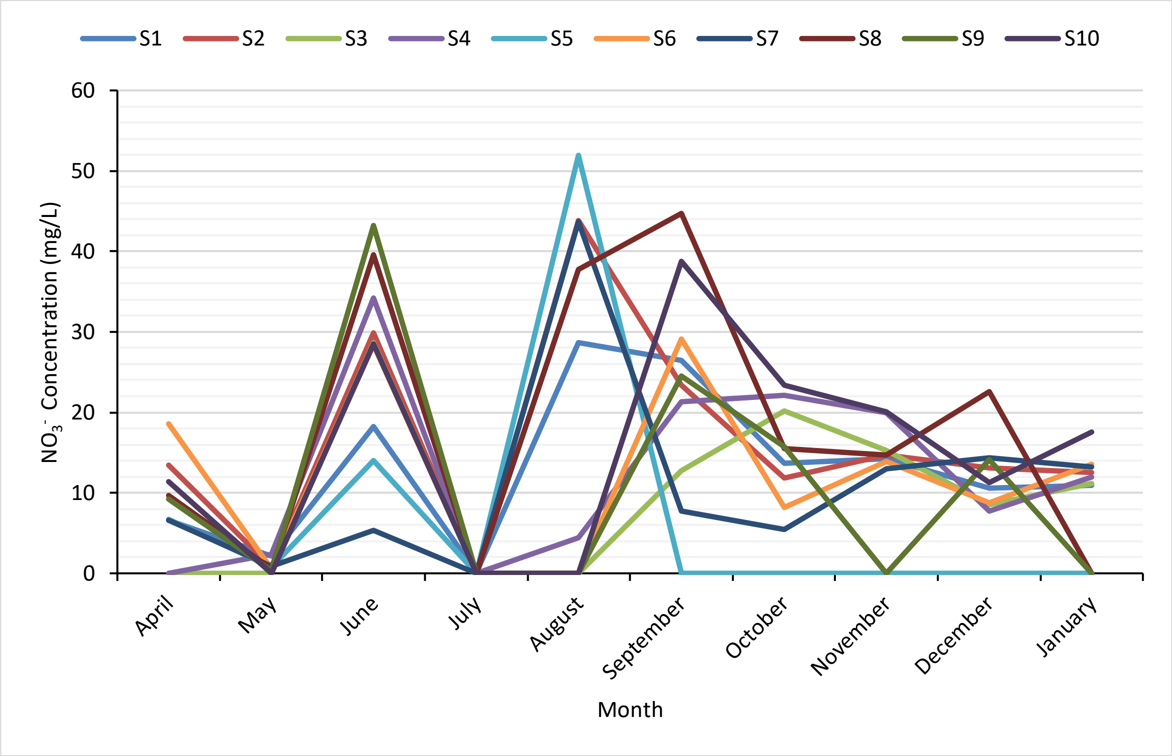

Figure 4.4. NO_3^- concentration (mg/l) over the 10-month sampling period.

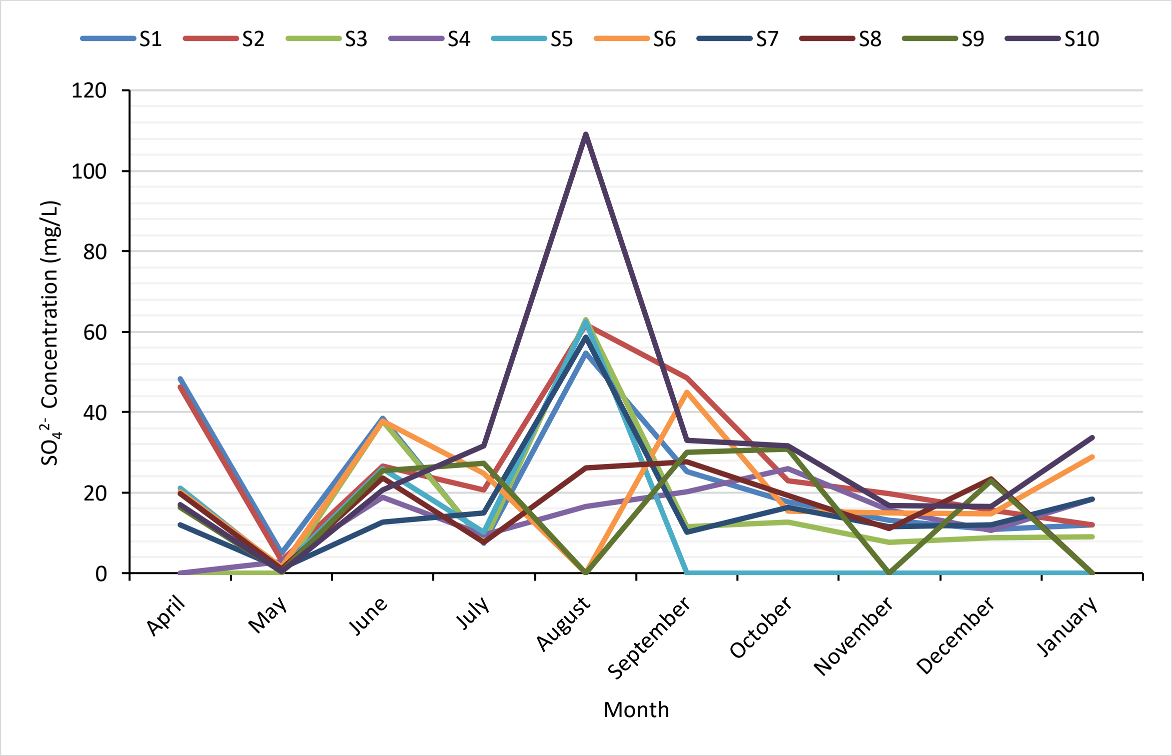

Figure 4.5. SO_4^{2-} concentration (mg/l) over the 10-month sampling period.

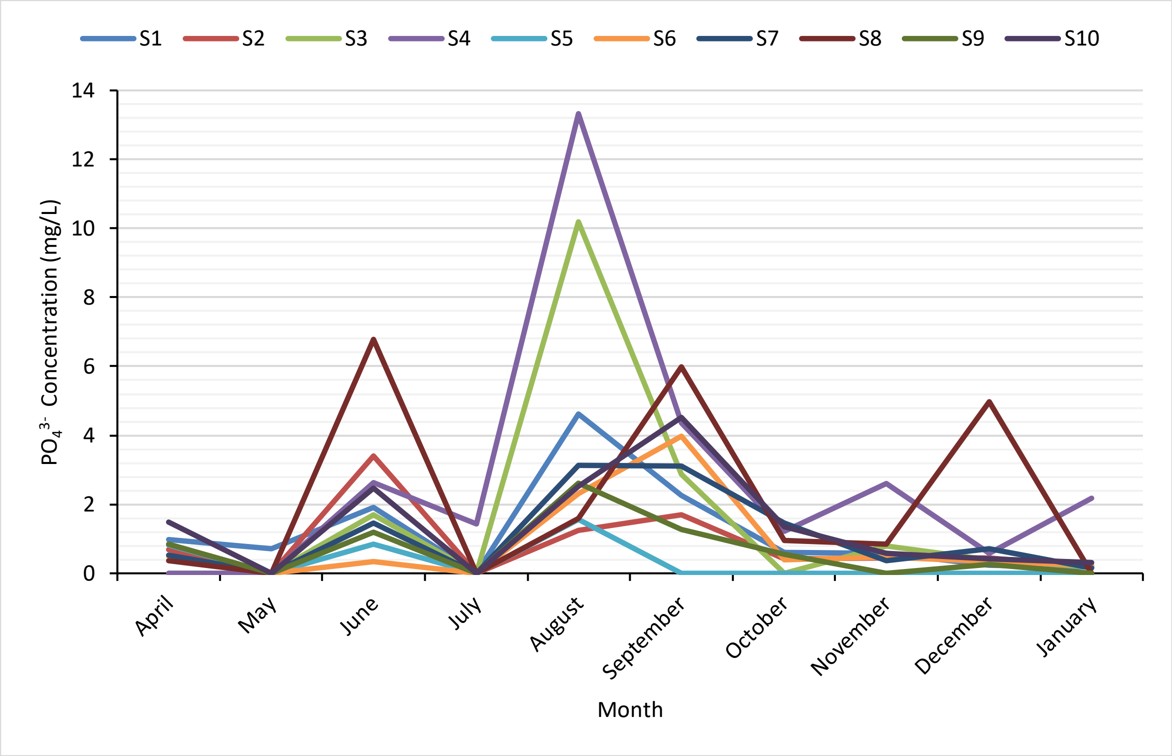

Figure 4.6. PO_4^{3-} concentration (mg/l) over the 10-month sampling period.

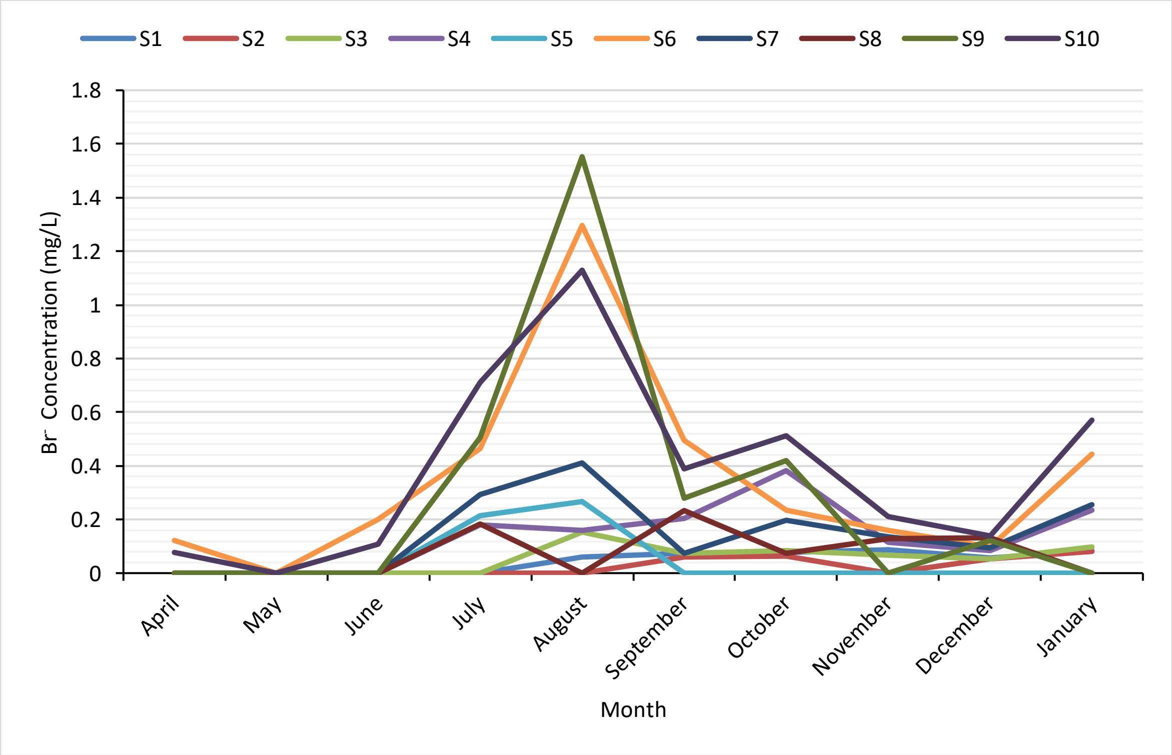

Figure 4.7. Br^- concentration (mg/l) over the 10-month sampling period.

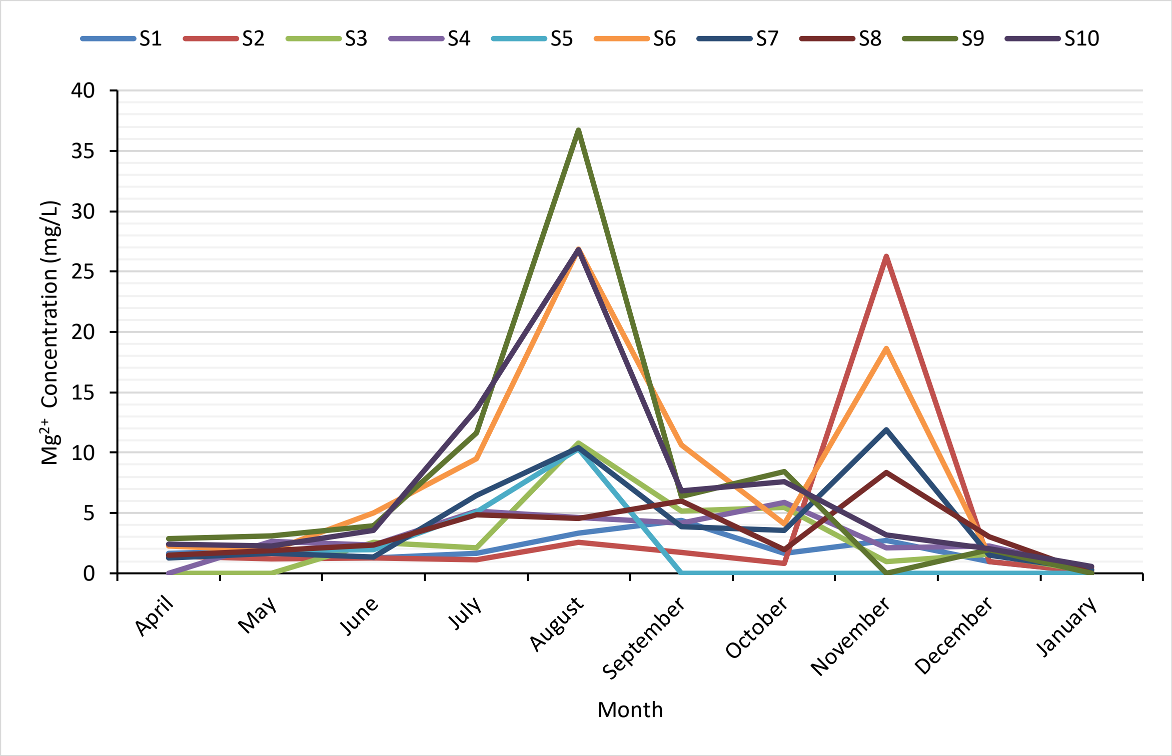

Figure 4.8. Mg^{2+} concentration (mg/l) over the 10-month sampling period.

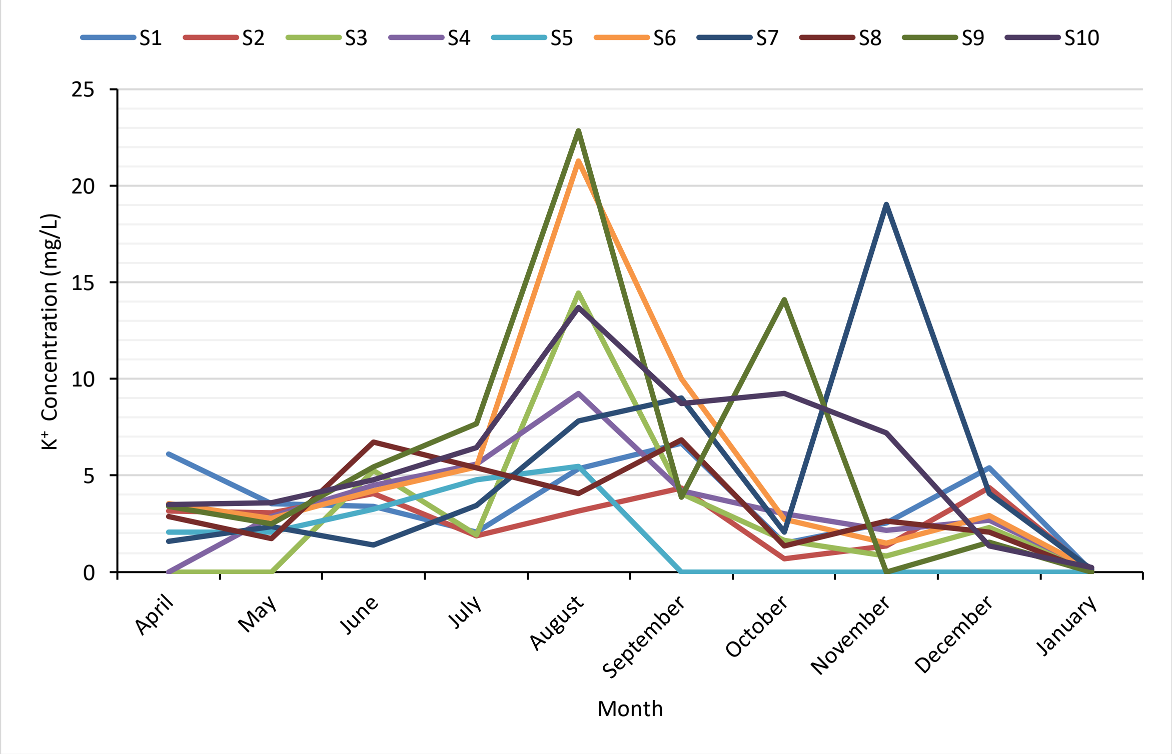

Figure 4.9. K^{+} concentration (mg/l) over the 10-month sampling period.

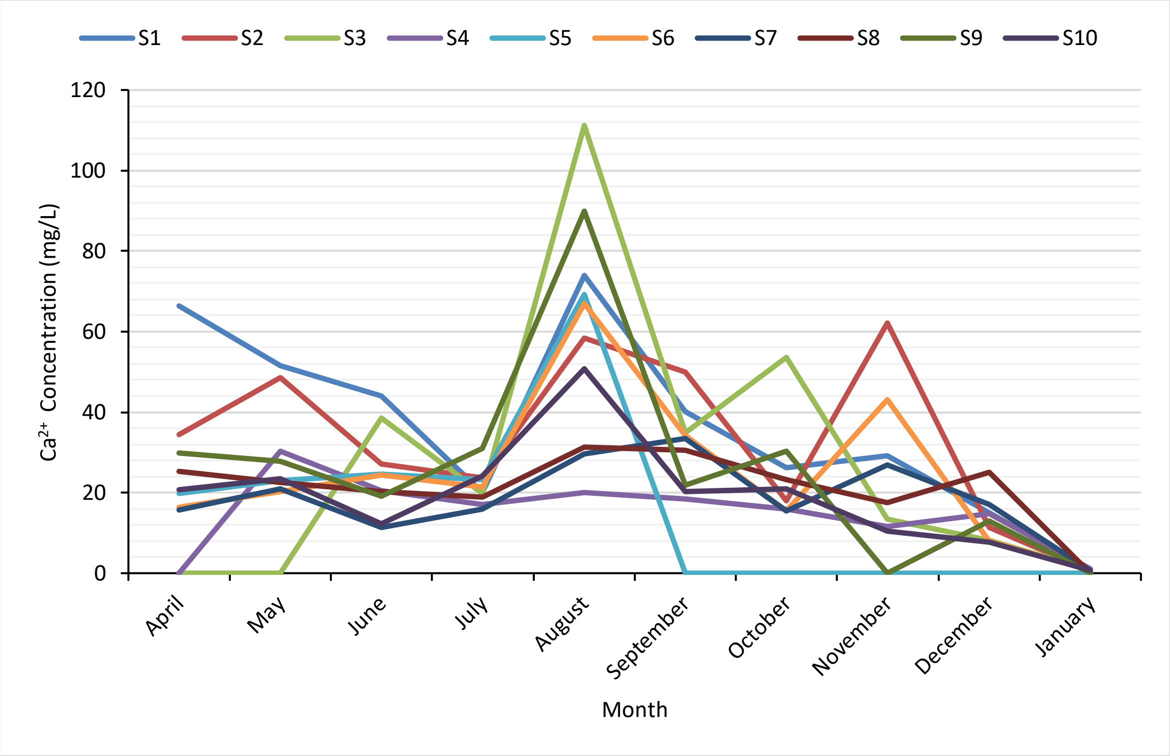

Figure 4.10. Ca^{2+} concentration (mg/l) over the 10-month sampling period.

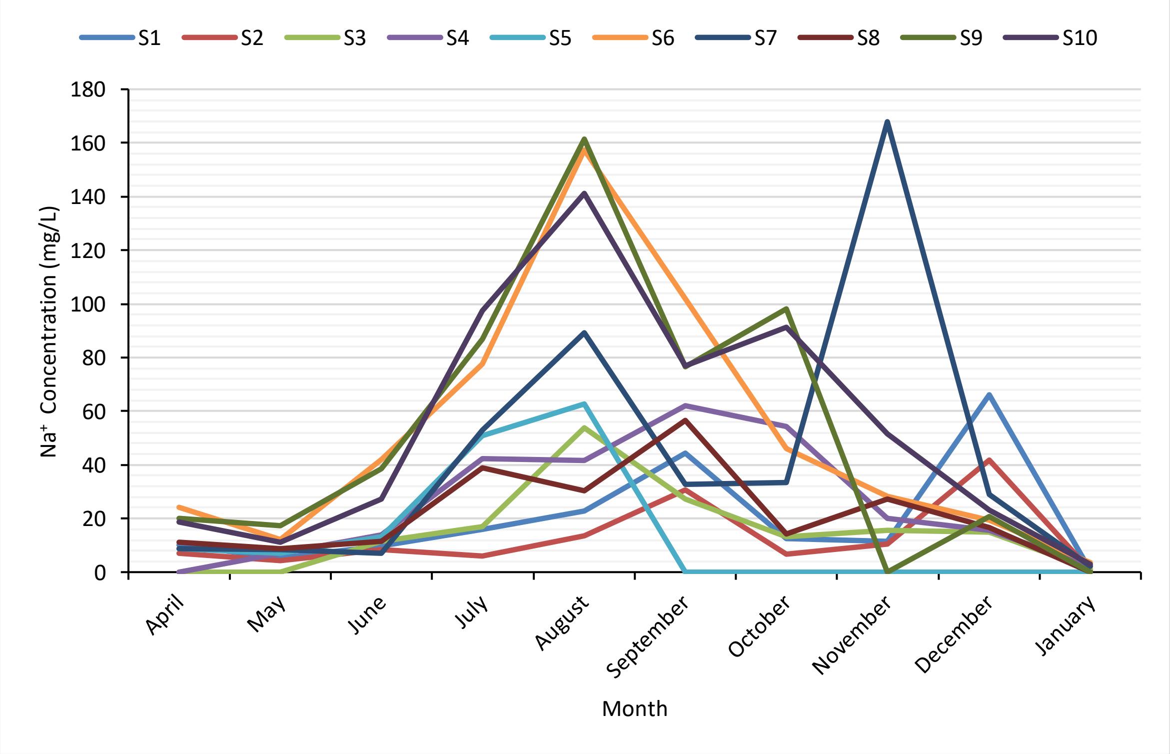

Figure 4.11. Na^{+} concentration (mg/l) over the 10-month sampling period.

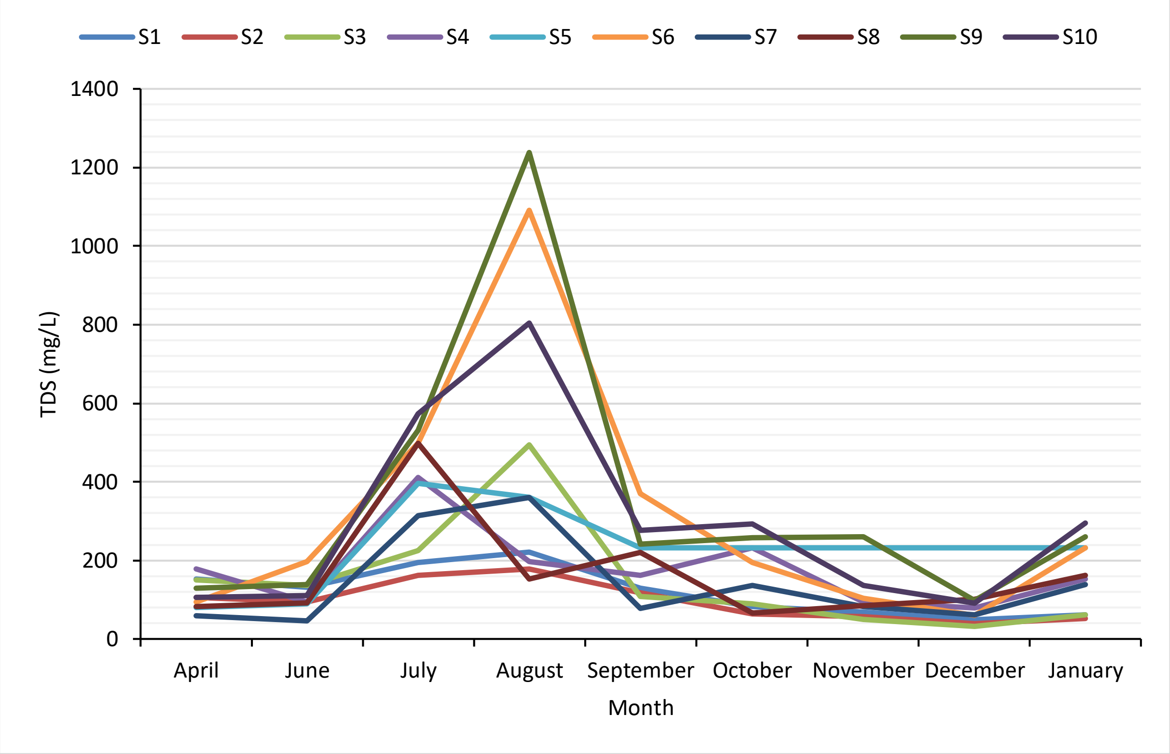

Figure 4.12. TDS (mg/l) results over the 10-month sampling period

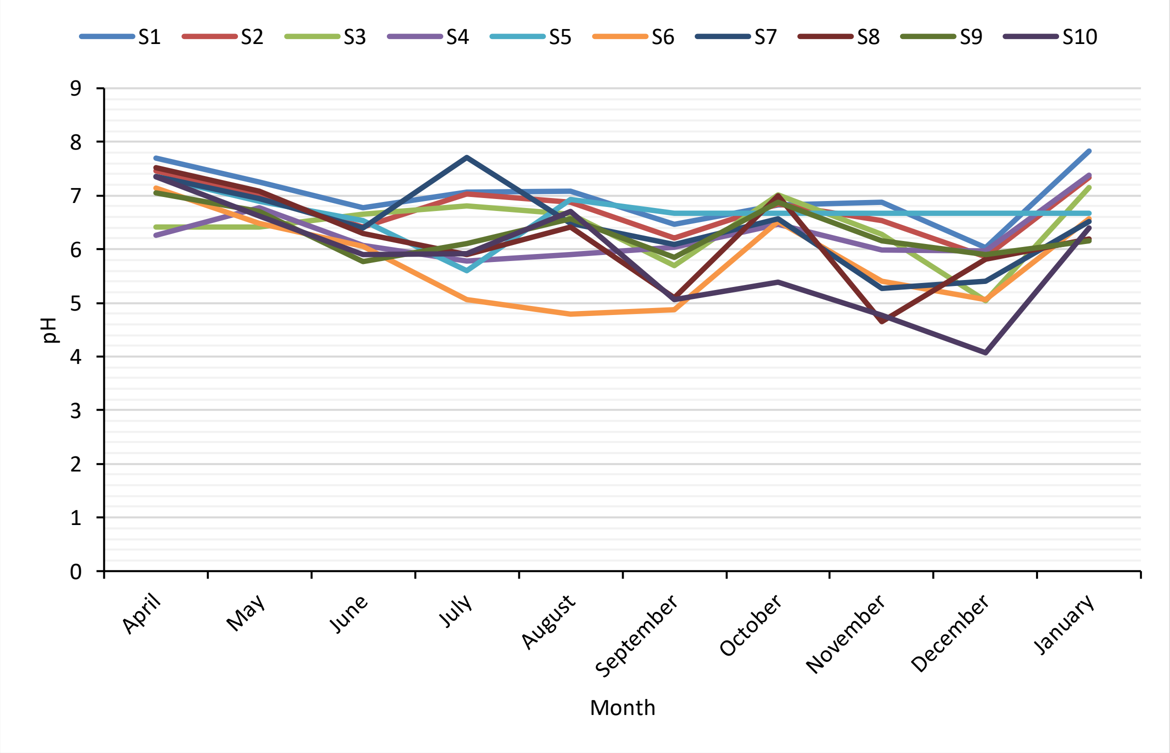

Figure 4.13. pH results over the 10-month sampling period.

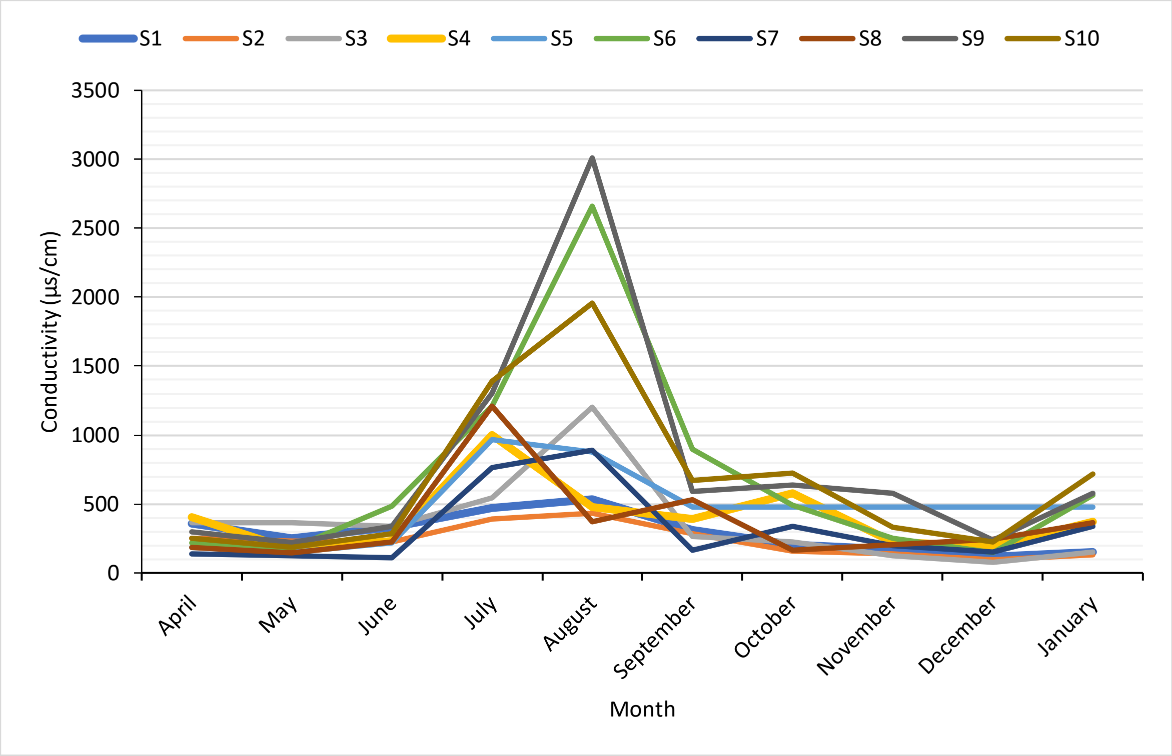

Figure 4.14. Conductivity (µs/cm) results for over the 10-month sampling period.

Table 4.1. Monthly average ion concentrations.

Ions	April (mg/l)	May (mg/l)	June (mg/l)	July (mg/l)	Aug (mg/l).	Sept. (mg/l)	Oct. (mg/l)	Nov. (mg/l)	Dec. (mg/l)	Jan. (mg/l)
F^-	0.1±0.0	ND	0.2±0.0	0.1±0.0	0.3±0.0	0.1±0.0	0.1±0.0	0.1±0.0	0.1±0.0	0.1±0.0
Cl^-	14.8±25.8	5.7±25.8	39.9±25.8	99.6±25.8	285.3±25.8	93.8±25.8	68.8±25.8	29.5±25.8	21.9±25.8	56.3±25.8
NO_2^-	2.6±1.2	0.2±1.2	ND	ND	ND	ND	ND	ND	ND	ND
NO_3^-	8.2±2.8	0.8±2.8	27±2.8	ND	21±2.8	22.9±2.8	13.6±2.8	12.6±2.8	11.1±2.8	9.1±2.8
SO_4^{2-}	20.1±3.7	1.6±3.7	26.8±3.7	16.2±3.7	45.2±3.7	25.1±3.7	19.3±3.7	11±3.7	13.5±3.7	13.3±3.7
PO_4^{3-}	0.6±0.5	0.1±0.5	2.3±0.5	0.1±0.5	4.3±0.5	3±0.5	0.7±0.5	0.7±0.5	0.8±0.5	0.3±0.5
Br^-	ND	ND	ND	0.3±0.1	0.5±0.1	0.2±0.1	0.2±0.1	0.1±0.1	0.1±0.1	0.2±0.1
Mg^{2+}	1.5±1.3	1.8±1.3	2.6±1.3	6.1±1.3	13.7±1.3	4.9±1.3	3.9±1.3	7.4±1.3	1.6±1.3	0.2±1.3
Ca^{2+}	22.9±4.8	26.8±4.8	24.2±4.8	21.5±4.8	60.1±4.8	28.4±4.8	21.9±4.8	21.4±4.8	12±4.8	0.6±4.8
K^+	2.6±0.9	2.5±0.9	4.3±0.9	4.5±0.9	10.7±0.9	5.8±0.9	3.6±0.9	3.7±0.9	2.7±0.9	0.1±0.9
Na^+	10.8±7.4	8.1±7.4	18.3±7.4	48.6±7.4	77.4±7.4	50.9±7.4	37±7.4	33.3±7.4	24.7±7.4	1.3±7.4

Table 4.2. Comparison of measured water composition to rainwater and seawater composition from the literature.

	Typical Sea Water*	Rainwater***	Current Study
F^- (mg/L)	1	0.04	0.12
Cl^- (mg/L)	18.9	3.89	**71.6**
SO_4^{2-} (mg/L)	2.6	2.24	**19.2**
Mg^{2+} (mg/L)	1.3	0.37	**4.37**
Ca^{2+} (mg/L)	400	1.74	23.98
K^+ (mg/L)	380	0.19	4.05
Na^+ (mg/L)	10.5	2.00	**31.04**
Br^- (mg/L)	65	NR	0.16
NO_3^- (mg/L)	NR	0.75	**12.63**
TDS (mg/L)	34.5	NR	**194**
pH	7.5-8.4**	6.25	6.38

*Reference: Lenntech, transferred from Magazine: Water Condition & Purification (2005)

**Reference: (Chester et. al., 2012)

*** Reference: (Gobre et. al., 2010)

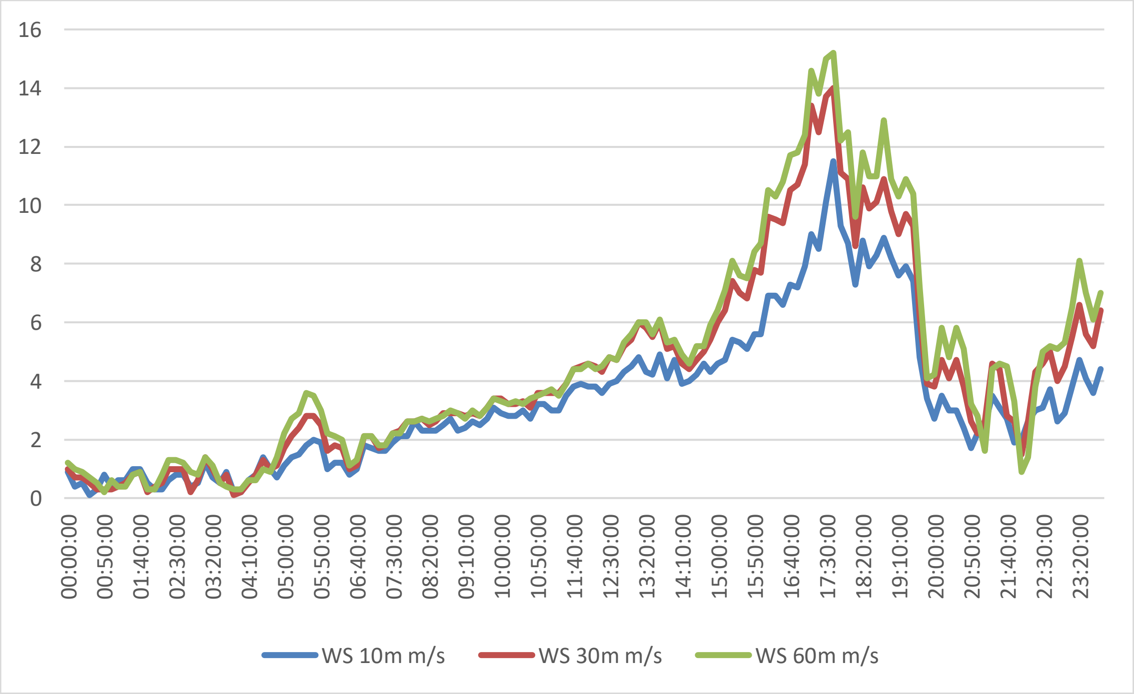

Figure 4.15. Wind speed on 27.07.2017 at different elevations with 10 min. intervals.

One particular event that may have contributed to the high ion concentrations in the fifth month (July 21-August 20, 2017) is the storm that occurred in Istanbul on 27.07.2017. Figure 4.15. shows the wind speed at the aforementioned date at three different elevations. Wind speed at 60 m had the maximum value which was 15.2 m/s at 17:40. And the dominant wind direction was from the North. As a result, and especially at the locations nearest the sea, maximum ion concentrations (Cl^-, Mg^{2+}, Na^+, K^+, Br^-), which may have originated from seawater, were observed.

4.2. Particulate Matter Results

This section presents the particulate matter data collected at each sampling device over the duration of the study. The results consist of the amount of particulate matter collected at the filter of each device and its composition. First, the mass of the particulate matter, which were determined by gravimetric method, are reported for each sampling point. Because each sampling device consists of 4 compartments oriented along 4 directions (north, south, east, and west), the results can also be used to analyze whether the collected mass is dependent on the direction. In second part, the focus is on trace elements due to their high impacts on the environment and human health. The analysis was conducted for the following metals: Cr, Mn, Fe, Ni, Cu, Zn, Al, Cd, Pb, Si, Co, Mo. Separate graphs were prepared for each sampling point.

4.2.1. Collected PM mass

Figures 4.16 to 4.25 show the monthly collected PM along the four different directions for all sampling points. The average monthly value is also shown on these graphs. The PM flux which is calculated as F=mass/area*time is summarized in Table 4.3. The collection area is equal to 0.0153 m^2 is standard for the device used in the current study and time is equal to 30 days. Monthly average collected mass ranged from 0.01 to 0.14 g. The data suggest that there is some variability from month to month. Specifically, the greatest collected mass was consistently in the month of April for all directions. However, the data suggest there is no significant difference along the 4 directions. This may be attributed to the complex wind patterns and turbulence effects which tend to settle the particulate matter equally in all four directions. Location wise, the highest collected mass was observed at sampling point S2 which is located near the gate of the campus where vehicles are likely to slow down and stop temporarily before accelerating again.

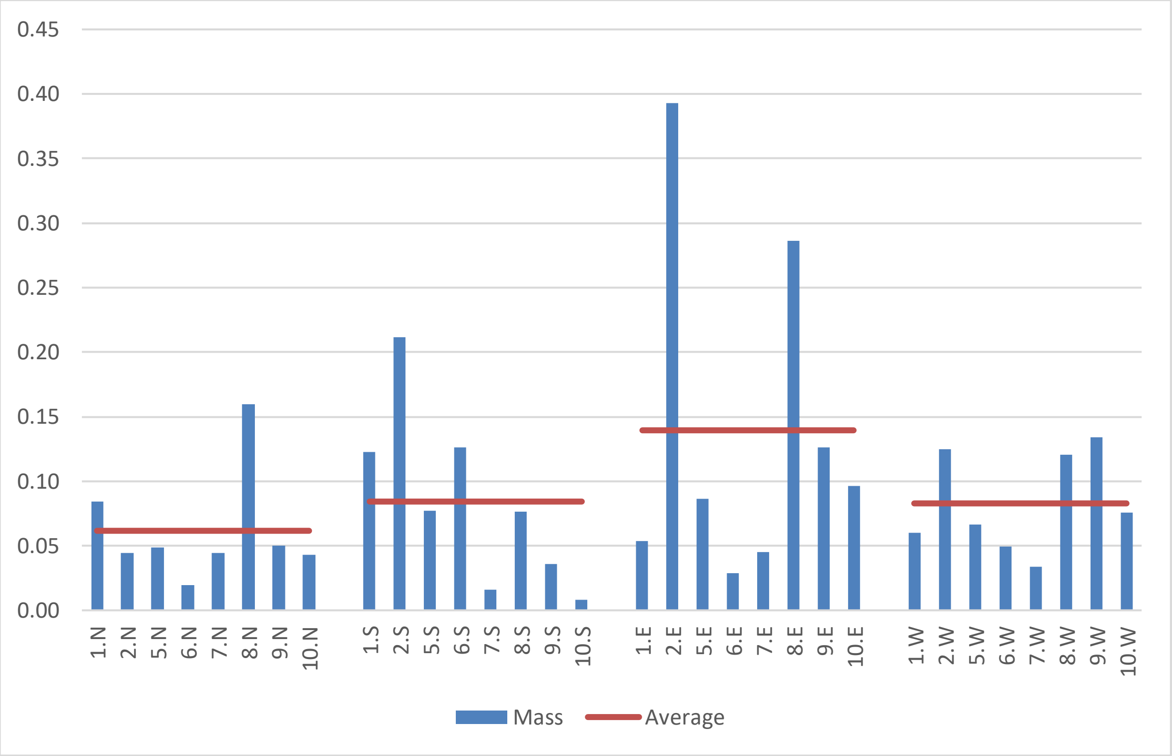

Figure 4.16. Mass of PM (g) for the period of 21 March to 20 April 2017.

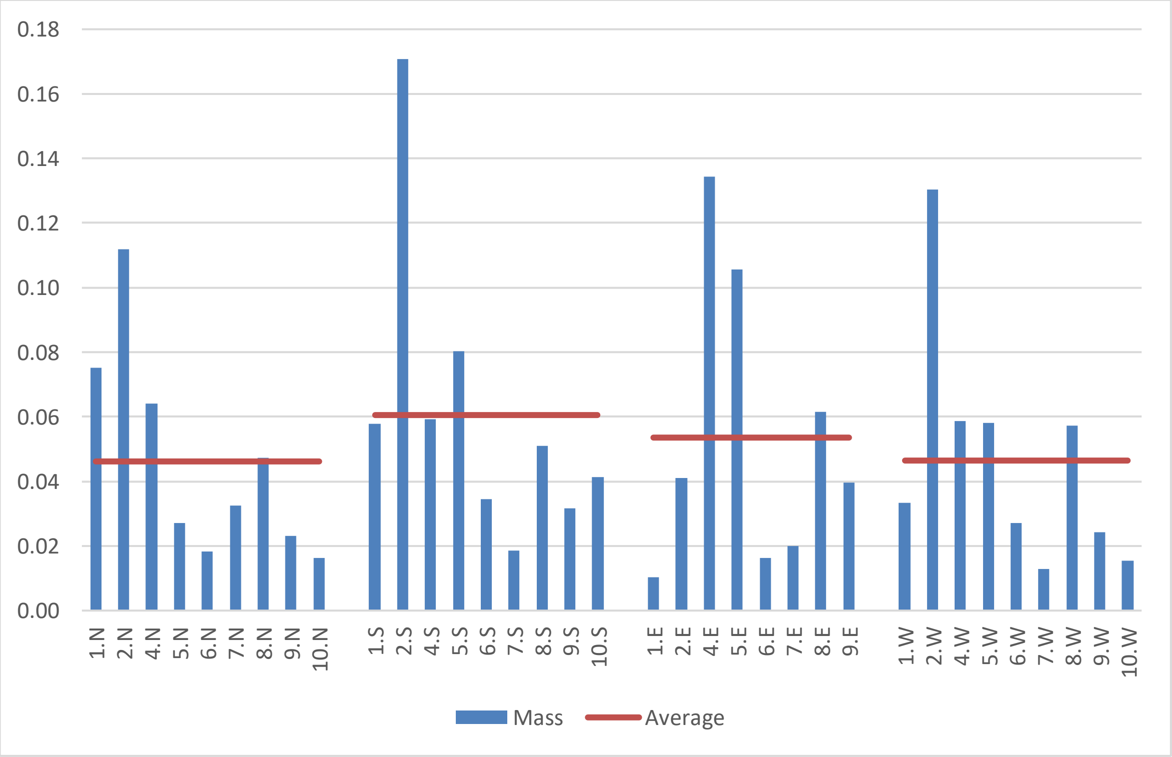

Figure 4.17. Mass of PM (g) for the period of 21 April to 20 May 2017.

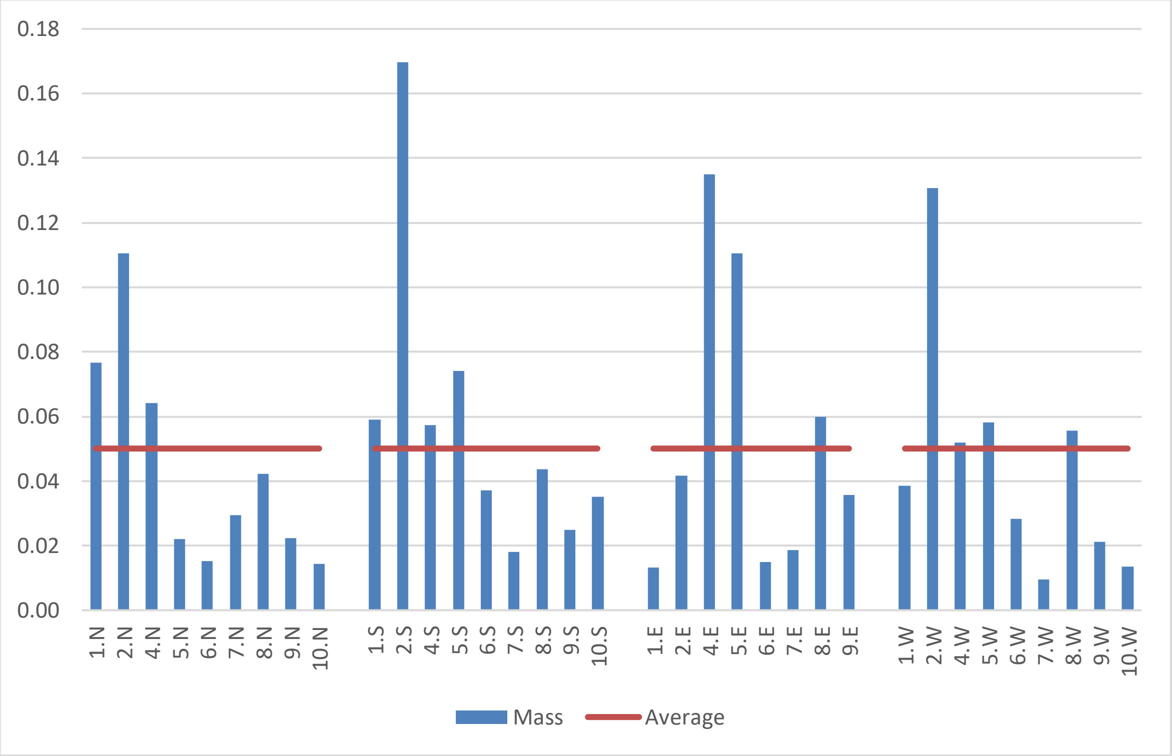

Figure 4.18. Mass of PM (g) for the period of 21 May to 20 June 2017.

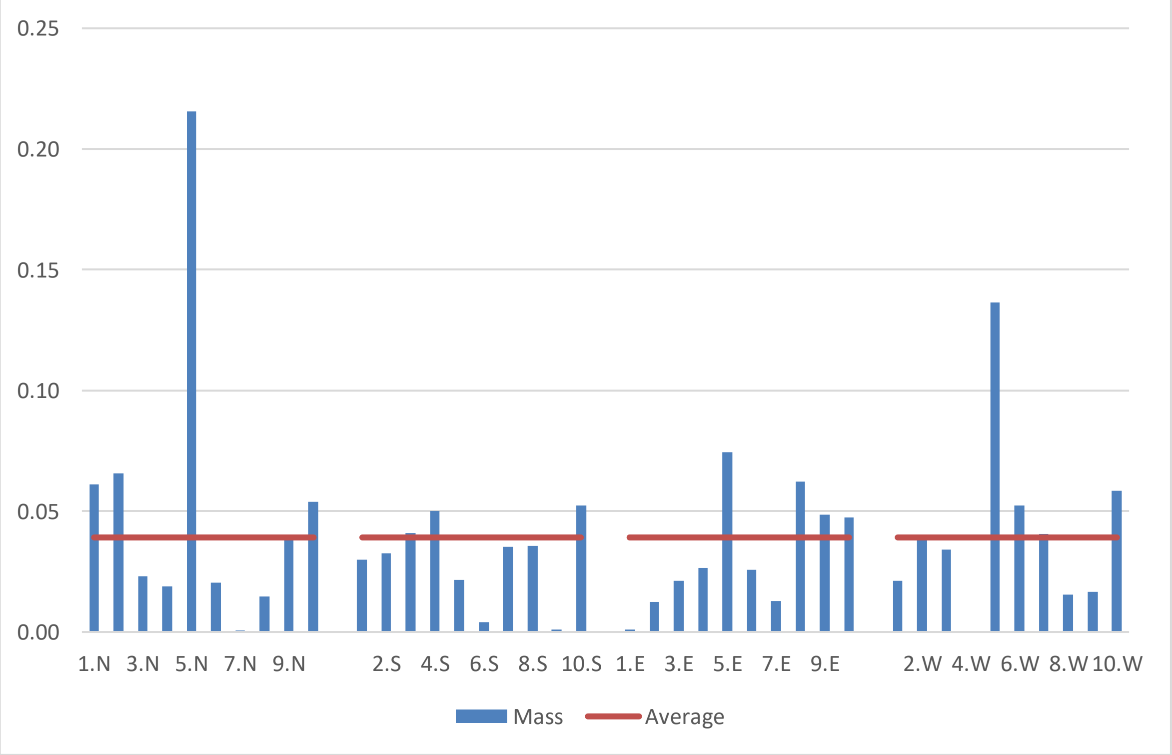

Figure 4.19. Mass of PM (g) for the period of 21 June to 20 July 2017.

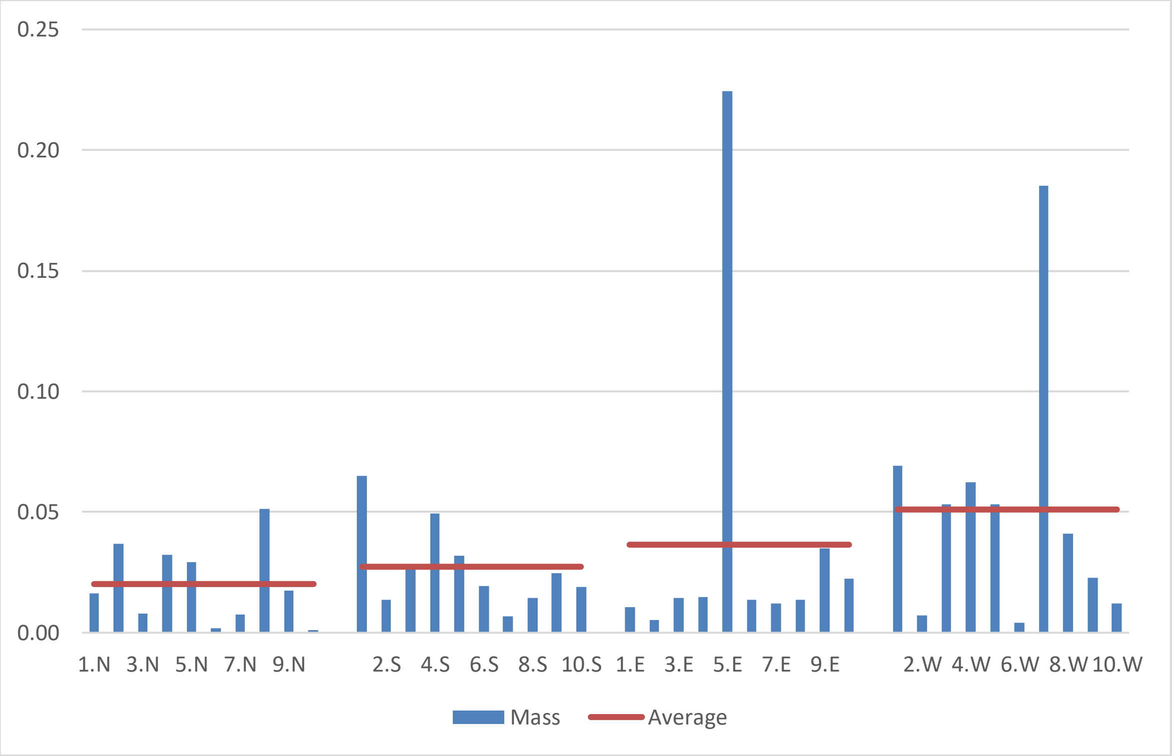

Figure 4.20. Mass of PM (g) for the period of 21 July to 20 August 2017.

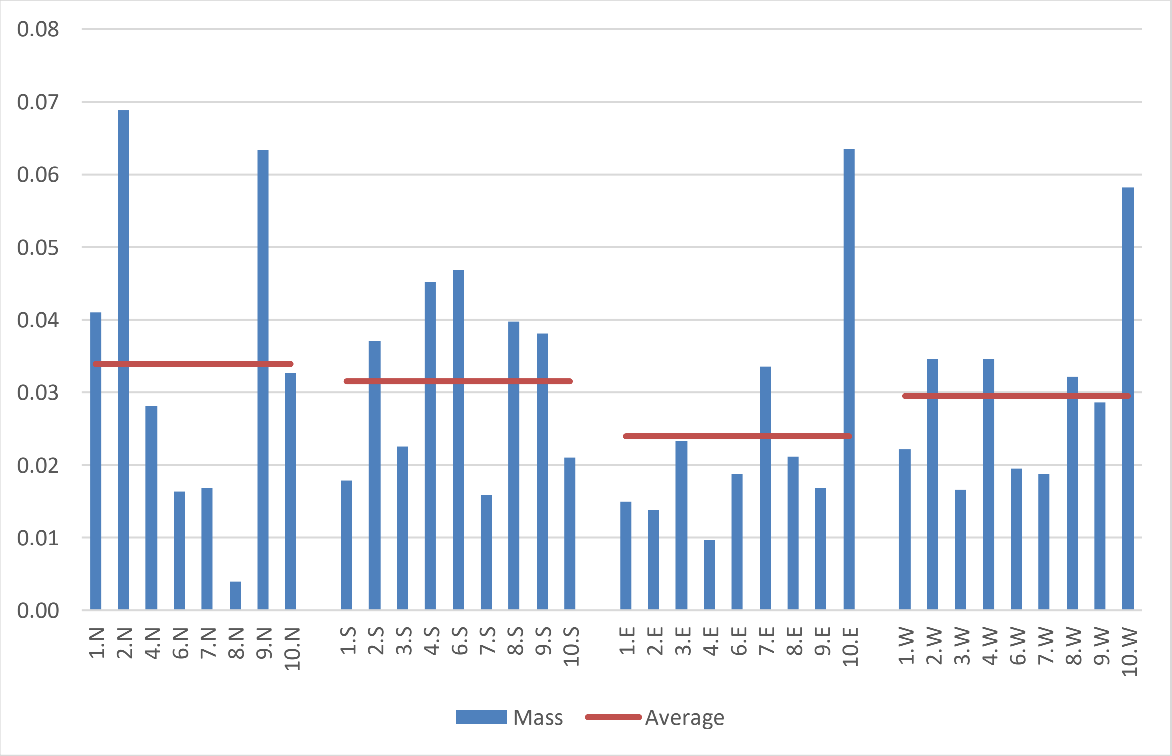

Figure 4.21. Mass of PM (g) for the period of 21 August to 20 Sept 2017.

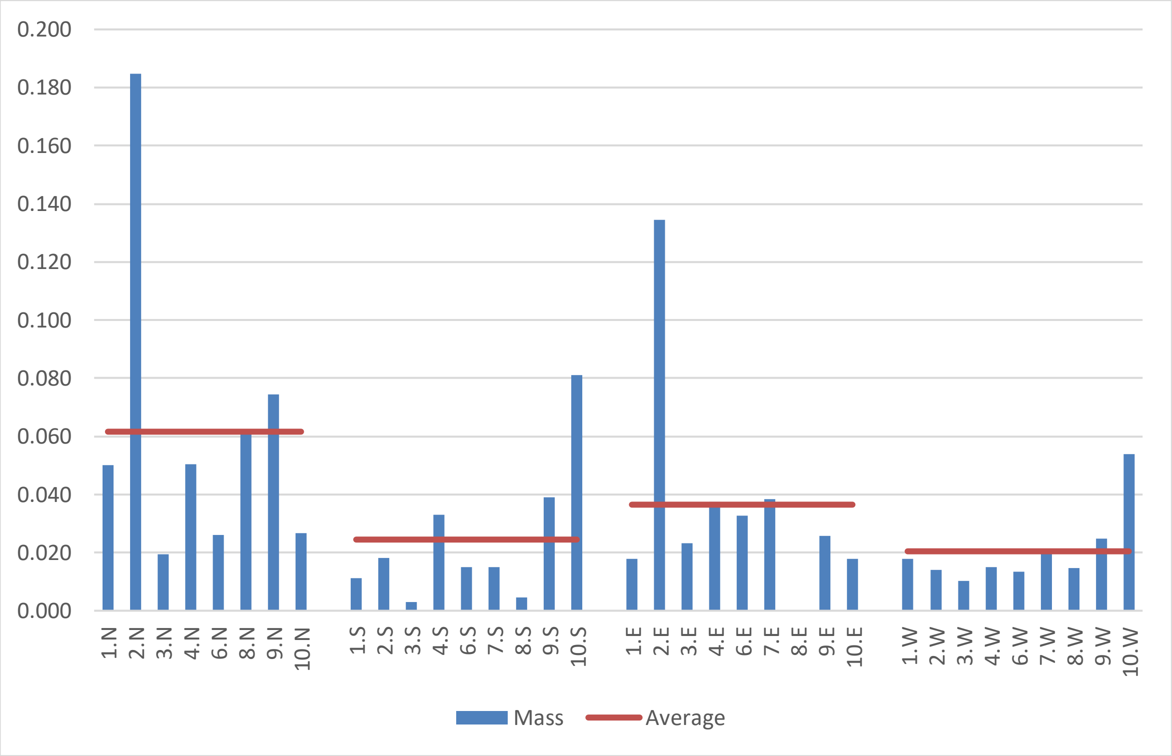

Figure 4.22. Mass of PM (g) for the period of 21 Sept to 20 October 2017.

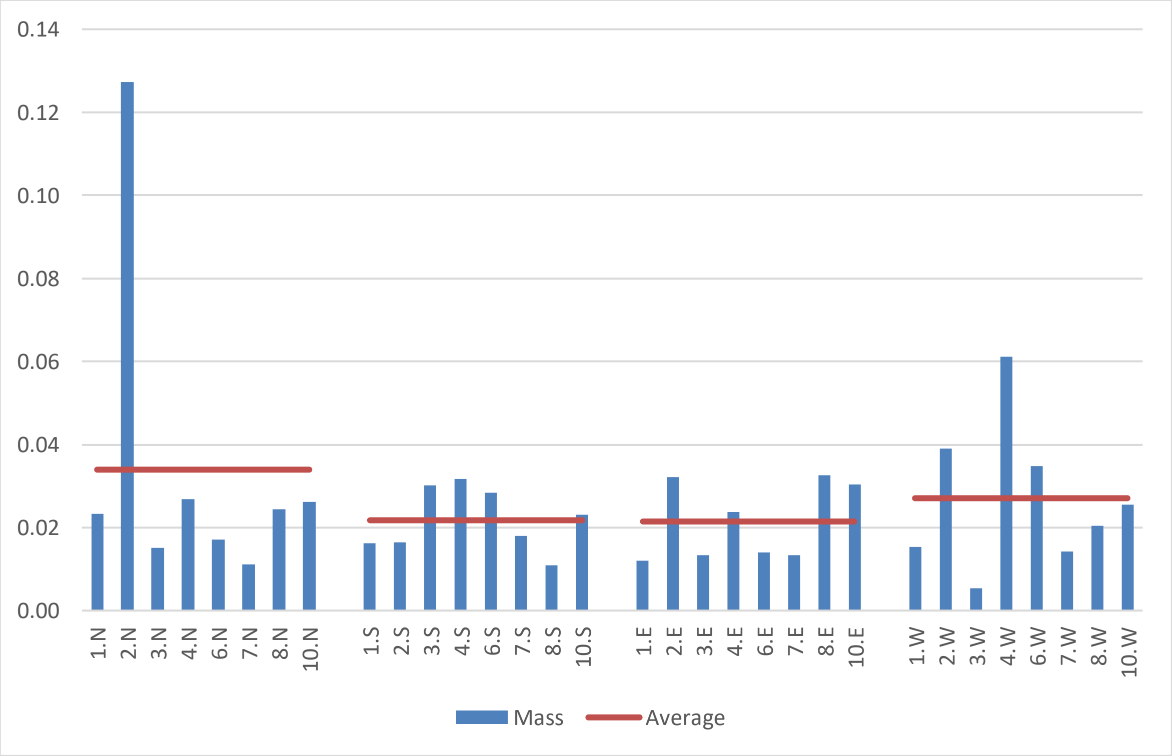

Figure 4.23. Mass of PM (g) for the period of 21 October to 20 November 2017.

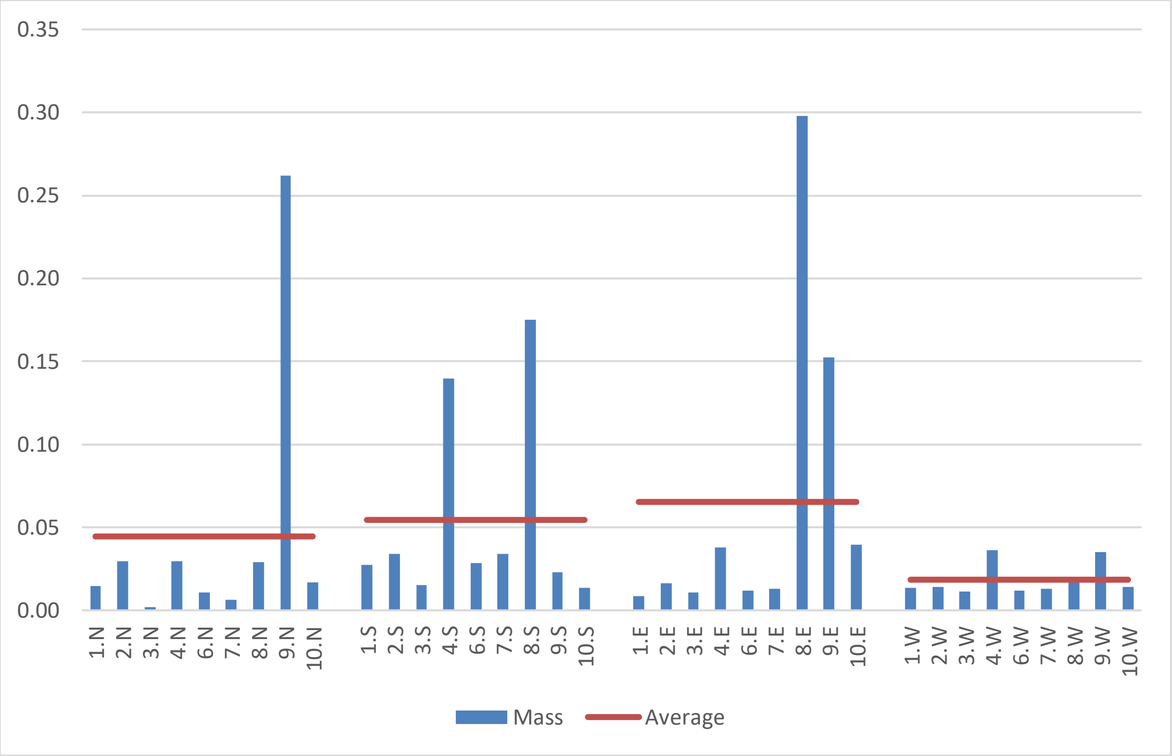

Figure 4.24. Mass of PM (g) for the period of 21 November to 20 December 2017.

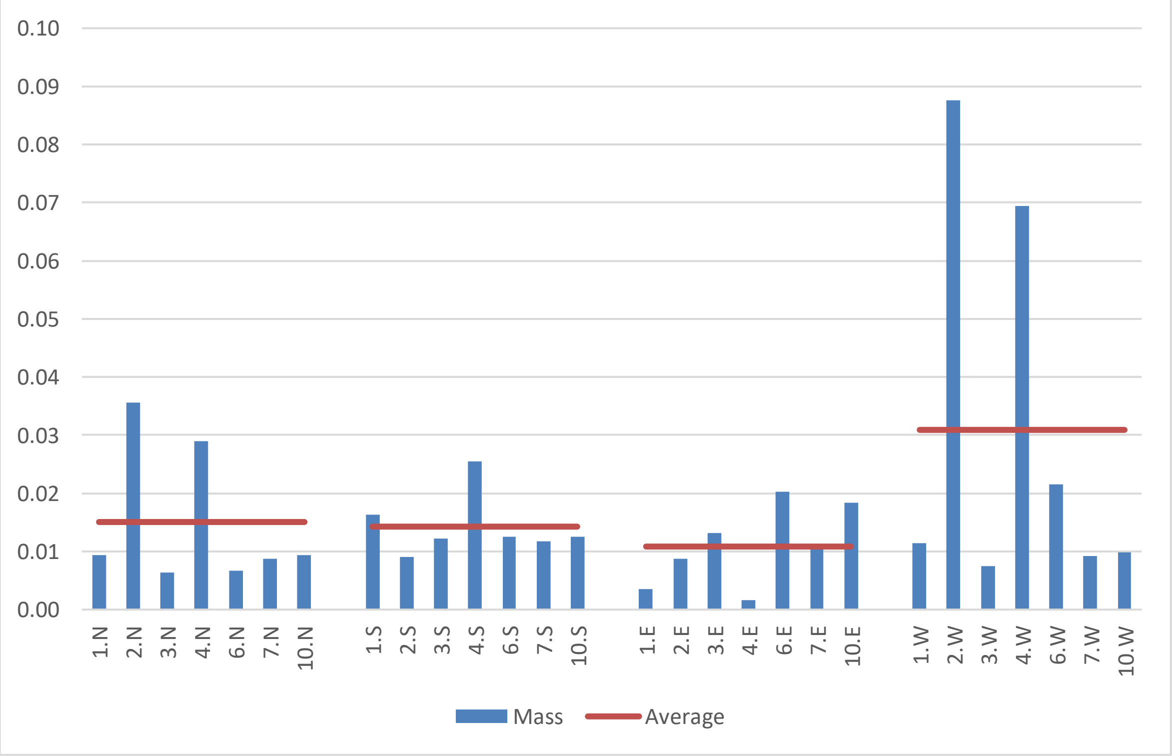

Figure 4.25. Mass of PM (g) for the period of 21 December 2017 to 20 January 2018.

Table 4.3. Monthly average PM flux g/m^2*day along each direction.

	North	South	East	West
April	0.13	0.17	0.31	0.17
May	0.11	0.13	0.11	0.11
June	0.11	0.11	0.11	0.11
July	0.09	0.09	0.09	0.09
August	0.04	0.07	0.09	0.11
September	0.07	0.07	0.04	0.07
October	0.13	0.04	0.09	0.04
November	0.07	0.04	0.04	0.07
December	0.09	0.11	0.15	0.04
January	0.04	0.02	0.02	0.07

4.2.2. PM metal composition

The airborne dust collected on the filters in the devices (Figure 3.4) were analyzed for the following metals Cr, Mn, Fe, Ni, Cu, Zn, Al, Cd, Pb, Si, Co, Mo. Initially, samples were analyzed for all directions separately; however, results revealed that there is no significant difference between directions. Therefore, combined results are reported. The monthly heavy metal contents at each sampling point are given in Figures 4.26 to 4.37. Table 4.4 presents the average metal concentrations for each month.

It is observed that the concentrations varied significantly over the duration of the study. The peak concentrations were mostly in the months of June and July. For some metals, the highest observed concentrations where mostly at S1 and S2. These two stations are located very near roadway close next to the University entrance. As such, cars are likely to brake and then accelerate. This has been reported in the literature that it leads to high metal emissions from tires and brakes (Guney et al., 2010).

Sampling point S5 which is located up the hill near the wind turbine had relatively high concentrations of Mn, Fe, Al, Si, Co. These metals are found in soils at relatively high levels. This could be attributed to the higher winds at this location and the bare exposed soils which can more readily release these metals. Because inorganic fraction of soil primarily consists of Al, Si, etc. but also it contains Mn, Co, Cu, Mo, Zn in smaller amounts (Pushkar, 2007). Table 4.5. summarizes the chemical composition of dust from the various studies published in the literature. This includes dusts released from brakes and tires, Saharan dust wet-deposited in the Iberian Peninsula during an extreme red rain event (21 to 23 Feb. 2017), street dust from Menomence River Watershed in Wisconsin, US, indoor dust in nursery school buildings, and street dust at Levent and Pendik, Istanbul, etc.

The particulate matter reported by Dong et al. (1984) were classified into fractions depending on the particle size of the urban street dust. USEPA (1992) dust limits are also reported in the Table along with the average metal concentrations observed in the current study. Most metal concentrations measured in this study fall in the range of concentrations observed in the literature.

However, it is observed that Fe, Zn, Pb and Al contents are at the higher end of the range of published data. According to Adachi et. al., (2004) tire dust is a significant pollutant, especially as a source of zinc in the urban environment. The values observed in this study are higher than the recommended values. As it will be discussed in section 4.5, although anthropogenic sources are a major contributor to the collected dust, a large fraction may also be coming from natural sources.

Table 4.4. Monthly metal concentrations.

Metal Concentrations (mg/g)	April	May	June	July	Aug.	Sept.	Oct.	Nov.	Dec.	Jan.
Cr	0.07±0.01	ND	0.04±0.01	0.05±0.01	0.02±0.01	0.02±0.01	0.03±0.01	0.01±0.01	0.01±0.01	0.02±0.01
Mn	0.37±0.03	0.02±0.03	0.18±0.03	0.24±0.03	0.19±0.03	0.13±0.03	0.23±0.03	0.07±0.03	0.15±0.03	0.1±0.03
Fe	13.15±1.56	0.81±1.56	12.58±1.56	18.14±1.56	8.79±1.56	8.06±1.56	11.85±1.56	4.31±1.56	5.95±1.56	9.22±1.56
Ni	0.06±0.01	ND	0.03±0.01	0.04±0.01	0.01±0.01	0.01±0.01	0.02±0.01	0.01±0.01	0.01±0.01	0.01±0.01
Cu	0.13±0.01	ND	0.05±0.01	0.06±0.01	0.04±0.01	0.04±0.01	0.05±0.01	0.02±0.01	0.03±0.01	0.02±0.01
Zn	10±4.64	1.26±4.64	39.81±4.64	45.73±4.64	11.18±4.64	8.67±4.64	21.77±4.64	5.5±4.64	10.71±4.64	17.55±4.64
Al	9.79±2.87	ND	2.16±2.87	31.32±2.87	8.92±2.87	6.03±2.87	17.71±2.87	3.6±2.87	6.54±2.87	9.86±2.87
Cd	ND	ND	8.85±0.88	0.01±0.88	ND	ND	ND	ND	ND	ND
Pb	0.6±1.02	0.03±1.02	11.13±1.02	2.02±1.02	1.74±1.02	2.48±1.02	1.62±1.02	0.86±1.02	0.67±1.02	0.67±1.02
Si	4.48±0.43	ND	1.47±0.43	1.87±0.43	0.6±0.43	0.48±0.43	0.49±0.43	0.39±0.43	0.24±0.43	0.26±0.43
Co	ND	ND	2.29±0.23	ND	ND	ND	ND	ND	ND	ND
Mo	ND	0.05±0.21	2.15±0.21	0.01±0.21	ND	ND	ND	ND	ND	ND

Table 4.5. Heavy metal composition data from the literature.

	Cr (mg/g)	Mn (mg/g)	Fe (mg/g)	Ni (mg/g)	Cu (mg/g)	Zn (mg/g)	Pb (mg/g)	Al (mg/g)
Saharan Dust[b]	0.1	0.7	0.3	ND	NR	0.4	ND	0.6
Sand[c]	ND	0.3	46.0	ND	0.2	0.4	0.1	3.2
Silt[c]	ND	0.3	34.3	0.1	0.2	0.8	0.4	5.6
Clay[c]	0.1	0.6	43.9	0.1	0.3	2.6	0.1	15.4
Indoor Dust[d]	ND	NR	4.2	ND	ND	0.1	ND	1.2
Street Dust - Levent, Istanbul[e]	NR	0.5	NR	ND	0.3	0.5	1.2	NR
Street Dust - Pendik, Istanbul[e]	NR	1.7	NR	ND	0.2	0.3	0.2	NR
USEPA[e] (1992)	NR	0.6	NR	ND	ND	0.1	ND	NR
Current Study	0.03	0.17	9.29	0.02	0.04	17.22	2.18	9.59
Highway dust- Istanbul[f]	NR	NR	NR	NR	0.047–1.358	0.190–1.852	0.105–0.555	NR
Highway surface soil-Galway, Ireland[f]	NR	NR	NR	NR	0.009–0.271	0.023–0.656	0.025–0.543	NR
Urban surface soil-Beijing, China[f]	NR	NR	NR	NR	0.024–0.457	0.025–0.196	0.025–0.207	NR
Urban surface soil-Hong Kong[f]	NR	NR	NR	NR	0.001–0.277	0.023–0.930	0.007–0.496	NR
Highway surface soil-Ibadan, Nigeria[f]	NR	NR	NR	NR	0.008–0.080	0.043–0.213	0.205–0.730	NR
Urban surface soil-Naples, Italy[f]	NR	NR	NR	NR	0.006–0.286	0.03–2.550	0.004–3.420	NR

NR: not reported
ND: none detected
b: Reference: Rodriquez- Navarro et al., (2018)
c: Reference: Dong et. al., (1984)
d: Reference: Darus et. al., (2012)
e: Reference: Yetimoglu et. al., (2007)
f: Reference: Guney et al., (2010)

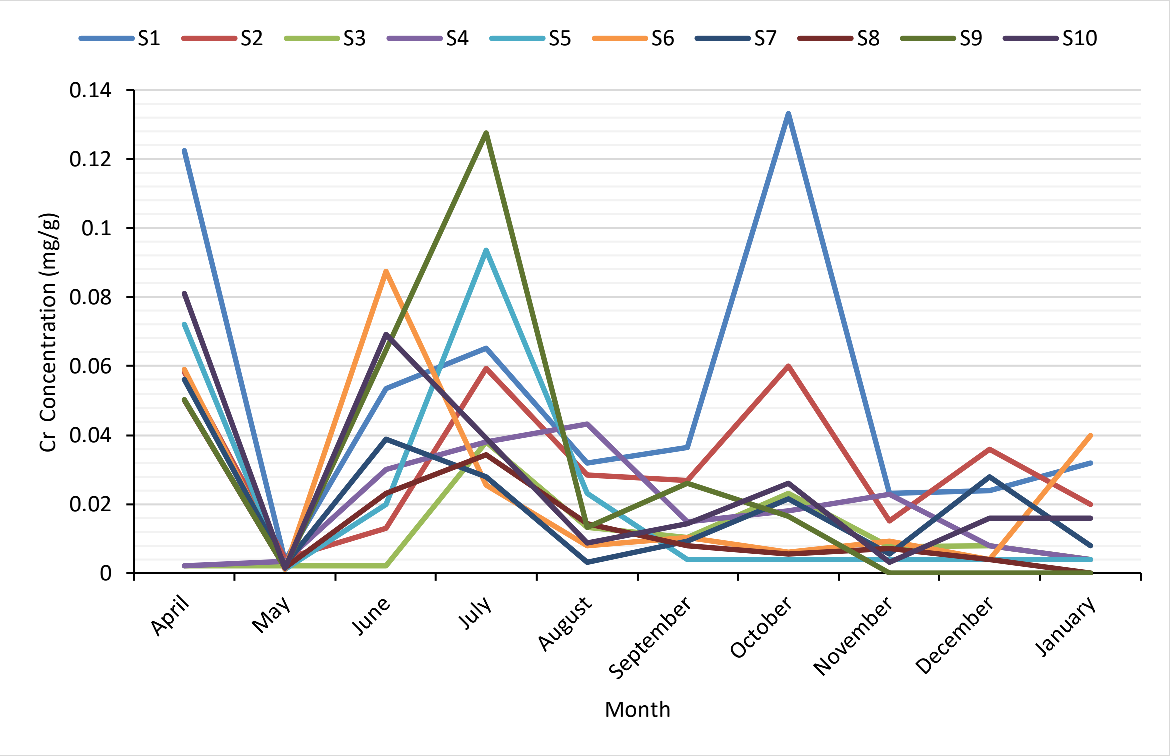

Figure 4.26. Cr results for the entire sampling period.

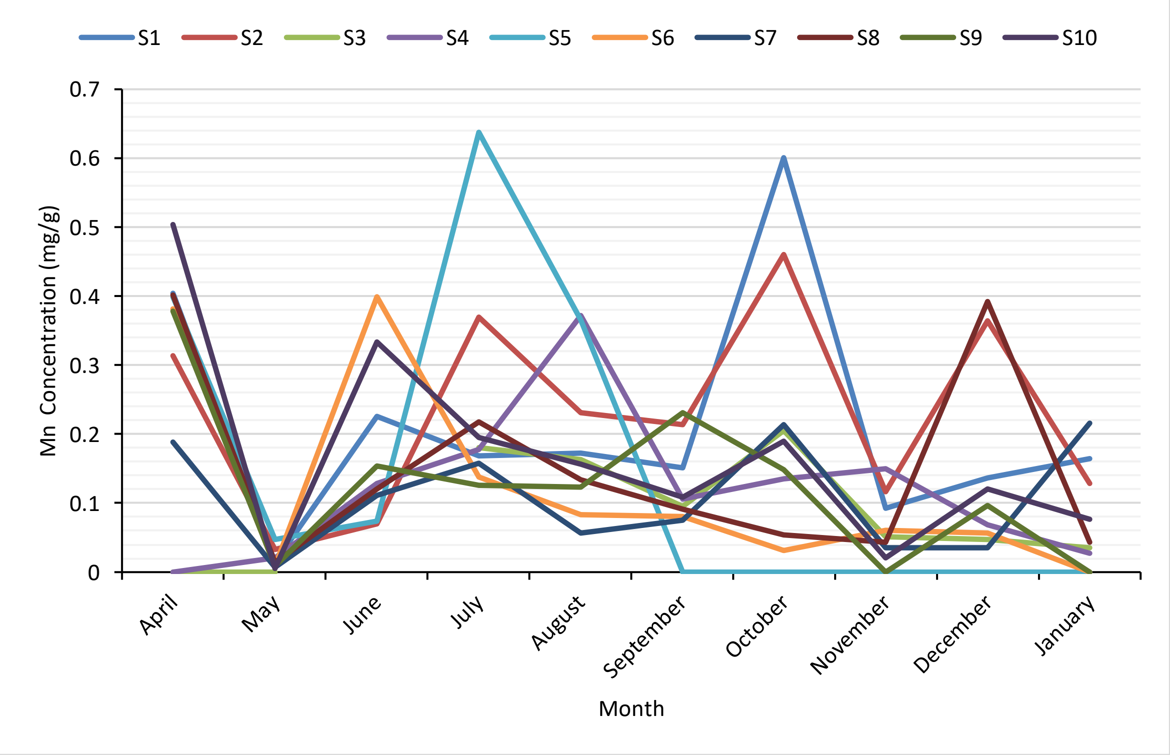

Figure 4.27. Mn results for the entire sampling period.

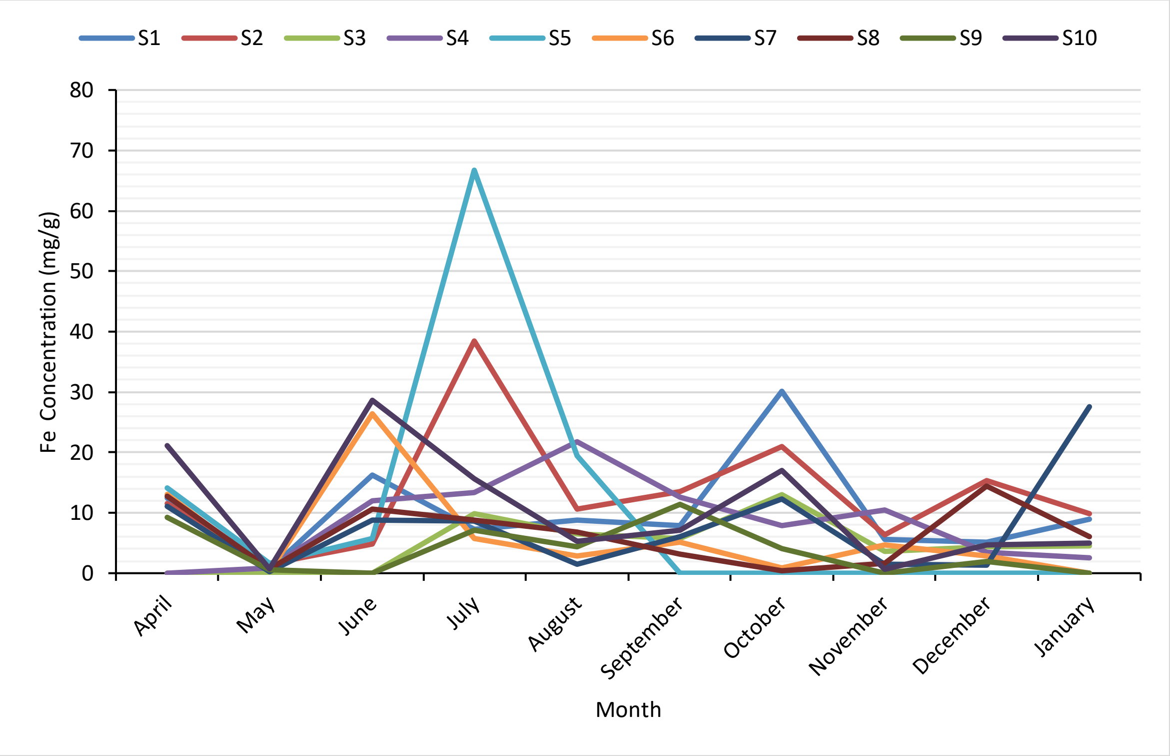

Figure 4.28. Fe results for the entire sampling period.

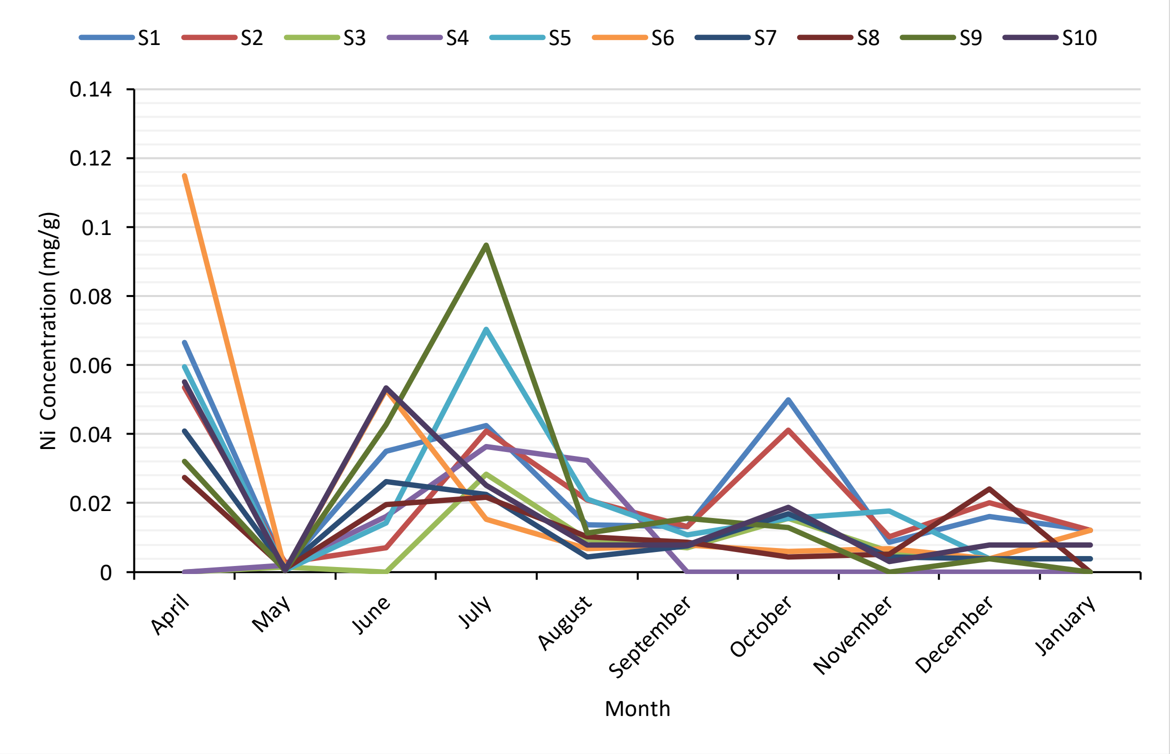

Figure 4.29. Ni results for the entire sampling period.

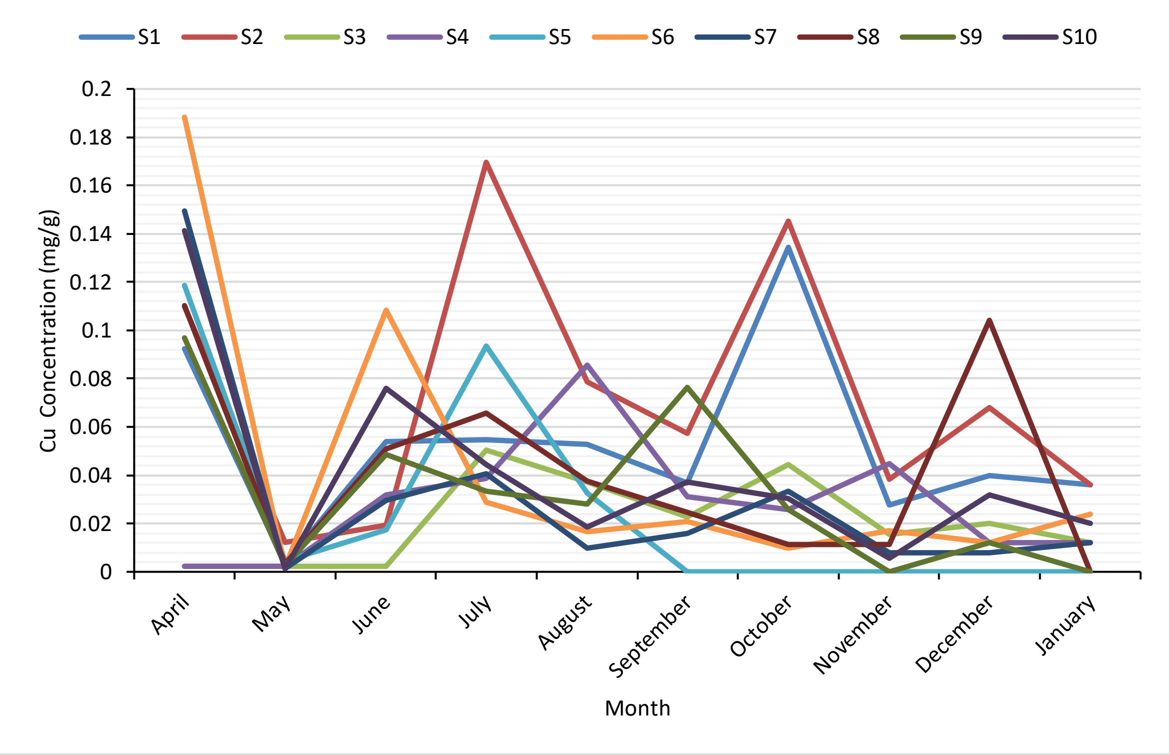

Figure 4.30. Cu results for the entire sampling period.

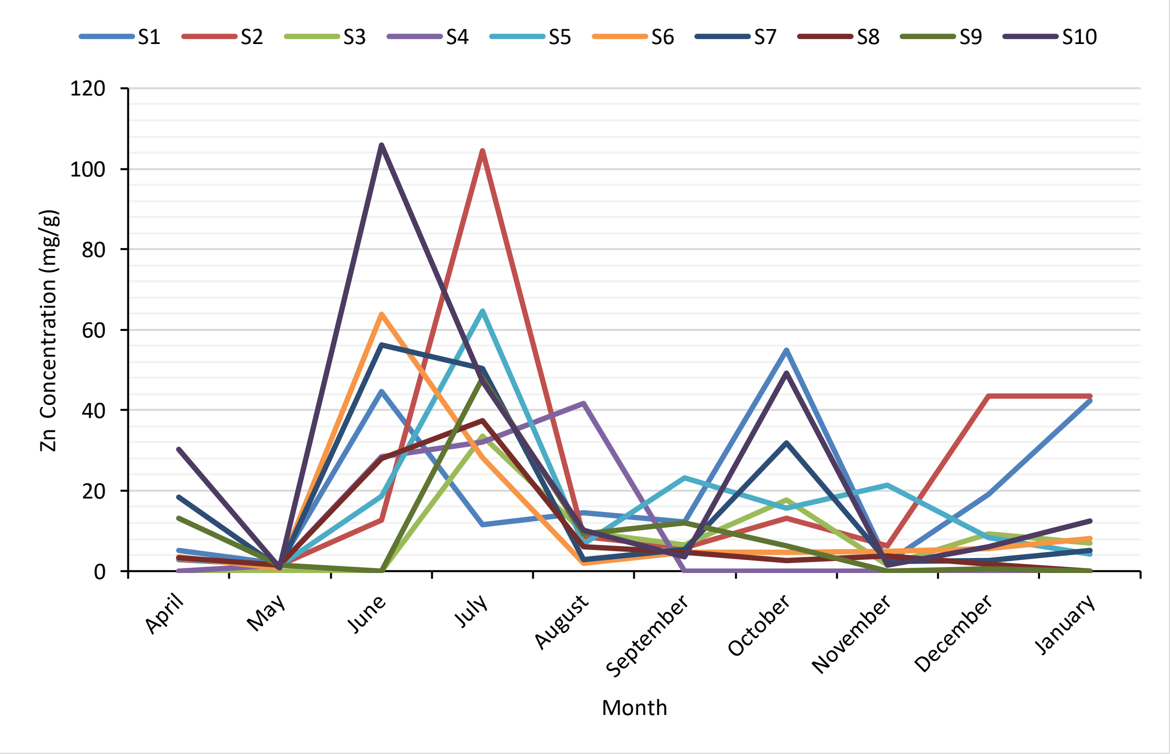

Figure 4.31. Zn results for the entire sampling period.

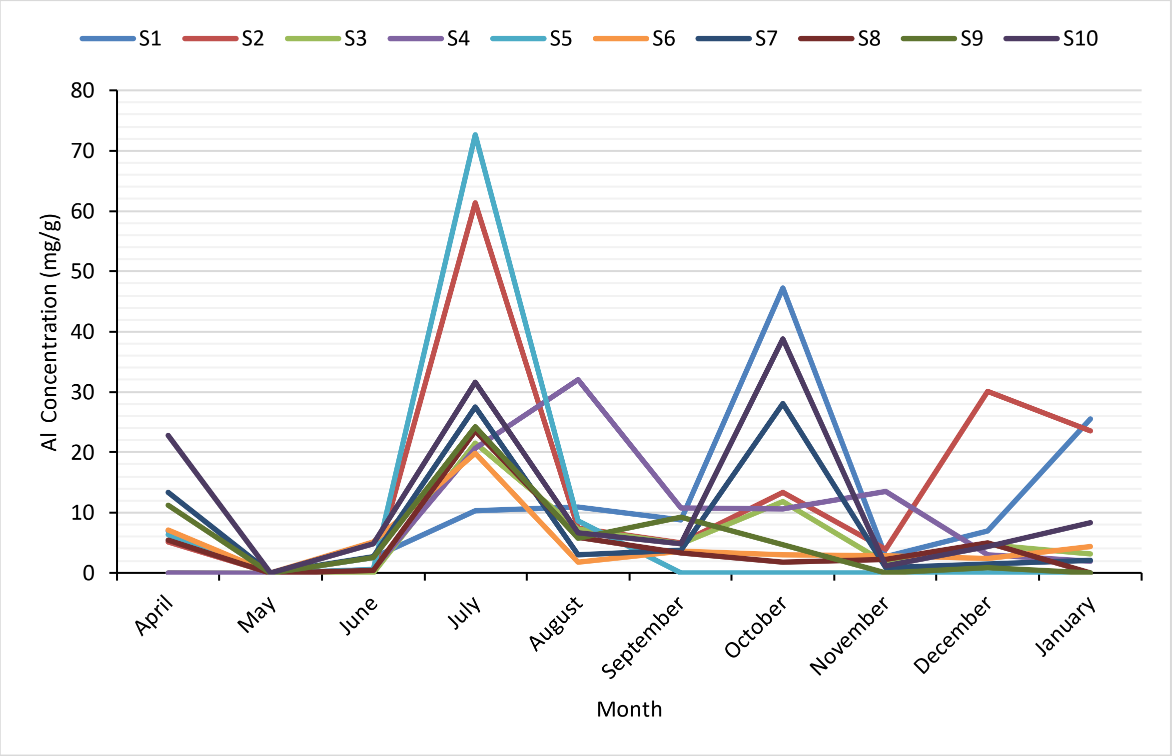

Figure 4.32. Al results for the entire sampling period.

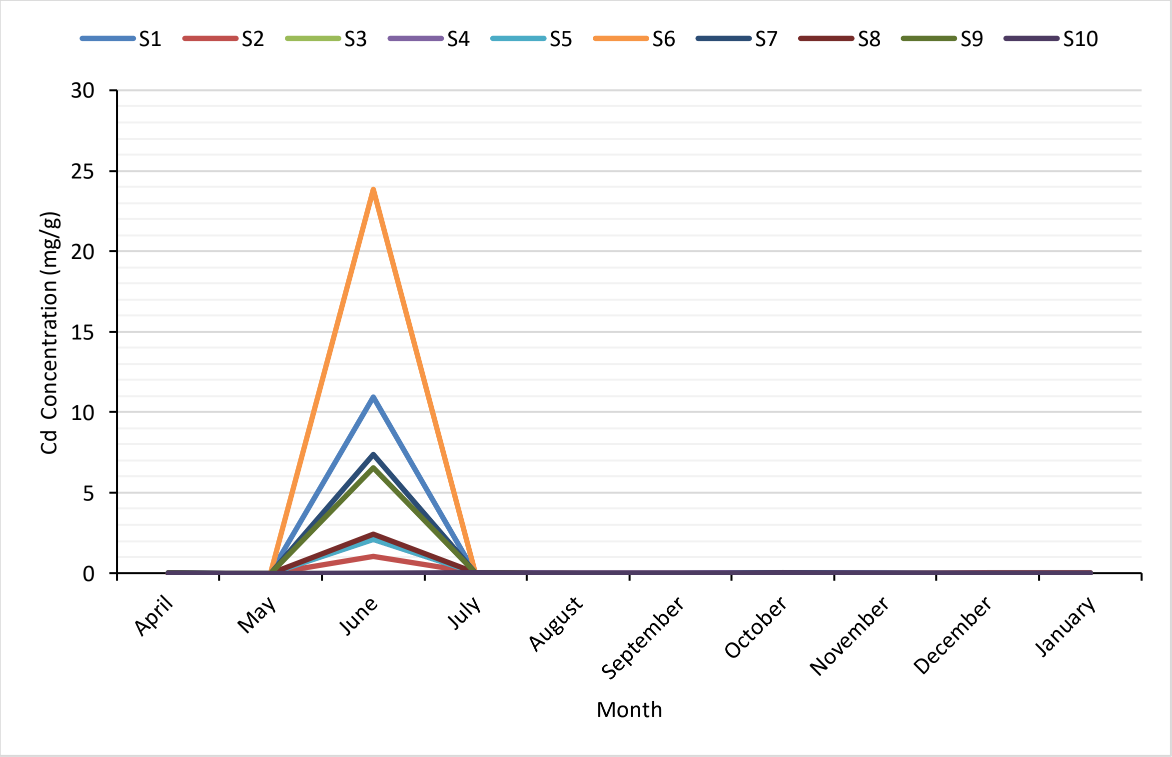

Figure 4.33. Cd results for the entire sampling period.

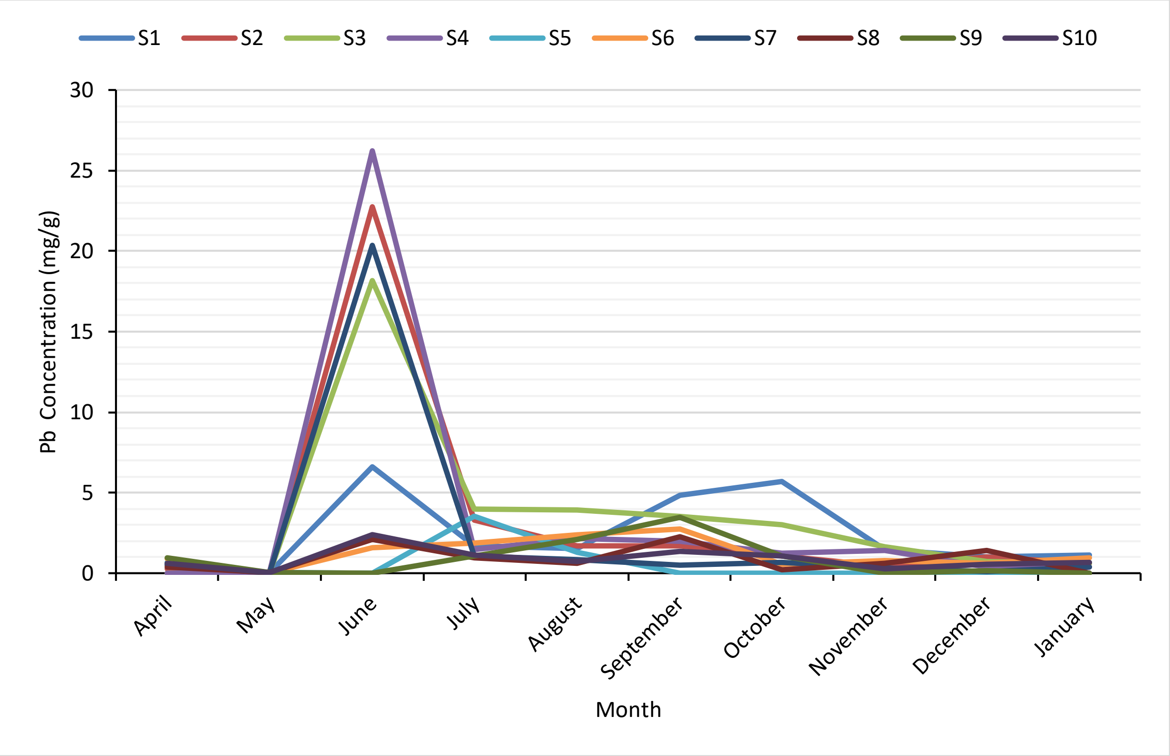

Figure 4.34. Pb results for the entire sampling period.

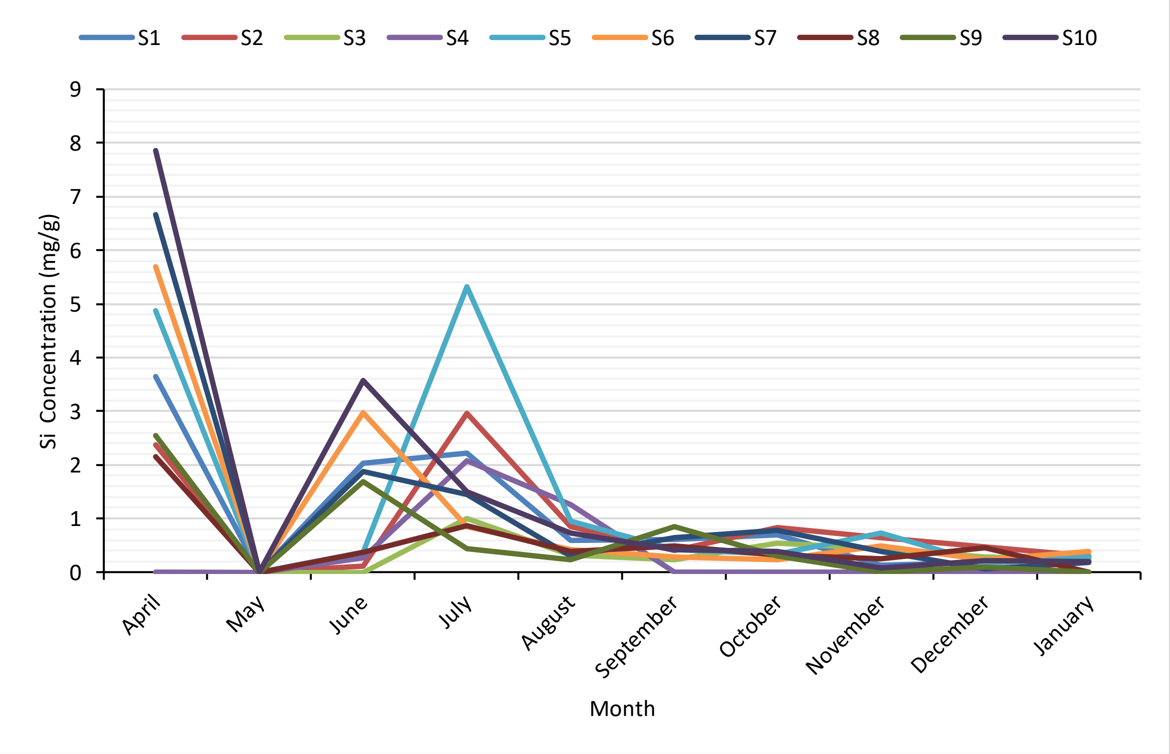

Figure 4.35. Si results for the entire sampling period.

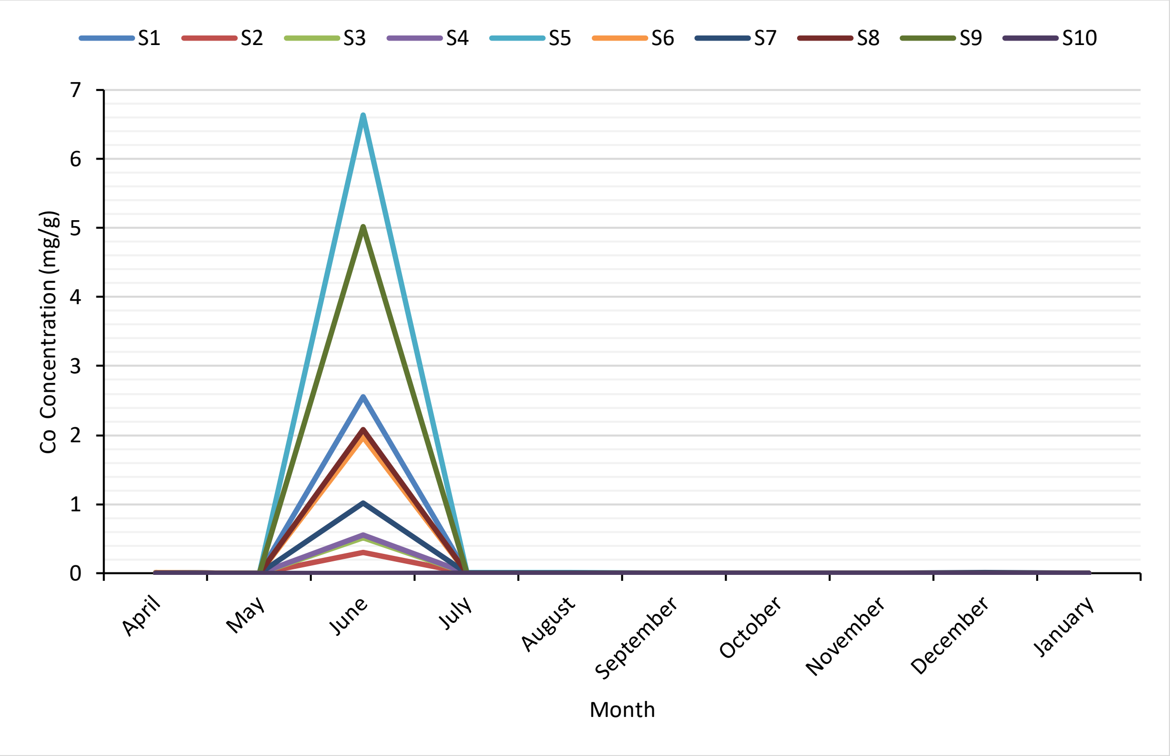

Figure 4.36. Co results for the entire sampling period.

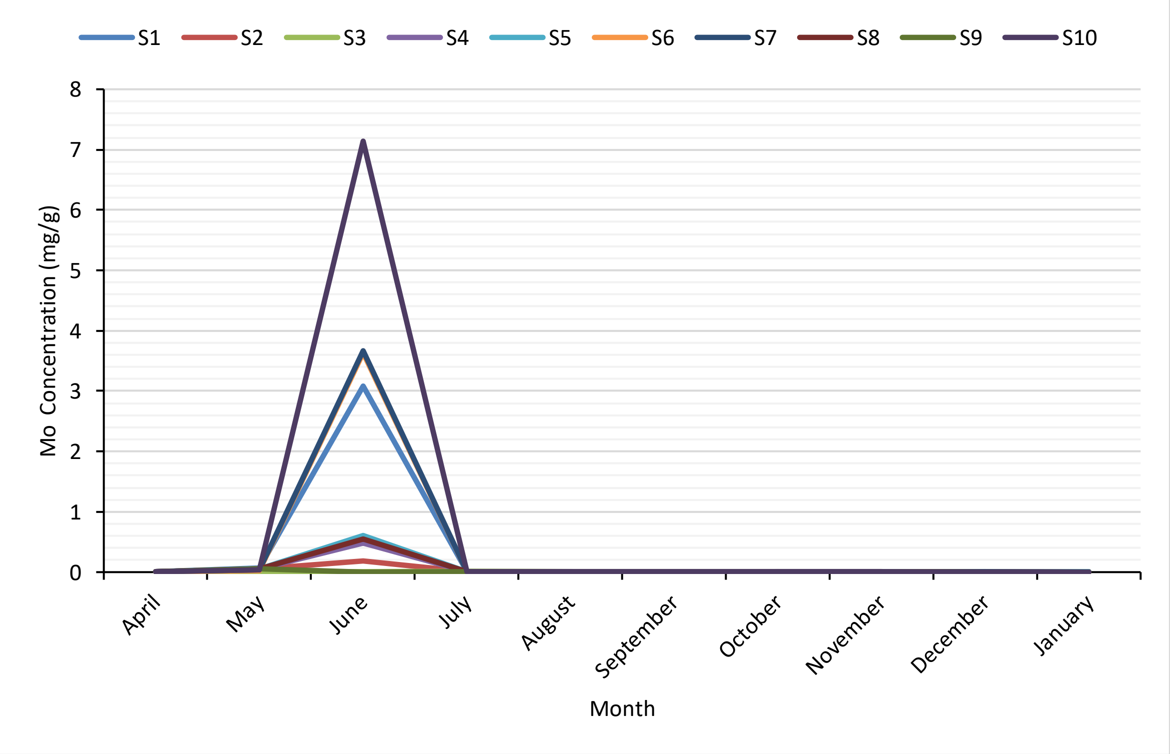

Figure 4.37. Mo results for the entire sampling period.

4.3. Meteorological Data

Meteorological data were obtained from the monitoring stations at Saritepe Campus. The meteorological data consisted of wind speed (WS), wind direction (WD), pressure, humidity, temperature, radiation and precipitation. The meteorological parameters were observed at 10-minute intervals. Table 4.5 shows the monthly average meteorological data during the study period. These values indicate that the average wind speed at the study area is about 3-4 m/s and these values do not change significantly from month to month. The dominant direction throughout the year is towards the south (from SE to SW). Humidity is relatively high, about 80% throughout the year. The average temperature varies from about 8 °C in winter to 25 °C in summer, while the radiation varies from about 60 W/m^2 in winter months to about 300 W/m^2 in the summer. Finally, monthly precipitation during the study period was highest in the months of November and December.

For the calculation of correlations between meteorological data and study parameters, monthly ions and metals have been used as well average monthly meteorological data. Specifically, the correlations between the 23 measured parameters (11 ions and 12 metals) and the meteorological parameters: Wind Speed (WS) at 10 m elevation, Wind Direction (WD) at 10 m elevation, Temperature, Precipitation and Humidity were examined.

The calculated Pearson’s correlations are reported in Table 4.6. and 4.7. The data suggest that the correlation with wind speed and direction is weak in part because the recorded monthly wind speed and directions does not seem to vary much. The data suggests that metal concentrations seem to increase with wind direction particularly towards the south west, but these correlations are low except for Si (r = 0.59) which has moderate correlation with wind direction. Similarly, temperature does not seem to have much correlation with the measured parameters. Precipitation has a clear negative correlation with the metal concentrations. The highest correlation was observed for precipitation and NO_3, (r = 0.72). For the ions associated with the sea water such as Cl, Na, SO_4 and K there is a weak negative correlation suggesting that precipitation may actually be diluting the effects of the nearby surf and wave action. Finally, the correlation data suggest that humidity does not seem to have much correlation indicating that the parameter concentrations are more influenced by the precipitation than the atmospheric humidity.

Table 4.6. Monthly average meteorological data.

	WS 10 m	WD 10 m	Air pressure	Humidity	Temperature	Precipitation
Unit:	m/s	°	hPa	%	°C	mm
April	4.13	SW	1006.55	81.61	8.45	80.4
May	2.91	SSE	1008.96	79.75	9.31	35.7
June	3.27	S	1006.51	78.00	13.79	43.5
July	3.24	S	1005.29	80.87	18.50	51.2
August	4.05	SE	1004.29	71.35	23.66	75.3
September	3.99	S	1003.24	80.45	24.61	21.1
October	3.81	SE	1004.91	70.29	22.81	25.6
November	3.79	SSE	1009.96	72.64	17.35	182.1
December	3.40	SSE	1007.66	78.74	13.57	100.7
January	4.58	SSW	1008.47	72.01	11.70	40.4

Table 4.7. Correlation between measured aqueous parameters and meteorological data.

Ion Name	WS	WD	Temperature	Precipitation	Humidity
Mg^+	0.17	0.019	0.19	-0.1	-0.02
K^+	0.30	0.09	0.12	-0.02	-0.09
Ca^{2+}	-0.24	0.22	-0.45	0.13	0.38
Na^+	0.39	0.04	0.27	-0.13	-0.18
F^-	-0.52	0.09	-0.49	-0.15	0.39
Cl^-	0.32	0.22	0.16	-0.14	0.04
NO_2^-	0.38	-0.22	0.34	0.11	-0.38
NO_3^-	0.06	-0.18	-0.16	**0.72**	-0.23
SO_4^{2-}	0.40	0.46	-0.44	-0.21	-0.13
PO_4^{3-}	-0.34	-0.34	0.12	0.48	0.34
Br^-	0.41	0.41	0.19	-0.2	-0.05

Table 4.8. Correlation between measured trace elements and meteorological data.

Element	WS	WD	Temperature	Precipitation	Humidity
Cr	0.2	0.49	-0.14	-0.16	0.36
Mn	0.2	0.30	0.02	-0.11	0.22
Fe	0.1	0.23	0.18	-0.30	0.15
Ni	0.1	0.49	-0.26	-0.03	0.43
Cu	0.3	0.47	-0.13	-0.04	0.36
Zn	-0.2	-0.13	0.12	-0.31	0.12
Al	0.0	-0.19	0.31	-0.21	0.02
Cd	-0.3	0.06	-0.15	-0.16	0.11
Pb	-0.3	0.00	0.06	-0.23	0.10
Si	0.1	0.59	-0.35	0.03	0.49
Co	-0.3	0.06	-0.15	-0.16	0.11
Mo	-0.3	0.06	-0.16	-0.17	0.12

4.4. Statistical Analysis Results

To gain further insight into the collected data, univariate statistics were calculated for the collected data. Table 4.9. and 4.10 give the statistics for the aqueous phase parameters and PM composition data. The statistics were calculated for the data collected over the entire 10 months period.

Correlation analyses revealed that ions/ions and aqueous phase metal/ PM metal concentrations are strongly correlation: Na/K (r = 0.96), Cl/Br (r = 0.96), Mg/Cl (r = 0.95), Na/Br (r = 0.94), Na/Cl (r = 0.92), Br/Mg (r = 0.90), K/Cl (r = 0.90) and high positively correlated ions like; Mg/Na (r = 0.89), K/Br (r = 0.88) and Mg/K (r = 0.87). According to Hinkle et. al., (1988) correlations between .90 to 1.00 are considered as very high and .70 to .90 are high, correlations between .50 to .70 are moderate, correlations between .30 to .50 are low correlation and .00 to .30 are considered as negligible.

The observed correlations clearly show very strong correlation between all metals. Similarly, there is a very strong positive correlation between Na, Cl, Mg, K ions which gives further evidence that these ions are originating from the same source, with the nearby sea as a possible source. This is further explored in Section 4.5. Besides sea salt (NaCl), Br^- ions also originate from marine aerosols.

Br^- ions is usually found in different salts such as NaBr which is highly soluble in water. However, Br^- is trace element for seawater due to its concentration typically 300 lowers than Cl (VanBriesen, 2014).

The data also indicate that the collected dust metal correlations are very highly positively correlated: Zn/Al (r = 0.94), Cr/Zn (r = 0.98), Cr/Al (r = 0.93), Mn/Zn (r = 0.90), Mn/Al (r = 0.95), Cr/Mo (r = 0.92), Co/Si (r = 0.97) and high positively correlated metals like; Fe/Cr (r = 0.85), Mn/Fe (0.78), Mn/Mo (0.85), Fe/Ni (0.83), Fe/Cu (0.78), Fe/Zn (0.78) Fe/Cd (0.83). The very high heavy metal correlations again suggest that they may be originating from the same anthropogenic activities such as transportation and burning processes. This will be investigated further in the next section.

Table 4.9. Descriptive statistics of the aqueous phase parameters for the entire sampling period.

	Mg	K	Ca	Na	F	Cl	NO2	NO3	SO4	PO4	Br
Mean	4.93	4.51	27.29	34.79	0.13	80.33	0.37	13.98	21.28	25.67	0.17
Standard Error	0.75	0.47	2.37	5.51	0.03	17.23	0.15	0.95	1.63	24.41	0.04
Median	3.99	3.79	28.53	28.64	0.11	58.94	0.15	13.57	19.74	1.15	0.12
Mode	#N/A	#N/A	#N/A	#N/A	#N/A	#N/A	#N/A	#N/A	#N/A	#N/A	#N/A
Standard Deviation	2.36	1.50	7.48	17.41	0.08	54.50	0.46	3.02	5.15	77.19	0.14
Sample Variance	5.58	2.25	55.93	303.28	0.01	2969.88	0.21	9.12	26.52	5958.50	0.02
Kurtosis	-0.15	0.86	-1.79	-1.05	7.64	-0.91	2.22	1.74	-0.30	10.00	-1.29
Skewness	0.96	1.05	-0.24	0.56	2.64	0.88	1.58	0.94	0.83	3.16	0.76
Range	7.42	5.06	20.11	52.02	0.28	153.64	1.43	10.85	15.66	244.71	0.36
Minimum	1.96	2.62	16.63	12.95	0.07	20.18	0.00	9.70	15.41	0.64	0.03
Maximum	9.38	7.68	36.74	64.97	0.35	173.82	1.43	20.55	31.06	245.35	0.39
Sum	49.26	45.13	272.85	347.86	1.30	803.33	3.74	139.81	212.80	256.65	1.72
Count	10.00	10.00	10.00	10.00	10.00	10.00	10.00	10.00	10.00	10.00	10.00
Largest (1)	9.38	7.68	36.74	64.97	0.35	173.82	1.43	20.55	31.06	245.35	0.39
Smallest (1)	1.96	2.62	16.63	12.95	0.07	20.18	0.00	9.70	15.41	0.64	0.03
Confidence Level (95.0%)	1.69	1.07	5.35	12.46	0.06	38.98	0.33	2.16	3.68	55.22	0.10

Table 4.10. Descriptive statistics of PM metal content data for entire sampling period.

	Cr	Mn	Fe	Zn	Al	Ni	Cu	Zn	Al	Cd	Pb	Si
Mean	0.03	0.17	9.29	17.22	9.59	0.02	0.04	17.22	9.59	0.89	2.18	1.03
Standard Error	0.01	0.03	1.56	4.64	2.87	0.01	0.01	4.64	2.87	0.88	1.02	0.43
Median	0.02	0.165	9.005	10.945	7.73	0.01	0.04	10.945	7.73	0	1.24	0.485
Mode	0.02	#N/A	#N/A	#N/A	#N/A	0.01	0.05	#N/A	#N/A	0	0.67	#N/A
Standard Deviation	0.02	0.10	4.95	14.68	9.09	0.02	0.04	14.68	9.09	2.80	3.23	1.34
Sample Variance	0.00	0.01	24.47	215.57	82.64	0.00	0.00	215.57	82.64	7.83	10.46	1.81
Kurtosis	0.53	0.87	0.19	0.44	3.34	1.44	4.25	0.44	3.34	10.00	8.53	5.33
Skewness	0.94	0.62	0.04	1.21	1.70	1.37	1.70	1.21	1.70	3.16	2.85	2.24
Range	0.07	0.35	17.33	44.47	31.32	0.06	0.13	44.47	31.32	8.85	11.10	4.48
Minimum	0.00	0.02	0.81	1.26	0.00	0.00	0.00	1.26	0.00	0.00	0.03	0.00
Maximum	0.07	0.37	18.14	45.73	31.32	0.06	0.13	45.73	31.32	8.85	11.13	4.48
Sum	0.27	1.68	92.86	172.18	95.93	0.20	0.44	172.18	95.93	8.86	21.82	10.28
Count	10.00	10.00	10.00	10.00	10.00	10.00	10.00	10.00	10.00	10.00	10.00	10.00
Largest (1)	0.07	0.37	18.14	45.73	31.32	0.06	0.13	45.73	31.32	8.85	11.13	4.48
Smallest (1)	0.00	0.02	0.81	1.26	0.00	0.00	0.00	1.26	0.00	0.00	0.03	0.00
Confidence Level (95.0%)	0.02	0.07	3.54	10.50	6.50	0.01	0.03	10.50	6.50	2.00	2.31	0.96

Table 4.11. Pearson correlations of the aqueous phase parameters for the entire sampling period.

	Mg	K	Ca	Na	F	Cl	NO_2	NO_3	SO_4	PO_4	Br
Mg	1.00										
K	**0.87**	1.00									
Ca	-0.12	-0.21	1.00								
Na	0.90	**0.97**	-0.35	1.00							
F	-0.18	-0.46	0.53	-0.49	1.00						
Cl	**0.95**	**0.91**	-0.18	**0.93**	-0.38	1.00					
NO_2	0.45	0.32	0.18	0.40	-0.15	0.40	1.00				
NO_3	-0.11	-0.23	-0.12	-0.22	0.23	-0.23	0.12	1.00			
SO_4	0.11	-0.05	0.19	0.02	0.45	0.09	0.35	0.27	1.00		
PO_4	-0.25	-0.16	-0.50	-0.12	-0.25	-0.13	-0.27	-0.02	-0.40	1.00	
Br	**0.91**	**0.89**	-0.37	**0.94**	-0.41	0.97	0.35	-0.16	0.16	-0.05	1.00

Table 4.12. Correlation of PM metal composition data for the entire sampling period.

	Cr	Mn	Fe	Ni	Cu	Zn	Al	Cd	Pb	Si	Co	Mo
Cr	1.00											
Mn	0.92	1.00										
Fe	0.85	0.78	1.00									
Ni	0.54	0.38	0.83	1.00								
Cu	0.51	0.52	0.78	0.64	1.00							
Zn	0.98	0.90	0.78	0.48	0.46	1.00						
Al	0.93	0.95	0.68	0.24	0.34	**0.94**	1.00					
Cd	0.54	0.38	0.83	1.00	0.64	0.48	0.24	1.00				
Pb	0.51	0.52	0.78	0.64	1.00	0.46	0.34	0.64	1.00			
Si	0.22	0.04	0.23	0.54	-0.29	0.19	0.06	0.54	-0.29	1.00		
Co	0.26	0.10	0.35	0.62	-0.16	0.21	0.09	0.62	-0.16	0.97	1.00	
Mo	0.92	0.85	0.61	0.24	0.27	0.96	0.95	0.24	0.27	0.12	0.10	1.00

4.5. Positive Matrix Factorization Source Apportionment Results

In the current investigation, 4 factors have been identified by PMF 5.0. Number of base runs was 20, number of base random seed was 8. For the run 13, the values of Q(Robust), Q(True), Q(true)/Qexp were 15369.9, 23937.3, 15.150, respectively. Following percentages mean that factor impact on the formation of the parameter. Factor 1 is characterized mostly by NO_3 (98.9%), SO_4 (91.9%), PO_4 (81.0%), F (59.7%). Comparison of factor fingerprints diagrams of summer and winter revealed that Factor 1 had higher contribution rate in summer season. Agricultural activities consist of many activities like field burning agricultural residues, cultivation, manure management, etc. Hence, agricultural soil can contain high rate of nutrients and, as a result, of plant activity organic N can be transformed to inorganic form such as NO_3 (Munch et. al., 2007). These results suggest that Factor 1 might be characterized as agricultural activity.

Factor 2 is characterized by Co (96.0%), Cu (61.7%), NO_2 (68.4%), Ni (55.7%), Cr (56.3%), Mn (56.6%), Pb (33.7%), Zn (5.2%), Mo (53.4%). According to Jolly et. al., (2013) agricultural soil can contain Co, Mo, Cu, and other trace metals as well, so biomass burning can be related to Factor 2. Overall, burning processes for heating and other purposes might be correspond to Factor 2.

Factor 3 is characterized by mostly Na (81.5%), Cl (83.4%), Br (91.8%), Mg (76.1%), K (53.8%). According to Heintzenberg et. al., (2000) Na, Cl and Mg are tracers of sea salt. Comparison of factor fingerprints diagrams of summer and winter revealed that Factor 3 had higher contribution rate in summer. According to these interpretations, Factor 3 appears to correspond to marine aerosol.

Factor 4 is characterized mostly by Si (94.9%), Al (94.7%), Fe (94.4%), Zn (94.6%), Cd (84.1%), Pb (35.8%) elements. Rhodes et. al., (2012) mentioned that tires can contain 1–2% zinc by weight, so factor 4 can be related with vehicle use. According to Guney et, al., (2010) motor vehicles which used leaded gasoline and wear brake linings due to traffic are widespread major source Pb and Zn, respectively. As a result, the roadway transportation might be corresponded to Factor 4.

Figure 4.39 shows the factor fingerprints for whole period of the investigation. Figure 4.40. and 4.41. shows the factor fingerprints for summer and winter seasons, respectively. Following figures and graphs show the pie charts of every element. Factor legend of diagrams as follows: Factor 1 is represented by red color, Factor 2 is represented by blue color, Factor 3 is represented by green color and Factor 4 is represented by yellow color.

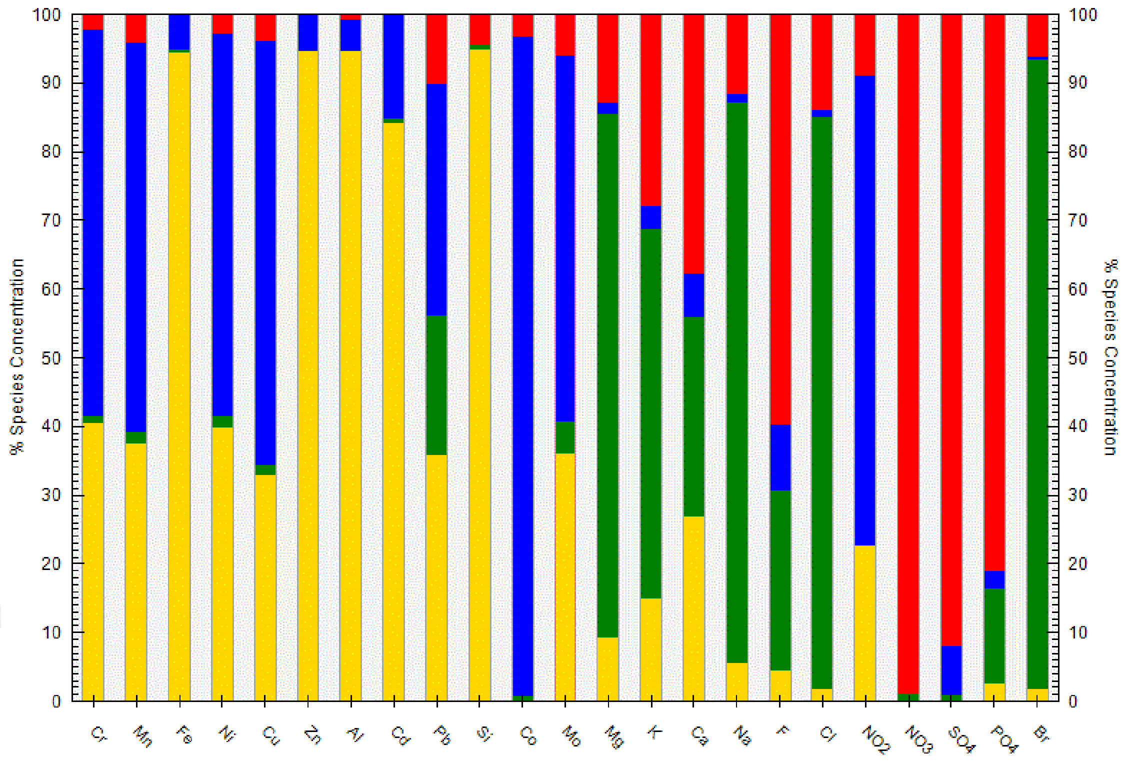

Figure 4.38. Factor fingerprints of each parameters for entire sampling duration.

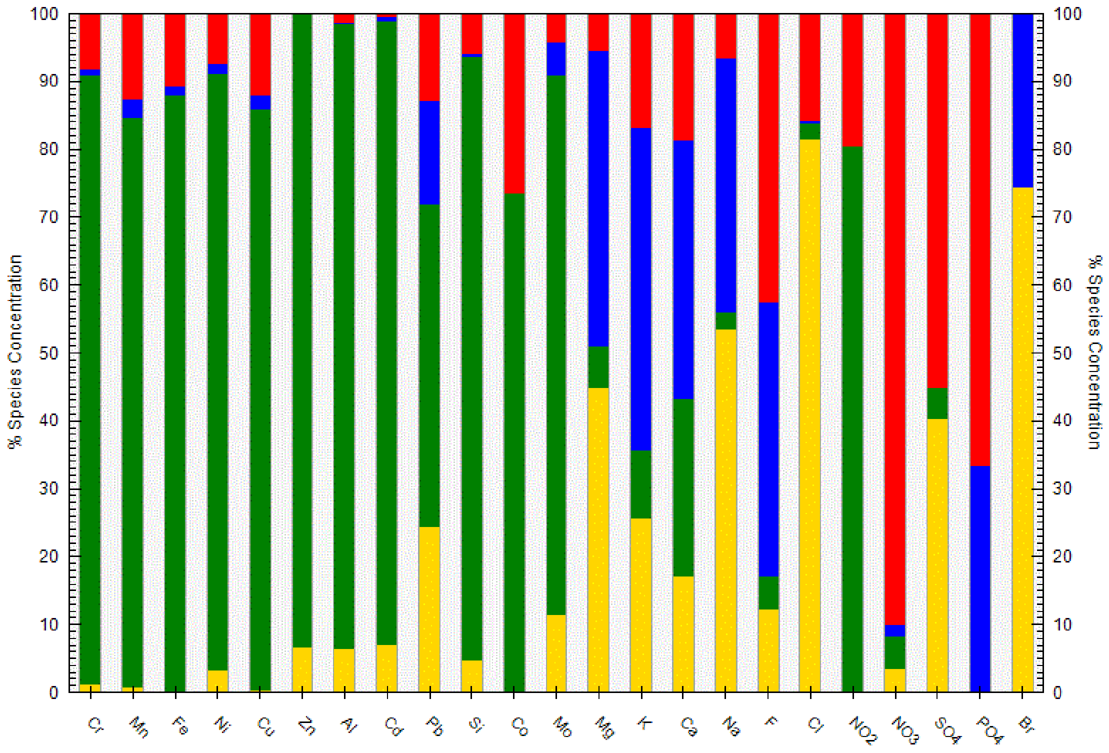

Figure 4.39. Factor fingerprints of each parameters for summer season.

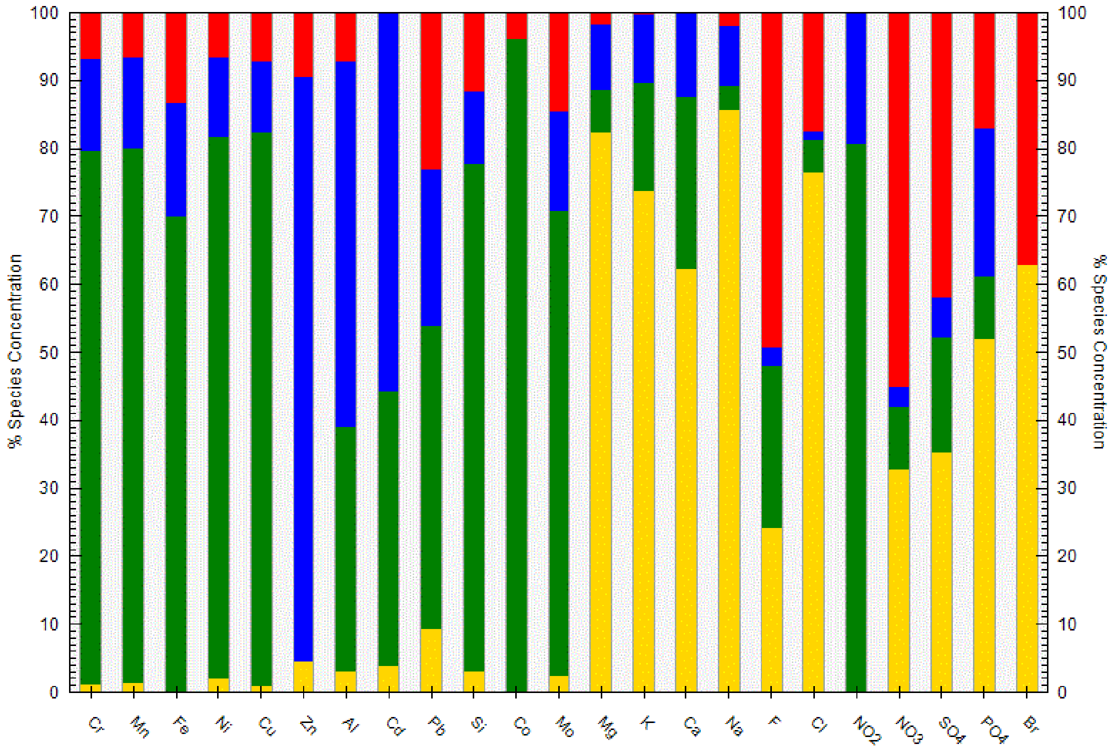

Figure 4.40. Factor fingerprints for of each parameters winter season.

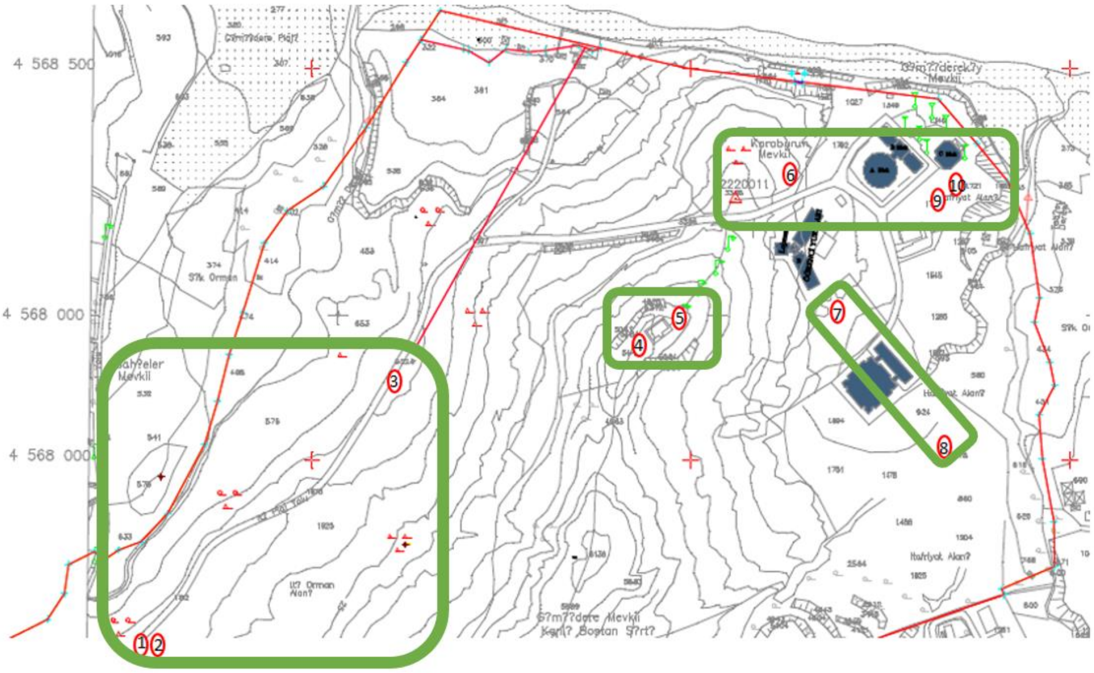

Figure 4.41. Map of selected groups of sampling devices.

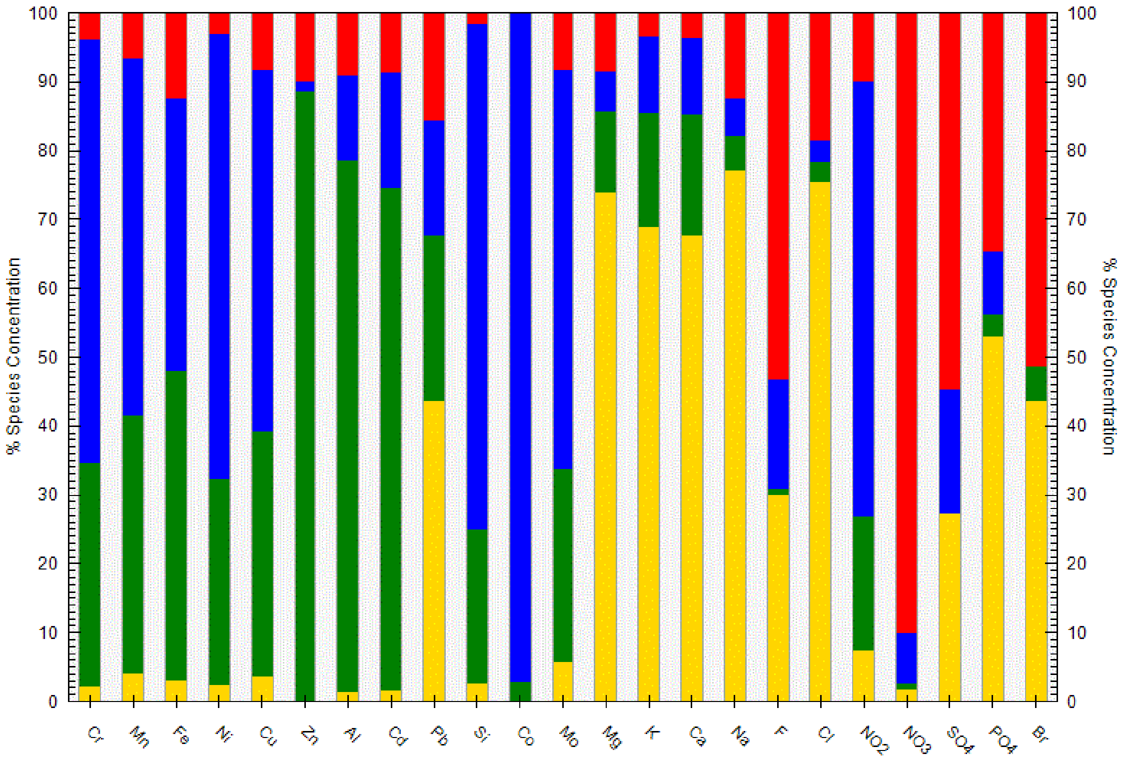

Figure 4.42. Factor fingerprints of group 1 sampling locations for entire sampling duration.

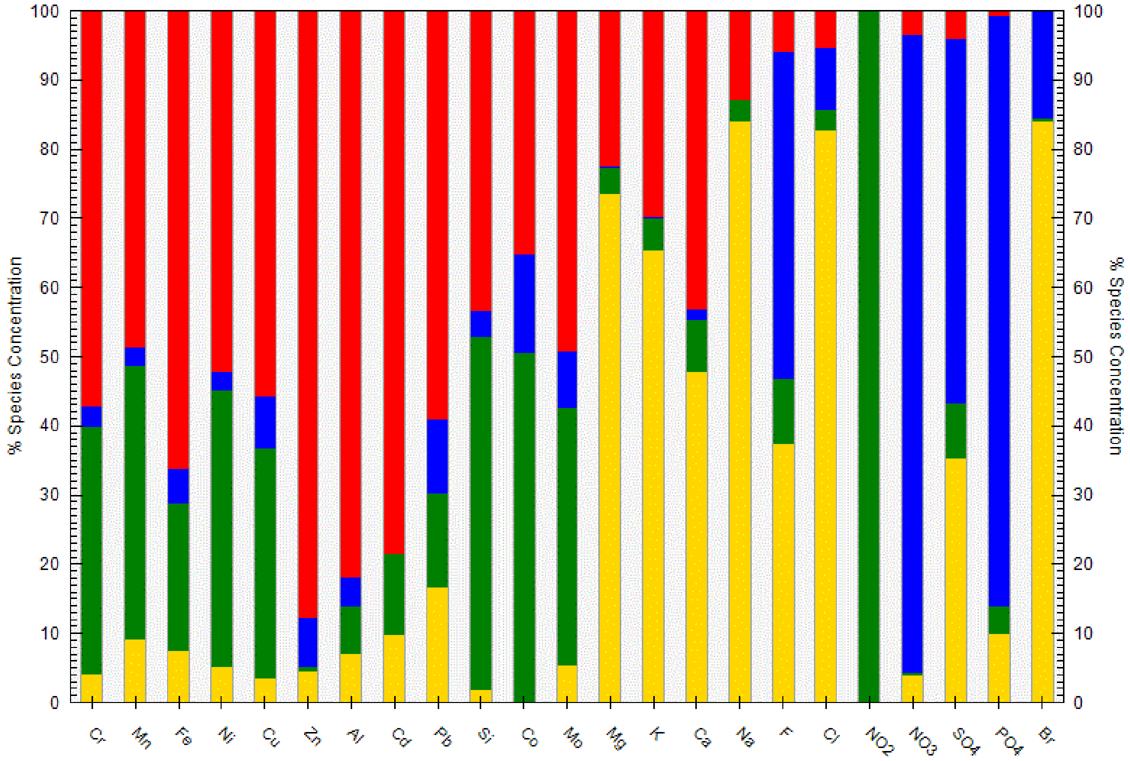

Figure 4.43. Factor fingerprints of group 2 sampling locations for entire sampling duration.

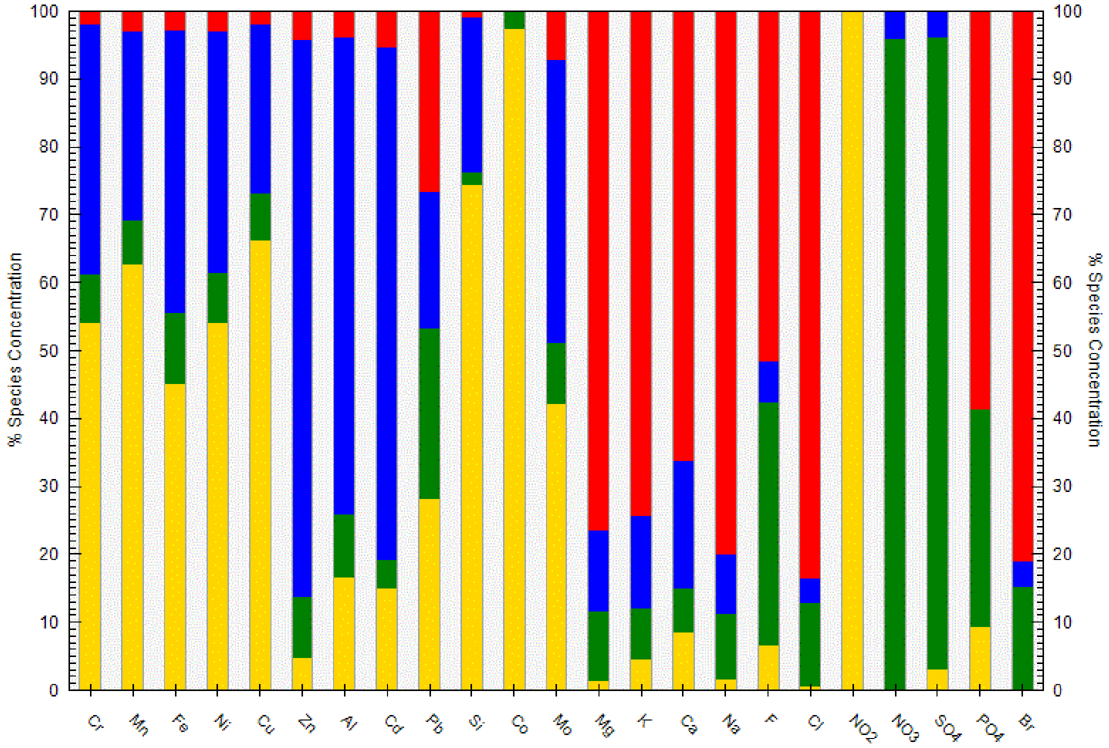

Figure 4.44. Factor fingerprints of group 3 sampling locations for entire sampling duration.

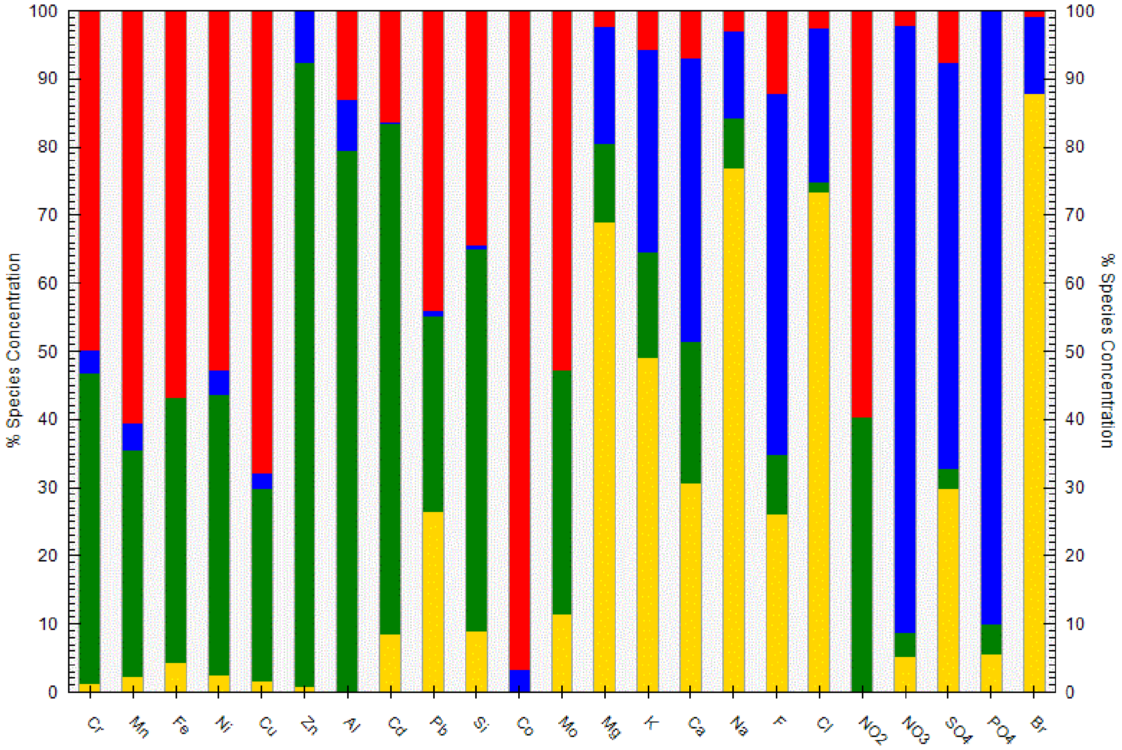

Figure 4.45. Factor fingerprints of group 4 sampling locations for entire sampling duration.

4.5.1. PMF Source Apportionment of Aqueous Phase Results

This section presents the pie charts which show the specific percentages of contributions of the different sources on each measured aqueous phase parameter. Figure 4.47 to 4.57 show the contributions of the aqueous phase parameters from the 4 factors for the entire sampling period. As mentioned before, Na (81.5%), Cl (83.4%), Br (91.8%), Mg (76.1%), K (53.8%), Ca (28.9%) are dominated by Factor 3 which corresponds to marine aerosols. NO_3 (98.9%), SO_4 (91.9%), PO_4 (81.0%), F (59.7%) are dominated by Factor 1 which might be related to agricultural activity. NO_2 (68.4%) is dominated by Factor 2 which is related to the burning processes.

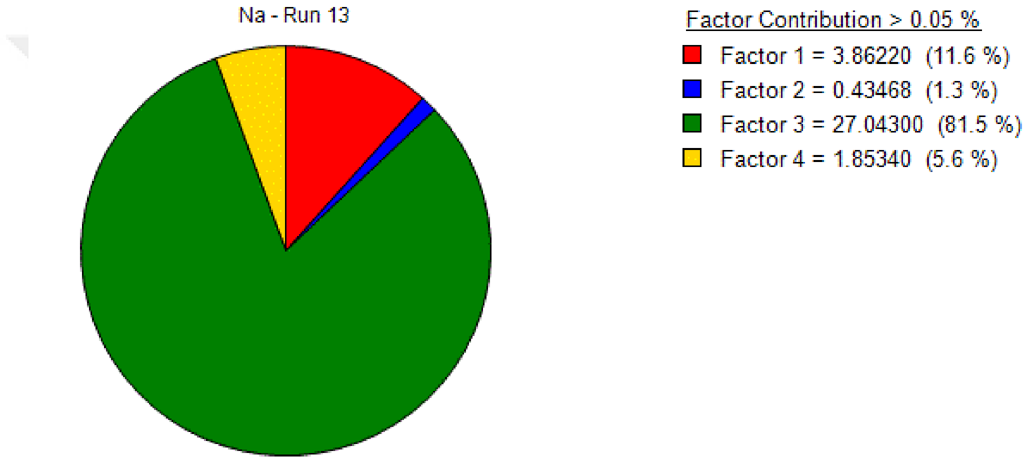

Figure 4.46. Factor contribution pie chart of Na.

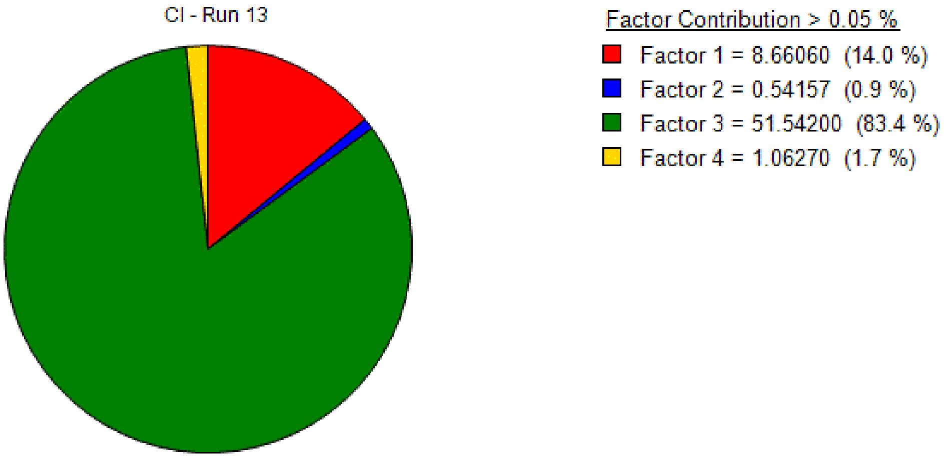

Figure 4.47. Factor contribution pie chart of Cl.

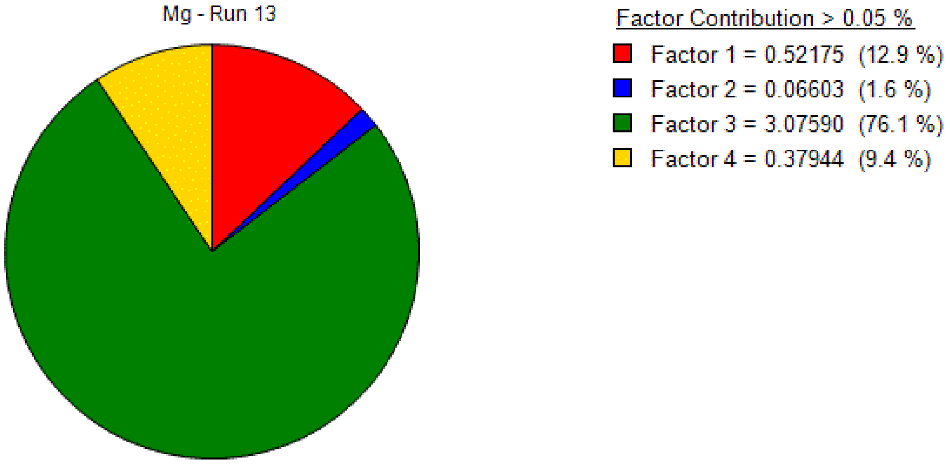

Figure 4.48. Factor contribution pie chart of Mg.

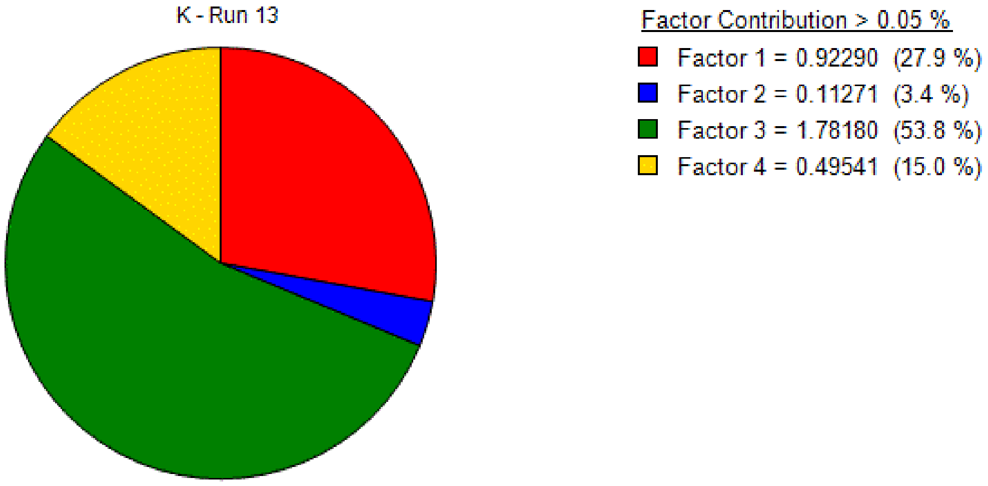

Figure 4.49. Factor contribution pie chart of K.

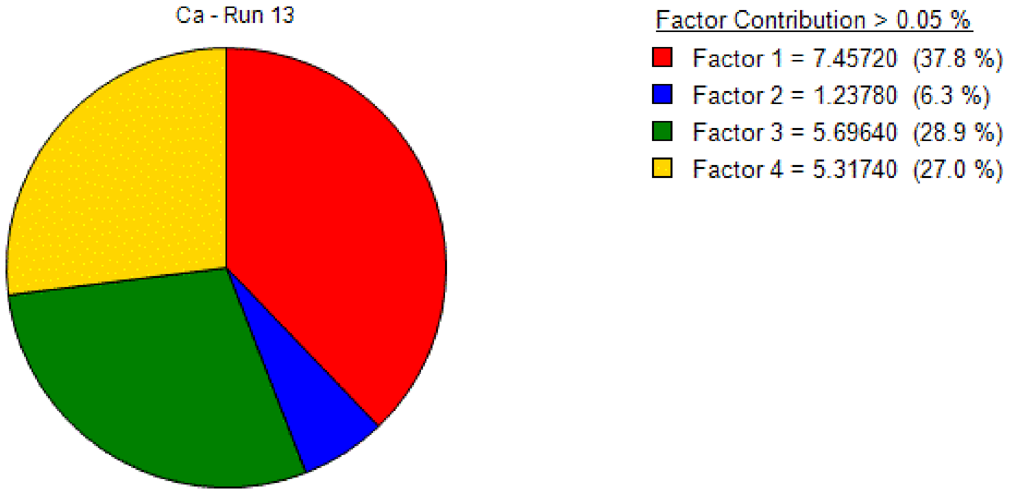

Figure 4.50. Factor contribution pie chart of Ca.

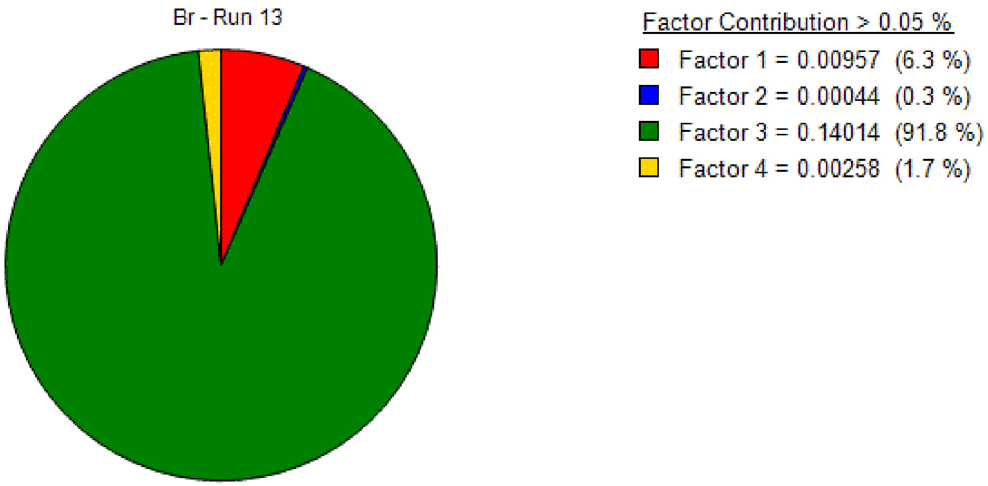

Figure 4.51. Factor contribution pie chart of Br.

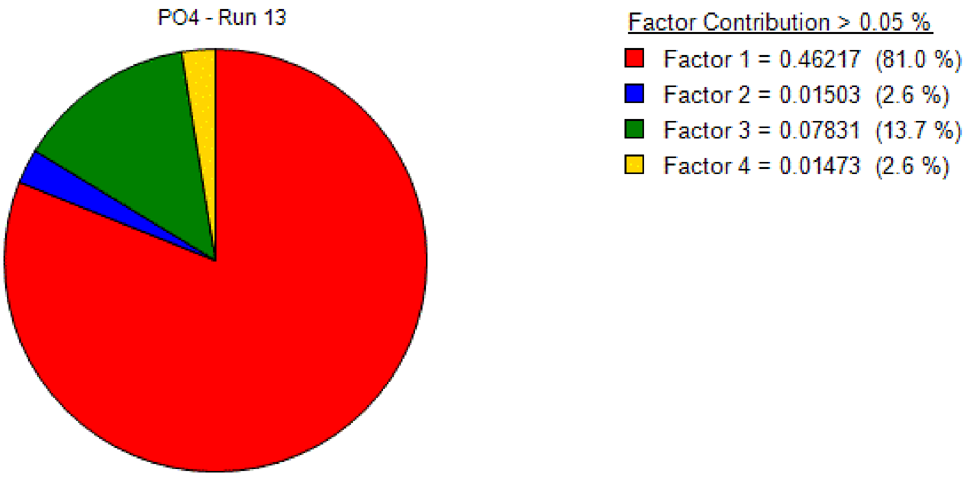

Figure 4.52. Factor contribution pie chart of PO_4.

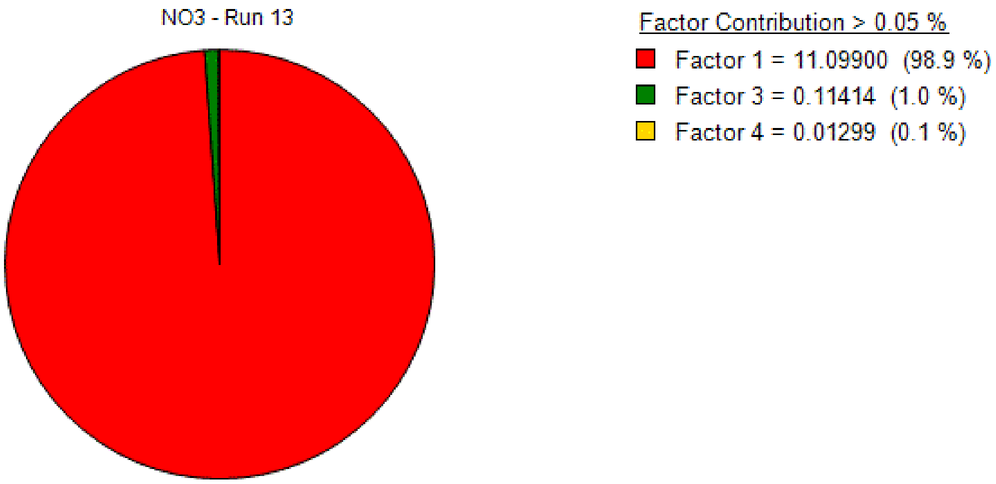

Figure 4.53. Factor contribution pie chart of NO_3.

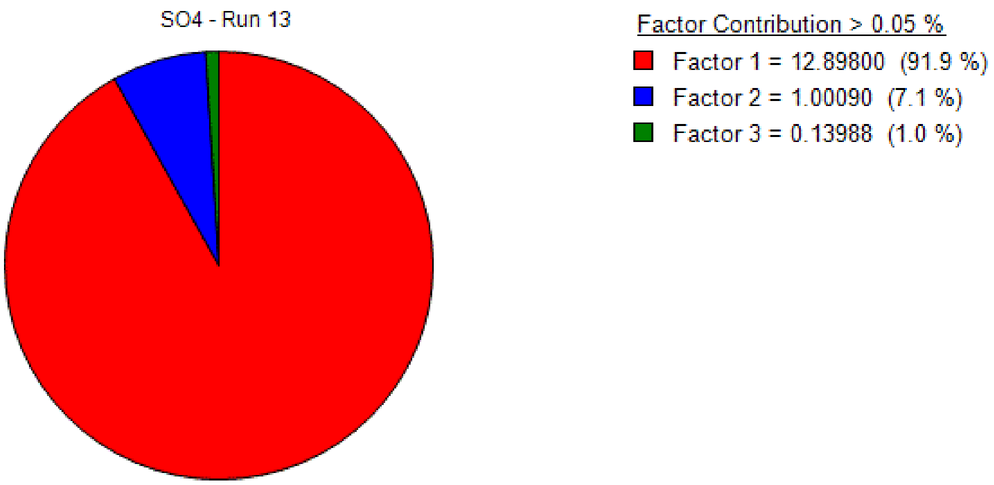

Figure 4.54. Factor contribution pie chart of SO_4.

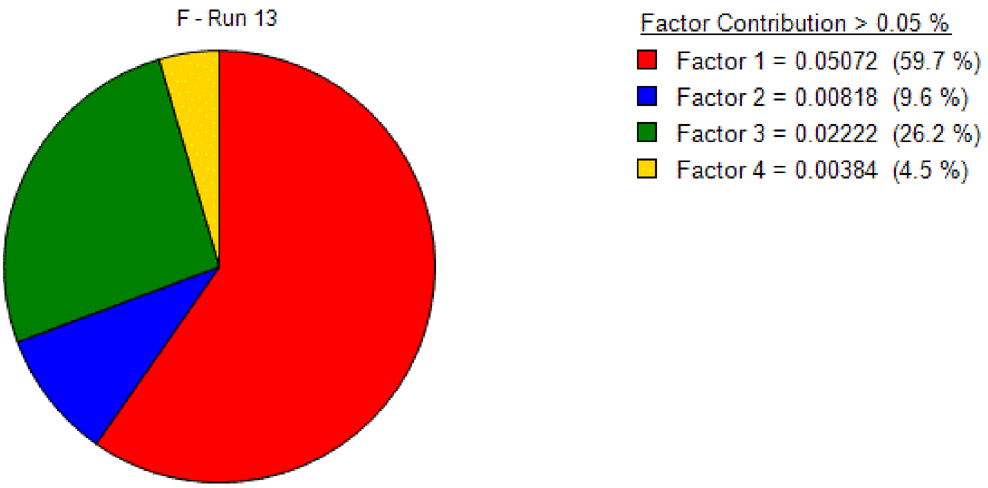

Figure 4.55. Factor contribution pie chart of F.

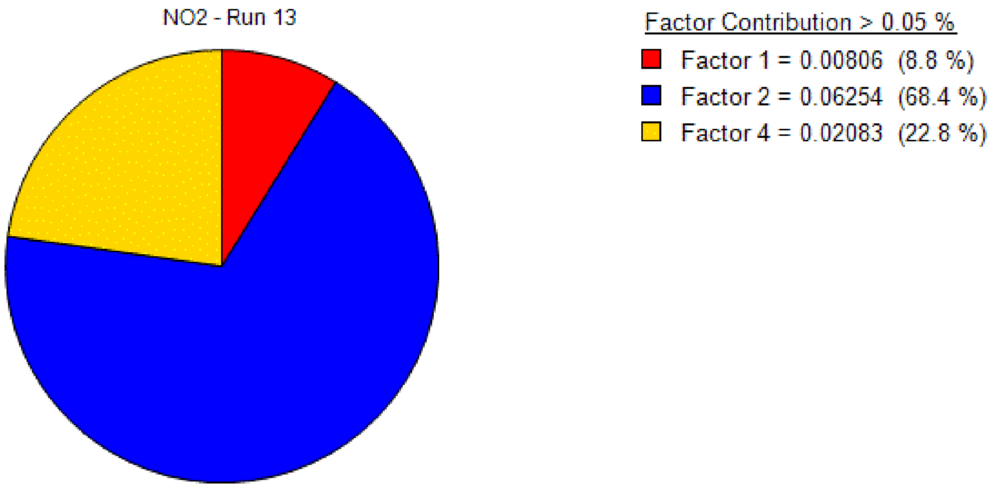

Figure 4.56. Factor contribution pie chart of NO_2.

4.5.2. PMF Source Apportionment of PM Results

This section presents the pie charts which show the specific percentages of contributions of the different sources on each measured parameter. Figure 4.58. to 4.69. show the contributions to heavy metals from the 4 factors for the entire sampling period. As mentioned before, Si (94.9%), Al (94.7%), Fe (94.4%), Zn (94.6%), Cd (84.1%), Pb (35.8%) are dominated by Factor 4 which might be originating roadway transportation. Co (96.0%), Cu (61.7%), Ni (55.7%), Cr (56.3%), Mn (56.6%), Pb (33.7%), Zn (5.2%), Mo (53.4%) are dominated by Factor 2 which can be related to burning processes. The other two factors have very little contribution.

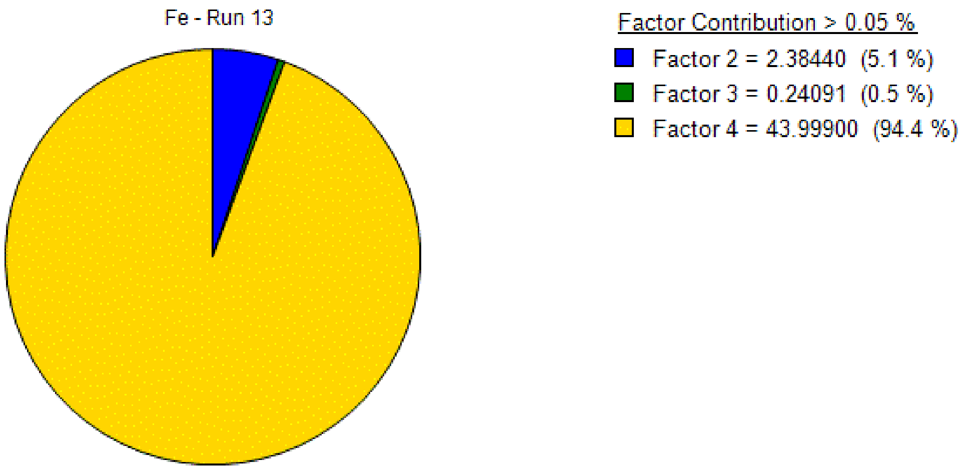

Figure 4.57. Factor Contribution Pie Chart of Fe.

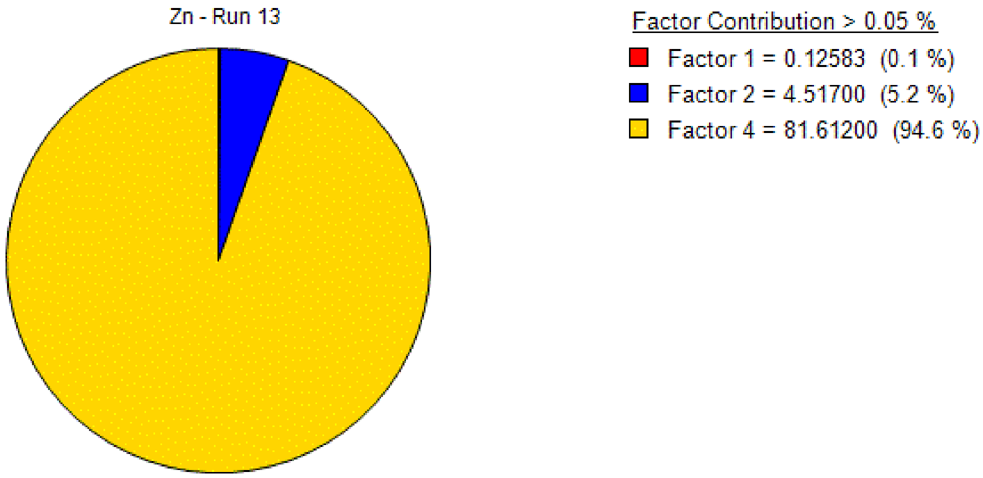

Figure 4.58. Factor Contribution Pie Chart of Zn.

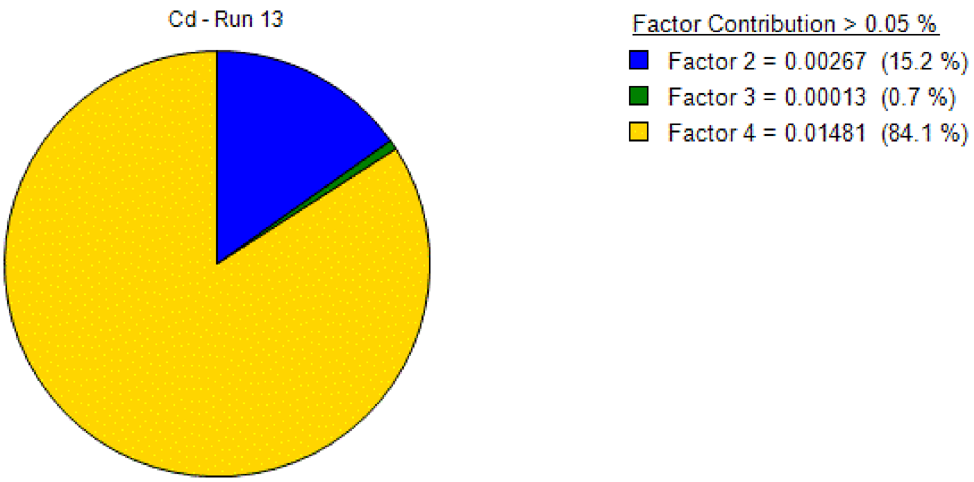

Figure 4.59. Factor Contribution Pie Chart of Cd.

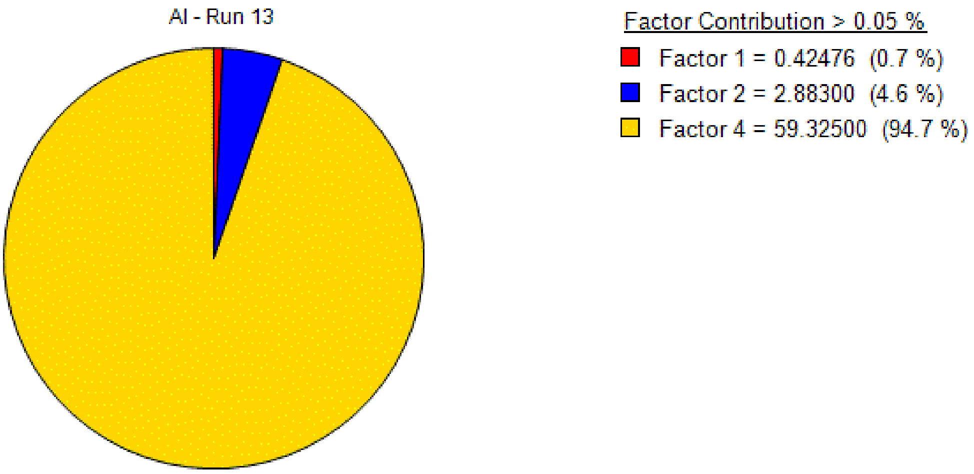

Figure 4.60. Factor Contribution Pie Chart of Al.

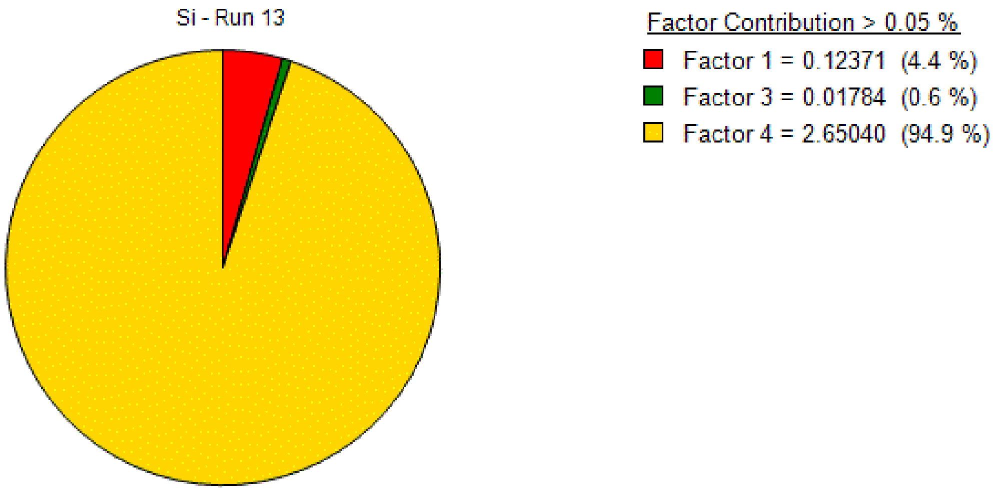

Figure 4.61. Factor Contribution Pie Chart of Si.

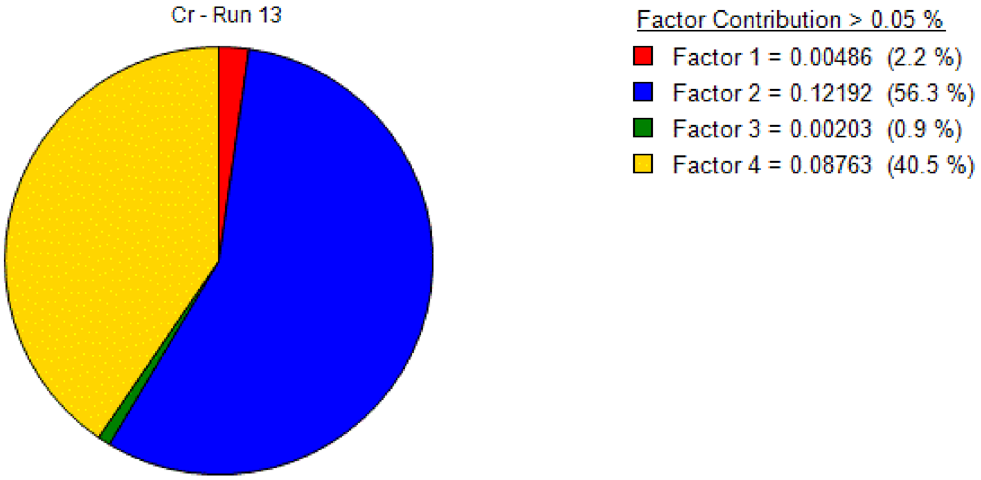

Figure 4.62. Factor Contribution Pie Chart of Cr.

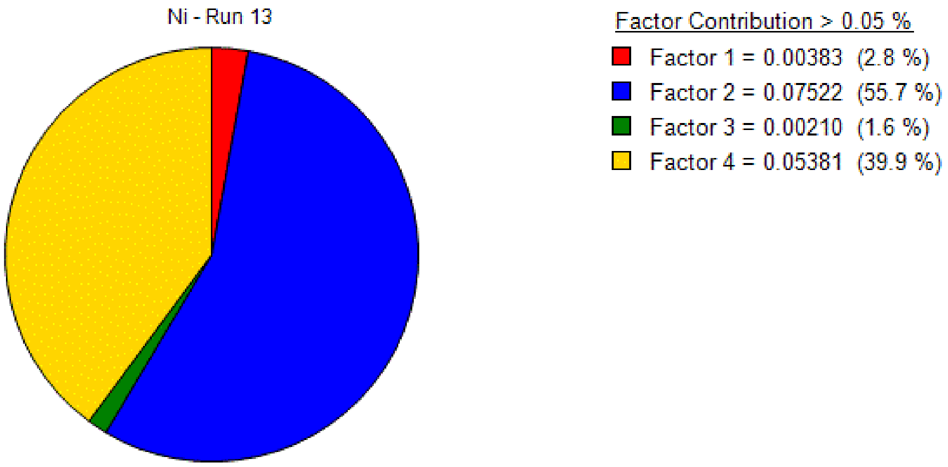

Figure 4.63. Factor Contribution Pie Chart of Ni.

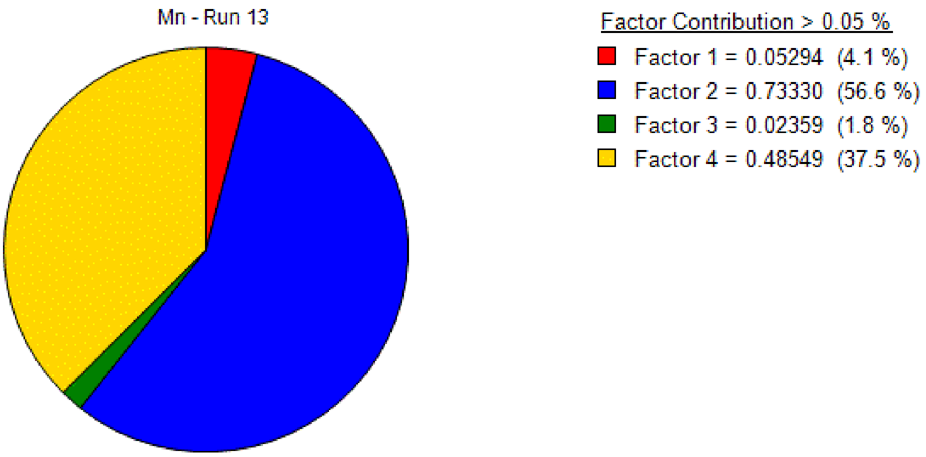

Figure 4.64. Factor Contribution Pie Chart of Mn.

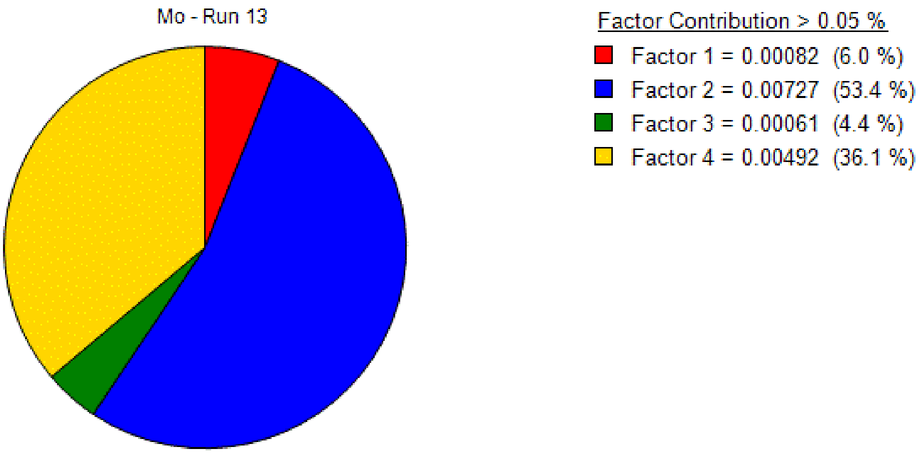

Figure 4.65. Factor Contribution Pie Chart of Mo.

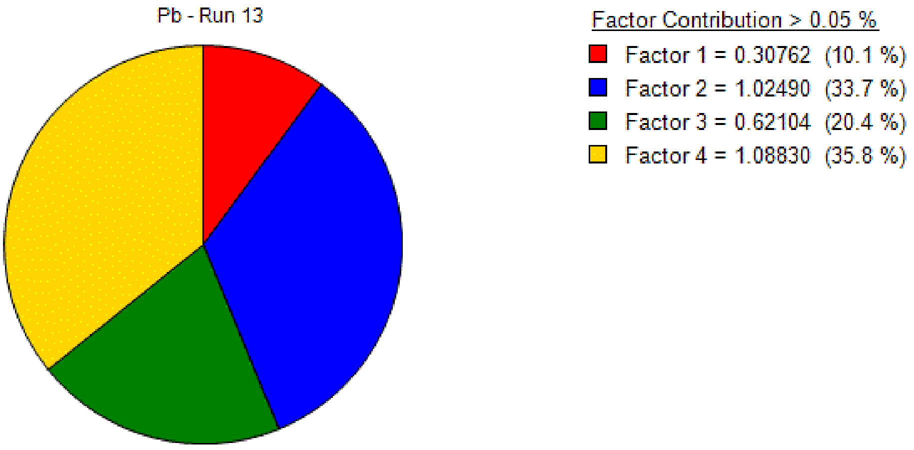

Figure 4.66. Factor Contribution Pie Chart of Pb.

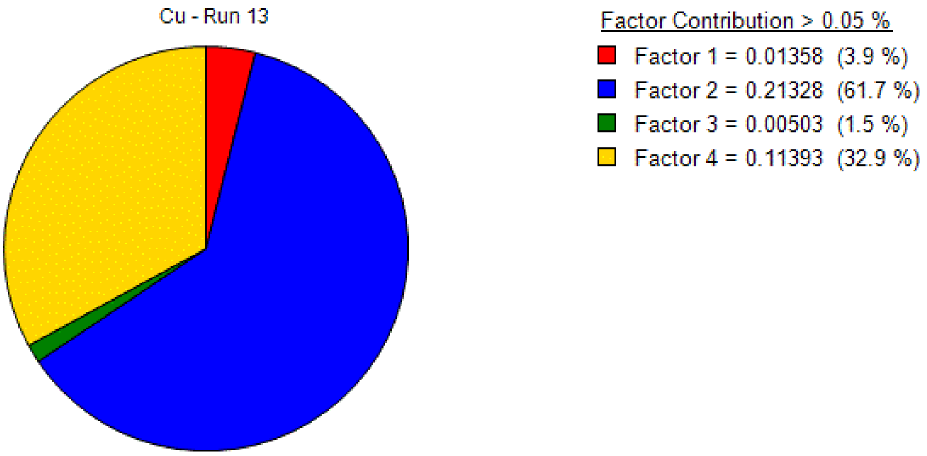

Figure 4.67. Factor Contribution Pie Chart of Cu.

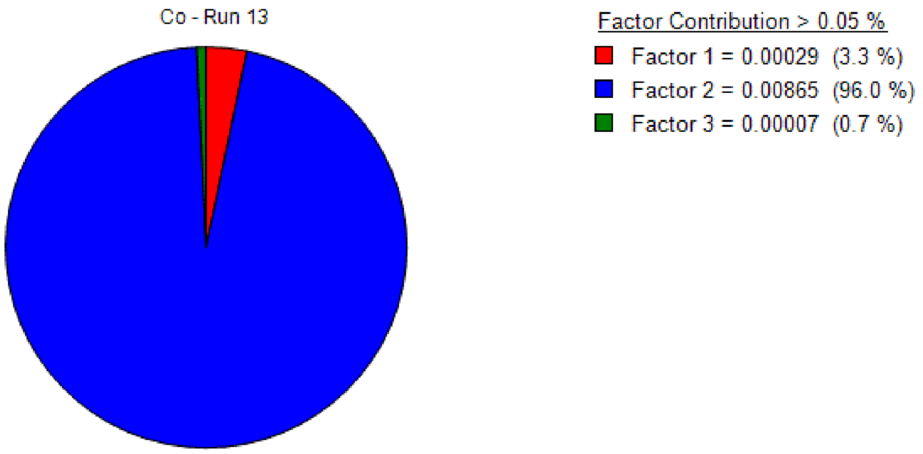

Figure 4.68. Factor Contribution Pie Chart of Co.

5. CONCLUSIONS AND RECOMMENDATIONS

The purpose of this study is to evaluate the concentrations and composition of particulate matter at the Saritepe Campus of Boğaziçi University. The campus is located at the Black Sea coast north west of the city of Istanbul. The study site was selected because of its proximity to the Black Sea and to the nearby highway system. The sea surf is known to contribute particulate matter emissions into the atmosphere. While some studies have focused on particulate matter studies along the Mediterranean Sea, less studies relating to the Black Sea can be found in the literature. Besides analyzing the solid and aqueous phases of the collected samples, a source apportionment study was also conducted to statistically determine the potential sources of the collected particulate matter.

Data were collected over a 10-month period starting from 21 March 2017 until 20 January 2018 from 10 locations distributed over the campus. In total 360 samples were collected over the 10 months period. The particulate matter composition was identified via sensitive laboratory techniques: ICP-OES, IC, AAS. Origins of PM were investigated by multivariate factor analysis technique (PMF 5.0). In total 26 parameters (F^-, Cl^-, NO_2^-, NO_3^-, SO_4^{2-}, PO_4^{3-}, Br^-, Mg^+, Ca^{2+}, K^+, Na^+, Cr, Mn, Fe, Ni, Cu, Zn, Al, Cd, Pb, Si, Co, Mo, pH, TDS and electrical conductivity) were analyzed. The sampling devices were located into different locations to allow comparing anthropogenic and natural activities effects. The sampling devices had compartments oriented along different directions to evaluate whether direction has any impact on the collected data.

The main findings of this study are summarized below:

Monthly concentrations varied widely with no clear pattern in the observed data over the duration of the study. However, some patterns may be observed. Nine parameters F^-, Cl^-, SO_4^{2-}, PO_4^{3-}, Br^-, Mg^{2+}, Ca^{2+}, K^+, Na^+ had a maximum value in the 5th month which was from July 21 to August 20 2018. Moreover, ion content shows that the collected water collected in the sampling devices appear to be a mix of seawater and to a larger extent rainwater. Wind direction did not have a significant impact on the collected PM and its composition. This may be attributed to atmospheric turbulence and the variable weather (wind/precipitation) conditions which do not favor one direction over the others. Metal contents Zn, Pb, Al and Fe are relatively high compared to the literature. However, most metal concentrations measured in this study fall in the range of concentrations observed in the literature. These levels were much higher than what is recommended by the USEPA.

The sampling locations which are closest to the sea S6, S9, S10 had the highest Cl^-, Br^-, Mg^{2+}, K^+, Na^+ concentrations. For some metals, the highest observed concentrations where mostly at S1 and S2 located very near the roadway, next to the University entrance. Sampling point S5 which is located up the hill near the wind turbine had relatively high concentrations of Mn, Fe, Al, Si, Co.

While interpreting the results, meteorological conditions were also considered. Correlation analysis between meteorological data and the 23 parameters revealed that there is no high (positive or negative) correlation between them except precipitation. Precipitation had a positive but low correlation which indicated that wet deposition is an important mechanism for the transport of the particulate matter to the Earth surface. The relatively low correlation also indicates that there are other factors that contribute to the settling of particulate matter. The ion concentrations were however very high positively correlated: Na/K ($r = 0.96$), Cl/Br ($r = 0.96$), Mg/Cl ($r = 0.95$), Na/Br ($r = 0.94$), Na/Cl ($r = 0.92$), Br/Mg ($r = 0.90$), K/Cl ($r = 0.90$), Mg/Na ($r = 0.89$), K/Br ($r = 0.88$) and Mg/K ($r = 0.87$). The strong correlation between ions gives further evidence that large fractions of these ions are originating from the same source.

Metal content in the collected PM are also very high positively correlated: Zn/Al ($r = 0.94$), Cr/Zn ($r = 0.98$), Cr/Al ($r = 0.93$), Mn/Zn ($r = 0.90$), Mn/Al ($r = 0.95$), Cr/Mo ($r = 0.92$), Co/Si ($r = 0.97$), Fe/Cr ($r = 0.85$), Mn/Fe (0.78), Mn/Mo (0.85), Fe/Ni (0.83), Fe/Cu (0.78), Fe/Zn (0.78) Fe/Cd (0.83). These high correlations between the different heavy metals suggest that they may be originating from the same anthropogenic activities such as transportation, burning processes, etc.

Source apportionment using the PMF 5.0 program developed by EPA reveals that the data are a contribution of 4 distinct sources. Factor 1 is characterized mostly by NO_3 (98.9%), SO_4 (91.9%), PO_4 (81.0%), F (59.7%) and is mostly attributed to agricultural activity. Factor 2 is characterized by Co (96.0%), Cu (61.7%), NO_2 (68.4%), Ni (55.7%), Cr (56.3%), Mn (56.6%), Pb (33.7%), Zn (5.2%), Mo (53.4%) that can be related to burning processes such as heating and other purposes. Factor 3 is characterized mostly by Na (81.5%), Cl (83.4%), Br (91.8%), Mg (76.1%), K (53.8%) which correspond to marine aerosol. Factor 4 is characterized by Si (94.9%), Al (94.7%), Fe (94.4%), Zn (94.6%), Cd (84.1%), Pb (35.8%) which is interpreted to be related to roadway transportation.

The data collected and the analyses performed in this study can serve as an example for other studies in Turkey. Specifically, the analyses can be repeated at other important locations with high levels of particulate matter such as in tunnels or at industrial zones.

The current analysis used passive simple devices that allow the collection of PMs over a relatively long time without differentiation between particulate matter size. Future studies could focus on advanced sampling techniques that collect air samples and filter them according to size prior to laboratory analysis. This is important because the size of the particulate matter has a significant impact on human health, particularly its ability to enter the respiratory system.

Future work could combine the data collected from this study along with data collected from other studies in Turkey and elsewhere in an open access database so that other researchers as well as the public can view and monitor air quality. For better visualization the data can be presented using a geographical information system.

Finally, the data presented in this study show that particulate matter can be transported over possibly large distances from the source to the receptors (in this case the Saritepe Campus). Future studies can include modeling studies that simulate the transport of the particulate matter taking into account meteorological conditions.

REFERENCES

Aceto, M., 2016. The use of ICP-MS in food traceability. In Advances in Food Traceability Techniques and Technologies, 137-164. Woodhead Publishing, Alessandria, Italy.

Adachi, K., Tainosho, Y., 2004. Characterization of heavy metal particles embedded in tire dust. Environment international, 30, 1009-1017.

Baykara, M., Im, U., Unal, A., 2019. Evaluation of impact of residential heating on air quality of megacity Istanbul by CMAQ. Science of the Total Environment, 651, 1688-1697.

Campbell, N. R., Ingram, J. C., 2014. Characterization of 234U/238U Activity Ratios and Potential Inorganic Uranium Complexation Species in Unregulated Water Sources in the Southwest Region of the Navajo Reservation. In Water Reclamation and Sustainability, 77-94. Elsevier, Flagstaff, AZ, USA.

Çapraz, Ö., Efe, B., Deniz, A., 2016. Study on the association between air pollution and mortality in İstanbul, 2007–2012. Atmospheric Pollution Research, 7, 147-154.

Celo, V., Dabek-Zlotorzynska, E., Mathieu, D., Okonskaia, I., 2010. Validation of simple microwave-assisted acid digestion method using micro vessels for analysis of trace elements in atmospheric $PM_{2.5}$ in monitoring and fingerprinting studies. The Open Chemical & Biomedical Methods Journal, 3, 143-152.

Charles, B., Fredeen, K. J., 1997. Concepts, instrumentation and techniques in inductively coupled plasma optical emission spectrometry. PerkinElmer Life and Analytical Sciences, CT, USA.

Chester, R., Jickells, T. D., 2012. Marine Geochemistry. Wiley/Blackwell Publishing, Chichester, West Sussex, UK; Hoboken, NJ, USA.

Cohen, A. J., Anderson, H. R., Ostro, B., Pandey, K. D., Krzyzanowski, M., Künzli, N., Smith, K. R., 2004. Urban air pollution. In: Ezzati, M., Lopez, A. D., Rodgers, A., Murray C. J. L., (Eds.), Comparative quantification of health risks, 2, 1353-1433, WHO, Geneva, Switzerland.

Comero, S., Capitani, L., Gawlik, B. M., 2009. Positive Matrix Factorisation (PMF)–An introduction to the chemometric evaluation of environmental monitoring data using PMF. Office for Official Publications of the European Communities, Luxembourg, 59.

Darus, F. M., Nasir, R. A., Sumari, S. M., Ismail, Z. S., Omar, N. A., 2012. Heavy metals composition of indoor dust in nursery schools building. Procedia-Social and Behavioral Sciences, 38, 169-175.

Demir, G., Yigit, S., Ozdemir, H., Borucu, G., Saral, A., 2010. Elemental concentrations of atmospheric aerosols and the soil samples on the selected playgrounds in Istanbul. Journal of Residuals Science & Technology, 7, 123-130.

Diapouli, E., Manousakas, M., Vratolis, S., Vasilatou, V., Maggos, T., Saraga, D., Eleftheriadis, K., 2017. Evolution of air pollution source contributions over one decade, derived by PM 10 and PM 2.5 source apportionment in two metropolitan urban areas in Greece. Atmospheric Environment, 416-430.

Directive of Air Quality Assessment and Management, 2008. Official gazette, 26898.

Dong, A., Chesters, G., Simsiman, G. V., 1984. Metal composition of soil, sediments, and urban dust and dirt samples from the Menomonee River Watershed, Wisconsin, USA. Water, Air, and Soil Pollution, 22, 257-275.

EEA, 2012. Particulate matter from natural sources and related reporting under the EU Air Quality Directive in 2008 and 2009, Technical Report.

Fenger, J., 2009. Air pollution in the last 50 years–From local to global. Atmospheric environment, 43, 13-22.

Flores, R. M., Kaya, N., Eşer, Ö., Saltan, Ş., 2017. The effect of mineral dust transport on PM10 concentrations and physical properties in Istanbul during 2007–2014. Atmospheric research, 197, 342-355.

Ghosh, S., Rabha, R., Chowdhury, M., Padhy, P. K., 2018. Source and chemical species characterization of PM10 and human health risk assessment of semi-urban, urban and industrial areas of West Bengal, India. Chemosphere, 207, 626-636.

Gobre, T., Salve, P. R., Krupadam, R. J., Bansiwal, A., Shastry, S., Wate, S. R., 2010. Chemical composition of precipitation in the coastal environment of India. Bulletin of environmental contamination and toxicology, 85, 48-53.

Güçlü, Y. S., Dabanlı, İ., Şişman, E., Şen, Z., 2019. Air quality identification by innovative trend diagram and AQ index combinations in Istanbul megacity. Atmospheric Pollution Research, 10, 88-96.

Guney, M., Onay, T. T., Copty, N. K., 2010. Impact of overland traffic on heavy metal levels in highway dust and soils of Istanbul, Turkey. Environmental monitoring and assessment, 164, 101-110.

Heij, G., Schneider, T., 1991. Acidification research in the Netherlands: Final report of the Dutch priority programme on acidification. Elsevier, Amsterdam, Netherlands.

Heintzenberg, J., Covert, D. C., Dingenen, R. V., 2000. Size distribution and chemical composition of marine aerosols: a compilation and review. Tellus B: Chemical and Physical Meteorology, 52, 1104-1122.

Hernández-Escamilla JA, Flores-Margez JP, Shukla MK, 2015. Particulate Matter: Capture and Quantification in Natural and Anthropogenic Sources. Environmental & Analytical Toxicology, 5, 281.

Hinkle, D. E., Wiersma, W., Jurs, S. G., 1988. Applied statistics for the behavioral sciences. Houghton Mifflin, Boston, USA.

Hosokawa, A., Reid, C. R., Latty, T., 2019. Slimes in the city: The diversity of myxomycetes from inner-city and semi-urban parks in Sydney, Australia. Fungal Ecology, 39, 37-44.

Im, U., 2009. Mesoscale modeling of aerosol levels in Istanbul using a high resolution MM5/CMAQ air quality modeling system, PhD Thesis, Bogazici University, Istanbul, Turkey.

Im, U., 2013. Impact of sea-salt emissions on the model performance and aerosol chemical composition and deposition in the East Mediterranean coastal regions. Atmospheric environment, 75, 329-340.

Im, U., Markakis, K., Unal, A., Kindap, T., Poupkou, A., Incecik, S., Mihalopoulos, N., 2010. Study of a winter PM episode in Istanbul using the high resolution WRF/CMAQ modeling system. Atmospheric Environment, 44, 3085-3094.

Jolly, Y. N., Islam, A., Akbar, S., 2013. Transfer of metals from soil to vegetables and possible health risk assessment. SpringerPlus, 2, 385.

Kabatas, B., Unal, A., Pierce, R. B., Kindap, T., Pozzoli, L., 2014. The contribution of Saharan dust in PM 10 concentration levels in Anatolian Peninsula of Turkey. Science of the Total Environment, 488, 413-421.

Kindap, T., 2008. Identifying the trans-boundary transport of air pollutants to the city of Istanbul under specific weather conditions. Water, air, and soil pollution, 189, 279-289.

Kindap, T., Unal, A., Chen, S. H., Hu, Y., Odman, M. T., Karaca, M., 2006. Long-range aerosol transport from Europe to Istanbul, Turkey. Atmospheric Environment, 40, 3536-3547.

Koçak, M., Theodosi, C., Zarmpas, P., Im, U., Bougiatioti, A., Yenigun, O., Mihalopoulos, N., 2011. Particulate matter (PM 10) in Istanbul: origin, source areas and potential impact on surrounding regions. Atmospheric Environment, 45, 6891-6900.

Landrigan, P. J., Fuller, R., Acosta, N. J., Adeyi, O., Arnold, R., Baldé, A. B., Chiles, T., 2018. The Lancet Commission on pollution and health. The Lancet, 391, 462-512.

Lenntech, Composition of seawater. https://www.lenntech.com/composition-seawater.html. Date accessed March 2019.

Li, X., Song, H., Zhai, S., Lu, S., Kong, Y., Xia, H., Zhao, H., 2019. Particulate matter pollution in Chinese cities: Areal-temporal variations and their relationships with meteorological conditions 2015–2017. Environmental Pollution, 246, 11-18.

Manousakas, M., Bairachtari, K., Kantarelou, V., Eleftheriadis, K., Vasilakos, C., Assimakopoulos, V. D., Maggos, T., 2019. The traffic signature on the vertical PM profile: Environmental and health risks within an urban roadside environment. Science of the Total Environment, 646, 448-459.

Markakis, K., Im, U., Unal, A., Melas, D., Yenigun, O., Incecik, S., 2012. Compilation of a GIS based high spatially and temporally resolved emission inventory for the greater Istanbul area. Atmospheric Pollution Research, 3, 112-125.

McMurry, P., Shepherd M., Vickery, J., 2006. Particulate Matter Science for Policy Makers: A NARSTO Assessment. and eds. Cambridge University Press, Cambridge, England.

Munch, J. C., Velthof, G. L., 2007. Denitrification and agriculture. In Biology of the nitrogen cycle, 331-341. Elsevier, Amsterdam, Netherlands.

Nagashima, H., Okamoto, T., 1999. Determination of inorganic anions by ion chromatography using a graphitized carbon column dynamically coated with cetyltrimethylammonium ions. Journal of Chromatography A, 855, 261-266.

Norris, G. A., Duvall, R., Brown, S. G., Bai, S., 2014. EPA Positive Matrix Factorization (PMF) 5.0 fundamentals and User Guide Prepared for the US Environmental Protection Agency Office of Research and Development, Washington, DC.

Ozdemir, H., Pozzoli, L., Kindap, T., Demir, G., Mertoglu, B., Mihalopoulos, N., Unal, A., 2014. Spatial and temporal analysis of black carbon aerosols in Istanbul megacity. Science of the Total Environment, 473, 451-458.

Pérez, N., Moreno, T., Querol, X., Alastuey, A., Bhatia, R., Spiro, B., Hanvey, M., 2010. Physicochemical variations in atmospheric aerosols recorded at sea onboard the Atlantic–Mediterranean 2008 Scholar Ship cruise (Part I): Particle mass concentrations, size ratios, and main chemical components. Atmospheric Environment, 44, 2552-2562.

Pushkar K., 2007. Competition Science Vision: Edaphic Factors, 1207-1212

Qian, P., Zhou, L., Zheng, X., Dong, Y., Wang, Y., 2014. Magnetic properties of airborne particulate matter in Shanghai during dust storm events and the implications for heavy metal contaminant sources. Environmental earth sciences, 72, 4167-4178.

Rhodes, E. P., Ren, Z., Mays, D. C., 2012. Zinc leaching from tire crumb rubber. Environmental science & technology, 46, 12856-12863.

Rizza, V., Stabile, L., Buonanno, G., Morawska, L., 2017. Variability of airborne particle metrics in an urban area. Environmental Pollution, 220, 625-635.

Rodriguez-Navarro, C., Di Lorenzo, F., Elert, K., 2018. Mineralogy and physicochemical features of Saharan dust wet deposited in the Iberian Peninsula during an extreme red rain event. Atmospheric Chemistry & Physics, 18, 13, 10089-10122.

Saliba, N. A., Massoud, R., 2010. A comparative review of PM levels, sources, and their likely fates in the Eastern Mediterranean Region. In Urban Airborne Particulate Matter. Springer, Berlin Heidelberg.

Salve, P. R., Maurya, A., Wate, S. R., Devotta, S., 2008. Chemical composition of major ions in rainwater. Bulletin of environmental contamination and toxicology, 80, 242-246.

Seinfeld, J. H., Pandis, S. N., Noone, K., 2006. Atmospheric chemistry and physics: from air pollution to climate change, 2nd ed., 57-383.

Song, Y., Zhang, Y., Xie, S., Zeng, L., Zheng, M., Salmon, L. G., Slanina, S., 2006. Source apportionment of $PM_{2.5}$ in Beijing by positive matrix factorization. Atmospheric Environment, 40, 1526-1537.

Tahmasbian, I., Nasrazadani, A., Shoja, H., Sinegani, A. A. S., 2014. The effects of human activities and different land-use on trace element pollution in urban topsoil of Isfahan (Iran). Environmental earth sciences, 71, 1551-1560.

Tao, J., Zhang, L., Cao, J., Zhong, L., Chen, D., Yang, Y., Xia, Y., 2017. Source apportionment of PM 2.5 at urban and suburban areas of the Pearl River Delta region, south China-With emphasis on ship emissions. Science of The Total Environment, 574, 1559-1570.

The Guardian Weekly, 2012. 60 years since the great smog of London in pictures https://www.theguardian.com/environment/gallery/2012/dec/05/60-years-great-smog-london-in-pictures. Date accessed March 2019.

Theodosi, C., Im, U., Bougiatioti, A., Zarmpas, P., Yenigun, O., Mihalopoulos, N., 2010. Aerosol chemical composition over Istanbul. Science of the Total Environment, 408, 2482-2491.

TMMOB Çevre Mühendisliği Odası, Hava Kirliliği Raporu, 2017.

Turkish Standards Institution, TS2341, 1976. Methods for The Measurement of Air Pollution Deposit Gauges.

Turkish Standards Institution, TS2342, 1976. Methods for The Installation and The Use of The Directional Dust Gauges

U.S. Environmental Protection Agency, 2017. What are the Air Quality Standards for PM, https://www.epa.gov/region1/airquality/PM-aq-standards.html. Date accessed March 2019.

USEPA, E., 1982. Method 120.1, Conductance (Specific Conductance, umhos at 25°C).

USEPA, E., 1982. Method 150.2, pH, Continuous Monitoring (Electrometric).

USEPA, E., 2007. Method 7000B, Flame Atomic Absorption Spectrophotometry.

USEPA, E., 2007. Method 3051a, Microwave Assisted Acid Digestion of Sediments, Sludges, Soils, And Oils.

USEPA, E., 2007. Method 9056a, Determination of Inorganic Anions by Ion Chromatography.

USEPA, E., 2018. Method 6010D, Inductively Coupled Plasma-Optical Emission Spectrometry.

Uygur, N., Saral, A., 2013. Evaluation of the effect of Marmara Sea on the characterization of the coastal line atmosphere in Istanbul. Journal of Engineering & Natural Sciences/Mühendislik ve Fen Bilimleri Dergisi, 31, 429-439.

VanBriesen, J. M., 2014. Potential drinking water effects of bromide discharges from coal-fired electric power plants. EPA NPDES Comments, 1-38.

Wiseman C. L., Zereini F., 2010. Airborne Particulate Matter, Platinum Group Elements and Human Health. In: Zereini F., Wiseman C. (Eds.), Urban Airborne Particulate Matter, 553-571. Springer, Berlin, Heidelberg.

World Health Organization. Occupational and Environmental Health Team., 1999. Hazard prevention and control in the work environment: airborne dust, Geneva, Switzerland.

Yetimoğlu, E. K., Ercan, Ö., Tosyali, K., 2007. Heavy Metal Contamination in Street Dusts of Istanbul. E-5 Highway. Journal of Analytical, Environmental and Cultural Heritage Chemistry, 97, 227-235.